Analysis and Performance Enhancement of Solar Photo-voltaic System in Indian Climate Conditions

A THESIS SUBMITTED TO
UNIVERSITY OF PETROLEUM AND ENERGY STUDIES

FOR THE AWARD OF
DOCTOR OF PHILOSOPHY
IN
ELECTRICAL ENGINEERING

BY

VINAY GUPTA

SUPERVISORS

DR. MADHU SHARMA
DR. RUPENDRA KUMAR PACHAURI
DR. K N DINESH BABU

DEPARTMENT OF ELECTRICAL ENGINEERING
SCHOOL OF ENGINEERING
UNIVERSITY OF PETROLEUM AND ENERGY STUDIES
DEHRADUN-248007, UTTARAKHAND, INDIA

AUGUST 2022

Analysis and Performance Enhancement of Solar Photo-voltaic System in Indian Climate Conditions

A thesis submitted to
University of Petroleum and Energy Studies

For the Award of
Doctor of Philosophy
in
Electrical Engineering

BY

Vinay Gupta
(SAP ID-500048428)
August 2022

Internal Supervisor
Dr. Madhu Sharma
Associate Professor
School of Engineering
University of Petroleum and Energy Studies

Internal Co-Supervisor
Dr. Rupendra Kumar Pachauri
Assistant Professor
School of Engineering
University of Petroleum and Energy Studies

External Supervisor
Dr. K N Dinesh Babu
Application Manager
Megger Group, Chennai

Department of Electrical Engineering
School of Engineering
University of Petroleum and Energy Studies
Dehradun-248007, Uttarakhand, INDIA

DECLARATION

04 August 2022

I declare that the thesis entitled "**Analysis and Performance Enhancement of Solar Photo-voltaic System in Indian Climate Conditions** "has been prepared by me under the guidance of **Dr. Madhu Sharma**, Associate Professor of School of Engineering, University of Petroleum and Energy Studies, Dehradun, **Dr. Rupendra Kumar Pachauri,** Assistant Professor of School of Engineering, University of Petroleum and Energy Studies, Dehradun and **Dr. K N Dinesh Babu**, Application Manager, Megger Group, Chennai. No part of this thesis has formed the basis for the award of any degree or fellowship previously.

Vinay Gupta
School of Engineering
University of Petroleum and Energy Studies, Dehradun
DATE: 04/08/2022

CERTIFICATE

I certify that **Mr. Vinay Gupta** has prepared his thesis entitled **"Analysis and Performance Enhancement of Solar Photo-voltaic System in Indian Climate Conditions",** for the award of PhD degree of the University of Petroleum & Energy Studies, under our guidance. He has carried out the work at the School of Engineering, University of Petroleum & Energy Studies.

Internal Supervisor

Madhu Sharma

Dr. Madhu Sharma
Associate Professor
School of Engineering
University of Petroleum and Energy Studies,
Dehradun Date: 04-08-2022

Internal Co-supervisor

Dr. Rupendra Kumar Pachauri
Assistant Professor
School of Engineering
University of Petroleum and Energy Studies,
Dehradun Date: 04-08-2022

CERTIFICATE

I certify that Mr. Vinay Gupta has prepared his thesis entitled “Analysis and Performance Enhancement of Solar Photo-voltaic System in Indian Climate Conditions”, for the award of PhD degree of the University of Petroleum & Energy Studies, under my guidance. He has carried out the work at the School of Engineering, University of Petroleum & Energy Studies.

External Supervisor

Dr. K N Dinesh Babu

Application Manager - APAC

Megger, Chennai

Mob: 09790920721

Email:

Dineshbabu.nagalingam@megger.com

Date:04/ August/2022

ABSTRACT

This research is focused on efficient power generation by the solar photovoltaic system. The following are the three major original contributions described in this study:

In remote PV systems, real-time monitoring systems are required to obtain all the parameters needed to estimate and optimize system performance. Many existing wired and wireless data acquisition systems (DAQ) rely on the expensive and complicated LABVIEW license software and monitor and record a limited number of parameters at a high cost. The wired data acquisition systems are only accessible close to the PV systems, and wireless data acquisition systems can monitor and record low voltage and low current at a high cost. A reliable, easy-to-use, and easily accessible data acquisition system for PV system sensing and monitoring is required for researchers and academia. These issues can be eliminated by using the developed wireless data acquisition system. In this thesis, we first described the design procedures for the suggested low-cost data acquisition system in a systematic manner, and the performance of the developed IoT enabled DAQ has been tested in harsh environmental conditions. Open-access software and cloud services were used to construct the suggested IoT enabled DAQ. Existing data acquisition systems, which are either continuously connected to the power supply or manually managed, necessitate the presence of humans to operate the system near the PV plant. The developed DAQ system can be turned on and off using a Wi-Fi enabled switch, depending on the

requirements. We can not only conserve energy but also extend the life of sensors in this way. The suggested DAQ system's information can be viewed from any location. The results of the experiments reveal that the created DAQ system is more durable, economical, trustworthy, and reliable and that it can be operated in harsh environments to observe and collect operational data from the PV system in order to study its behavior. Secondly, we investigated the performance of a 106W PV system under different weather conditions over a one-year period using an IoT enabled monitoring system. The results revealed that the exposure of 12 months of 106W PV panels under different seasons in Jaipur reduced the PV system's efficiency by 24.5% in summer, by 15.6% in winter, by 5.14% in post-monsoon and by 1.95% in monsoon. In the summer, the average air dust density was 0.35 mg/m^3, reducing efficiency by 24.5% over four months. Despite the decrease in air dust density in winter, the reduction in efficiency of the panel is high because bird droppings are more common in this period. The PV panels' maximum efficiency is reached at a panel temperature of 41 °C in the summer and 48 °C in the winter.

Finally, a novel installation method is developed that provides self-cleaning and hailstorm protection for PV modules. The performance of PV modules with the developed self-cleaning method is investigated in different climate conditions and compared to conventional ones. The goal of this research is to increase the efficiency of solar photovoltaic systems while minimising cleaning costs, less cleaning time, and ensuring effectiveness and adaptability. The performance of the developed PV technique was examined in this study by considering a variety of factors, such as cleaning performance, cost, energy consumption, land use and effectiveness during hailstorm. The experimental results show that the proposed system improved efficiency by 18.37%, 13.33%, and 6.47%, respectively, in the summer, winter, and post-monsoon seasons, when compared to the fixed PV system. The experimental results also revealed

that the energy consumption is very low when compared to the amount of energy gained. The proposed system not only cleans the PV system but also protects it from hailstorms. The findings of this study reveal that the efficiency of the PV system has improved significantly, and thus an increase in electricity production in different climate conditions.

ACKNOWLEDGEMENT

First and foremost, I want to express my heartfelt gratitude to my superiors, Dr. Madhu Sharma, Dr. Rupendra Kumar Pachauri, and Dr. K N Dinesh Babu, for their support during the entire course of my research project. Their professionalism, perspicacity, and patience have provided technical, direction, and spiritual assistance throughout my PhD research project. I am grateful for all their time, ideas, and emotional support in making my PhD fruitful and exciting experience. Even during challenging moments in my PhD pursuit, their passion and enthusiasm for research was infectious and motivating for me.

Secondly, I want to express my gratitude to the teaching and non-teaching staff of the department of Electrical Engineering, Manipal University Jaipur for their assistance in providing necessary lab space, equipment, and devices that facilitate my research project. Furthermore, I would like to appreciate the positive work environment built by the management of Manipal University Jaipur.

A very special thanks to the members of the School Research Committee at the University of Petroleum and Energy Studies, Dehradun, who gave me several advice and suggestions to make my research productive.

Finally, I would like to be thankful to my parents, wife, brothers, sisters, and loving daughters for their unwavering backing and encouragement in my pursuit of a doctorate degree.

LIST OF FIGURES

LIST OF TABLES

LIST OF ABERRATIONS

G_I	Solar Irradiance
T_A	Ambient Temperature
V_S	Battery Operating voltage
I_{Ts}	Current to battery
I_{Fs}	Current from battery
P_{Ts}	Power to Battery
S_W	Wind Speed
S_{Dir}	Wind Speed Direction
S_v	Wind Velocity
BP	Barometric Pressure
W/G speed	Wind Generator Speed
T_{MOD}	Module Temperature
Dust	Dust density
T_S	Soil Temperature
S_{HF}	Soil Heat Flux
V_{AC}	Output AC voltage of Inverter
I_{AC}	Output AC current of Inverter
V_L	Load voltage

I_L	Load current
P_L	Load power
V_u	Utility voltage
I_{TU}	Current to utility Grid
I_{FU}	Current from utility grid
P_{BU}	Backup output power
P_{Ts}	Power to utility grid
P_{Fs}	Power from utility grid
V_{BU}	Back up output voltage
V_{IR}	Voltage of the refrigerator input
W/GV	Wind Generator voltage
W/GC	Wind Generator Current
I_{SC}	Short Circuit Current
V_{OC}	Open Circuit Voltage
P_{out}	Output Power
P_{max}	Maximum Power
H	Efficiency of PV system

TABLE OF CONTENTS

CHAPTER I

INTRODUCTION

1.1 Motivation

The energy crisis and global warming are the most crucial issues confronting humanity today. Electrical energy demand has risen dramatically in recent years because of economic and population growth in both developing and industrialized countries. Because of the continued use of fossil fuels, air pollution and global warming have reached alarming levels. According to the International Energy Agency, India's energy demand will increase by 30 % by 2040 [1]. As the demand for electricity grows, pollutant levels rise. For India, overcoming this power demand in the approaching era will be a difficult task. To meet the growing demand, the country is looking for a different energy strategy that combines multiple sources of hybrid energy to support sustainability and reduce greenhouse gas emissions. Traditional energy sources are being replaced by the worldwide development of renewable energy sources. The wind, sunlight, biomass, and water are the sources of sustainable energy. They are ample and natural form of source. From the last decades, solar energy has become the most promising and fastest-growing sustainable energy source among the renewable sources to generate Electrical Energy because of free, natural, ample availability of solar radiation, with an incredible price decrease and zero operating noise [2].

India's geographical location makes it ideal for solar-powered electricity generation. India's government has implemented a policy to encourage the use of renewable energy sources, particularly solar energy. India’s current

solar power price is $0.033-0.038 per kilowatt hour (kWh), which is stable at 20–30% lower than India's existing thermal energy cost, up to half the cost of a new coal-fired power plant [3]. In terms of total renewable energy installed capacity, India currently ranks fifth in the world. A target of 175 GW of renewable energy capacity, including 100 GW from solar, has been established by the Indian government for installation by the year 2022 [4]. Semi-arid and desert regions are more suitable for large-scale solar PV plants where abundant solar radiation is available for the generation of electricity using solar energy [5]. The fundamental issue of installing solar PV energy systems in dry and hot areas is dirt deposition on panel surfaces, which, in addition to high temperatures, is the main challenge [6]. Both significantly diminish the efficiency of solar panels and thereby increase electricity costs, resulting in a lack of competitiveness of solar energy systems with plenty of fossil fuels such as natural gas [7].

The low efficiency of a photovoltaic system, which ranges from 12 to 20%, is its most serious flaw [8]. Photovoltaic system performance is influenced by a variety of elements, including the local environment, weather conditions, installation factors and dust deposition. Because of these factors, PV systems have a significant challenge during operation.

The main factor of degrading the generation of PV modules is dust accumulation on the PV module surface that causes huge energy losses during a long-term utilization. Dust accumulation for long time damages the layer of the panel, resulting in less output and a decreasing lifespan [9].

Dust storms, high ambient temperatures, excessive relative humidity and intense solar radiation are all elements that can degrade PV system productivity [8]. These issues are local and vary from one region to another [10].

The rate of dust settlement is affected by the dust's chemical characteristics, size, form, and weight and different environmental circumstances, such as humidity, ambient temperature, dust storms, pollution, wind speed, and wind direction. Surrounding activities such as human actions, vehicle movement, and volcanic discharges can also increase dust deposition [11,12,13].

In India, the monthly reduction in PV panel efficiency is greater than 70% [14]. This will have an impact on the price of energy, the payback period, and other factors. It is therefore necessary to clean the PV system on a regular basis at a low cost and with limited resources.

Apart from dust accumulation, solar PV panels are affected by hailstorms as well. The number of hailstorms has increased in the last few years, especially in India, which is dangerous for the solar PV system. A heavy hailstorm can affect the surface of the front glass and break the solar cell. When cracks occur on the front surface of glass, they reduce the solar radiation that enters the solar cell. If cracks occur in a solar cell, current is reduced, and the cell is totally isolated. Hailstorms reduce not only total electricity generation but also PV module life. Thus, hailstorm protection for solar PV panels is critical [15].

Solar radiation is the most essential element affecting the PV module's performance. Dust on the PV module prevents solar radiation from reaching the solar cell directly [16,17]. This produces an irregularity in the generation of output power and decreases the reliability of the solar PV module [18]. Thus, to raise the reliability of the PV module, reducing the chance of degradation and financial losses, suitable and economical mitigation method is required to be developed.

The loss in the output power of the modules can be avoided if the modules are cleaned periodically. Several cleaning methods and techniques have been developed to mitigate the effect of dust deposition. These methods & techniques are costly depending on the type of cleaning system.

Most existing cleaning methods require water for cleaning the PV system [19]. Water is scarce in hot and dry climates. The use of water for the cleaning of the PV system is incompatible with the aims of economic development and environmental protection. Some mechanical and autonomous cleaning methods necessitate the use of separate cleaning mechanisms, which can be very expensive and require more energy consumption [20]. Separate cleaning systems increase capital costs while running on fossil fuels. This research attempts to deal with these issues based on the true need for a cost-effective, efficient and automated technology for cleaning dirt deposition and hailstorm protection.

In remote PV systems, real-time monitoring systems are required to obtain all the parameters needed to estimate and optimize system performance. Many existing wired and wireless data acquisition systems rely on the expensive and complicated LABVIEW license software [21]. The wired DAQ systems are only accessible close to the PV systems, and wireless data acquisition systems can monitor and record the limited number of parameters at a high cost. There are only a few open-access wireless data acquisition systems that can monitor and record low voltage and low current. [22]. A reliable, easy-to-use, and easily accessible data acquisition system for PV system sensing and monitoring is required for researchers and academia.

1.2 Objectives

The following objectives have been identified to carry out the research work under the title “Analysis and Performance Enhancement of Solar Photo-voltaic System in Indian Climate Conditions” as

- To investigate the effect of dust on the performance of the PV module for all weather conditions using the IoT based data logger.

- Design and development of the novel installation method to enhance the performance of the PV module, which provides the self-clearing mechanism and protection from hailstorm.
- To compare the cost and land-use of the proposed system with conventional (fixed) ones.

1.3 Research Methodology

The performance of installed PV systems at different places depends on the atmosphere and local conditions. It is not possible to predict the performance and the production capacity of energy without a thorough investigation of the location. Field tests and scientific analysis of the data at the site are important. To examine the performance of solar panels in various seasons and Jaipur's weather conditions, we installed two polycrystalline silicon PV panels of 53 W each on the roof of Manipal University Jaipur. The solar panels were connected in parallel, and the output terminals were connected to the resistive load. The PV solar panels have an inclination of 27^{o} to the south and are located at a latitude of 26.84^{o} and longitude of 75.56^{o}.

The project started by modules installation in a fixed position with respect to the sun's position. This position has been selected to enable the modules to collect maximum sunlight during the day as much as possible. The system comprises of four Node MCU ESP8266/ESP32 modules, the DHT22/11 temperature and humidity sensor module, the INA260/219 sensor module, the LM35 temperature sensor, anemometer, and ThingSpeak. For solar radiation, an EKO MS40M pyranometer is used. All sensors were tested and calibrated properly before the system was mounted. The standard multimeter (AplabVC97) is used to calibrate the INA260/219 sensor. The values of voltage and current measured by the INA260/219 sensor and standard meter are noted at the same time. The DHT22/11 sensor and LM35 sensor have been calibrated by the HTC HD-

304 humidity and temperature meter. The DHT22/11 humidity sensor was calibrated using vapor created inside an encased container that housed both the DTH22/11 and the HTC HD-304. Both the HTC HD-304 meter and the DHT22/11 sensor's measurements are recoded at the same time. The LM35 sensor was mounted on the back side of the PV panel using a highly thermally conductive adhesive. The wind speed was measured using a commercially available INSPEED VORTEX wind speed sensor. For the calibration of the dust sensor, we employed the firm calibration curve. We tested the sensing element of the GP2Y1010AU0F sensor with various dust levels, which were confirmed to be within the sensor's limits. The results of the entire calibration were repeatable. All sensors are then connected and installed to the IoT enabled data acquisition system for gathering various parameters such as wind speed, dust level, relative humidity, ambient and PV surface temperatures, and power output. The calibration process was repeated every month.

Measurements were recorded at an interval of 5 minutes from 7.00 am to 6.00 pm for a period of one year (Sept. 2019 to Sept. 2020). The values have been collected from 7:00 am to 6:00 pm, as the solar radiation is available during these times. We calculated the operating efficiency based on average solar radiation, average output power, and the PV system's area during the time periods or seasons and compared the average efficiency of the clean and unclean PV panels.

The period of investigation is split into four seasons for better understanding, such as post-monsoon (From the middle of September to the middle of December), winter (From the middle of December to the middle of March), summer (From the middle of March to the middle of June), and monsoon (From the middle of June to the middle of September).To investigate the performance of the PV panels in different seasons, one set of 106 W PV panels, connected in parallel, was cleaned on the first day of the start of each season, whereas the second set of PV

panels was cleaned on a weekly basis and noted the values of voltage, current, power, and surface temperature of the panels, as well as environmental parameters for the entire season. On the last day of the season, the P-V and V-I curves for dirty and cleaned PV panels were drawn. Data is taken for dirty and cleaned with the same solar radiation, ambient temperature, and relative humidity.

To investigate the performance of the proposed self-cleaning PV sliding system, we incorporated three PV panels of 20 W with a sliding structure and installed them on the rooftop of Manipal University Jaipur. The solar panels were connected in parallel, and the output terminals were connected to the resistive load. Another set of three PV panels of 20 W was installed with a conventional method, i.e., fixed. The effectiveness of the proposed cleaning system is tested on photovoltaic panels in Jaipur, India, for all seasons. Both sets of three polycrystalline solar panels are mounted on a 27° south-facing structure and are located at a latitude of 26.84^{o} and longitude of 75.56 ^{o}.

The experiment was divided into two sections. In the first section, we installed one set of three PV panels without any cleaning method, and on the second set of three PV panels, we implemented the proposed cleaning technique and measured the output power of both sets for all seasons (about one year). In the second section, we used weekly and daily manual cleaning on the first set of PV panels and applied the proposed self-cleaning technique to the second PV panel set, and then recorded the output power of both sets for four weeks and one month respectively. The performance of the proposed self-cleaning PV sliding system is determined based on cleaning efficiency, energy usage, land use, and cost considerations. A data logger is used to record the performance parameters.

Measurements were recorded at an interval of 5 minutes from 7.00 am to 6.00 pm for a period of one year (Dec. 2019 to Apr. 2021). The values

have been collected from 7:00 am to 6:00 pm, as the solar radiation available during these times. We calculated the normalized efficiency for all seasons and compared the normalized efficiency of the clean and unclean PV panels. The ratio of the measured power to the power rating at STC compared to the irradiance divided by the STC irradiance gives the normalized efficiency,

$$\eta_N = \frac{P/P_{STC}}{I_m/I_{STC}} \quad \text{---------- (1.1)}$$

where P is the measured power, P_{STC} is the STC rated power, I_m is the measured irradiance, and I_{STC} is the reference irradiance (1,000 W/m^2) [23,24].

1.4 Chapter scheme

The structure of this report is as follows: The first chapter provides an overview of dirt deposition and its causes, the cleaning method, and research objectives and methodology. The second chapter discusses the literature review on the impact of the dust on the PV system and factors that influence dust deposition. We discuss the hail development and its effect on the PV system. This chapter also discusses existing cleaning techniques for PV systems and PV data acquisition systems. The developed IoT enabled data acquisition system is described in the third chapter, including their components, design, validation process and performance. The performance of a PV system in the Indian semi-arid region (Jaipur) during various seasons is described using a developed IoT enabled data acquisition system in the fourth chapter. The fifth chapter discusses the developed self-cleaning PV sliding technique, including its components, design, operation, suitability, and performance in various seasons, followed by the conclusion in chapter six.

CHAPTER 2

LITERATURE SURVEY

The first section of this chapter provides a detailed description of previous and ongoing research on the impact of dust settlement on the electrical, thermal, and optical characteristics of PV systems and the factors that influence dust deposition. Following that, the impact of a hailstorm on the PV system and existing PV cleaning techniques were presented. Finally, a brief overview of the PV system's wired and wireless data acquisition systems is provided.

A literature review has been done in the following areas:

- The impact of dust settlement on the PV system's performance
- Factors affect the dust deposition.
- Impact of the hailstorm on the PV system's performance
- Cleaning Techniques for the PV system
- Data Acquisition System for PV system

2.1 Impact of dust settlement on the PV system's performance

Dust is a tiny solid element below 250 µm in the radius. Bird droppings, plant products, pollens, sand, hair, and microfibers are also referred as dust when placed on the PV module's surface. The principal source of dust in desert regions is soil, whereas soiling can take place in many other places, as snow and other particles are included. However, there are numerous local sources of deposited dust, such as discharges from coal-based plants, vehicle movements, vehicle emissions, and human activities in large cities [25]. The suspension of dust and its deposits in the desert

and semi-arid regions is a natural phenomenon, and the amount of suspended dust is very high. The rate of dust settlement is affected by the dust's chemical characteristics, size, form, and weight and different environmental circumstances, such as humidity, ambient temperature, dust storms, pollution, wind speed, and wind direction [11-13]. Dust particles have two types of effects on the operation of the PV module: the effect of airborne dust particles and the effect of dust settlement on the PV module's front surface [26]. Both air pollution and PV module soiling may drastically reduce PV power generation and result in considerable financial losses in most regions with significant solar energy. [27].

The PV module output is governed by the solar radiation and temperature. Dust deteriorates the PV panel's performance by impacting the intensity of the solar radiation, surfaces, and partial shades [10]. Dust degrades the PV module's performances by affecting the electrical characteristics, optical characteristics and thermal characteristic of the PV module.

2.1.1 Influence on the Electrical Characteristics

El-Shobokshy and Hussein [28] performed the experiment to examine the effect of the physical characteristics of dust elements accumulated on the PV panel. They used cement, carbon, and limestone (three types of limestone elements) having an average diameter of 10, 5, 50, 60, 80 μ m. The variations in four parameters short circuit current, output power, solar radiation and fill factor with dust deposition densities are shown in Fig. 2.1.

The result has shown that for carbon particles deposition with 28g/m^2, the short circuit current more reduces compared to cement with 73g/m^2 for 10 micro m, and limestone with 125g/m^2 for 50 μ m, 168g/m^2 for 60 μm and 250g/m^2 for 80 μ m. They found that carbon particles collect more solar energy compare to cement and limestone particles. Thus, carbon particles reduce the solar light entering the solar module and also increase

the surface temperature of the PV module. They reported that small dust particles are more evenly distributed than coarser dust particles, decreasing the intervals between dust particles through which sunlight can pass. With the small amount of coarse dust deposit, there are sufficient spaces to enter sunlight to the solar module. These ways small dust particles have more scattering losses compared to that of the larger dust particles. PV module performance is influenced by dust settlement density and dust properties. The study has been done by Hassan et al. [29] in Egypt and Asl-Soleimani [30] in Tahan Iraq. They found that 66% and more than 60% output power of PV module can be decreased in six months & one year respectively.

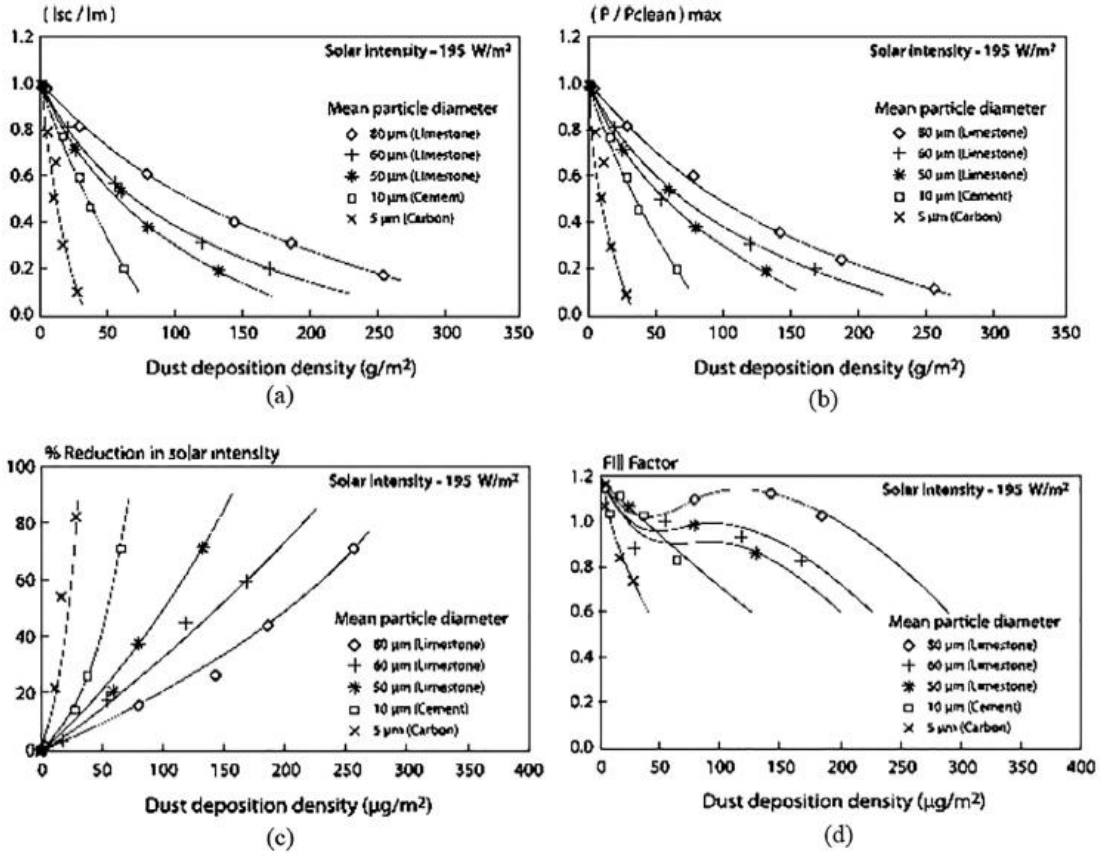

Fig. 2.1 (a) Variation in Short Circuit current with dust deposition density; (b) Variation in output power with dust deposition density; (c) Variation in solar intensity with dust deposition density; (d) Variation in fill-factor with dust deposition density [28]

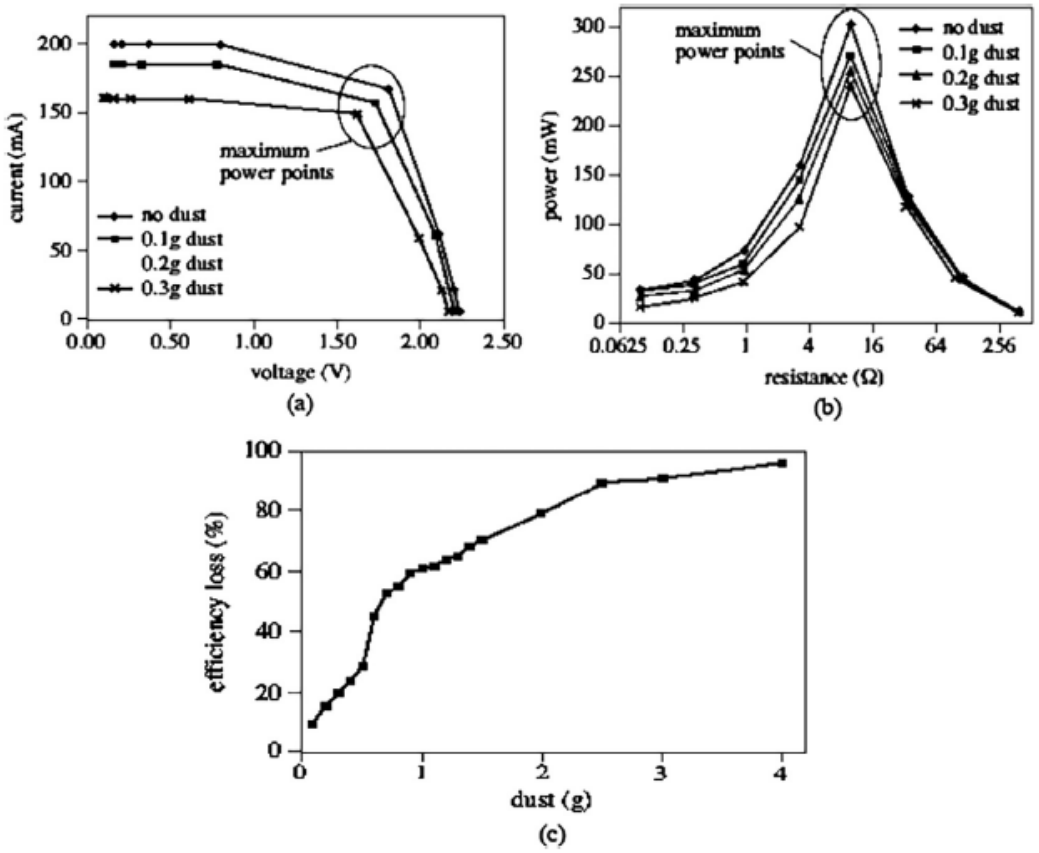

Fig.2.2 (a) I-V curves for different dust accumulation on the solar panel; (b) Power - load resistance curves for different dust accumulation; (c) Variation in efficiency loss with dust deposition [31]

To determine the effect of dust deposition, Molki et al. [31] covered the PV module with fine clay that was randomly distributed. They observed that the efficiency of PV modules declines by 10%, 16%, and 20% for 0.1 g, 0.2 g, and 0.3 g, respectively. They also concluded that there was a negative exponential connection between the amount of dust deposition and the maximum output power loss, as shown in Fig. 2.2.

Another study was done by Sulaiman et al. [32] with mud and talcum powder, shows that the power losses of the PV module reach 18% and 16.2%, respectively, and also found that the dirt accumulation on the front sheet of the PV module can decrease the 50% efficiency.

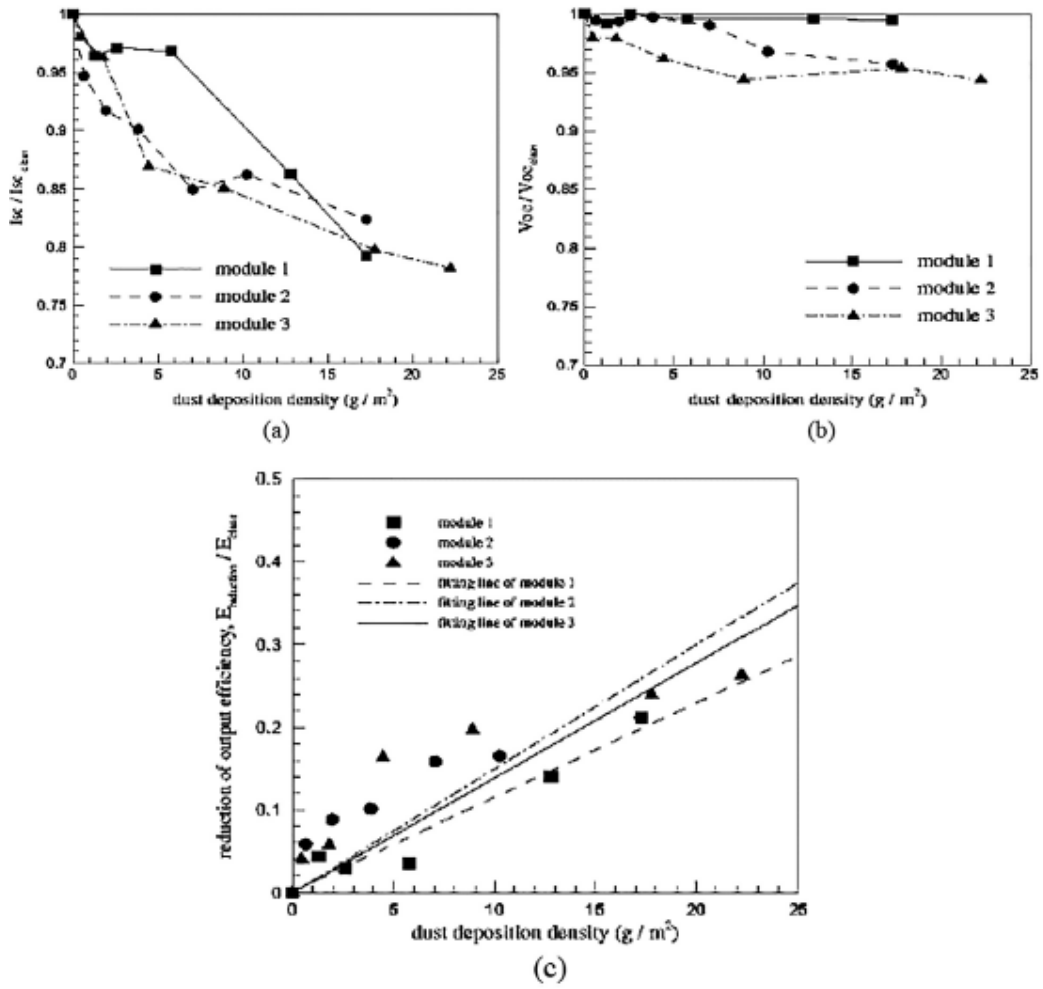

Fig. 2.3 (a) Change in short circuit current with different dust densities; (b) Change in open circuit voltage for different dust densities; (c) reduction in output efficiency with different dust density [34]

Kaldellis et al. [33] performed the experiment to examine the impact of the dust settles on the PV module. For this investigation, they used three types of dust: ash particles (less than 10µ m diameters), limestone (less than 60 µm) and red soil (less than 150 µ m), which are usually seen in urban and other environments. Fig. 2.3 shows the variation in the PV module's parameters with the dust deposition density. The drop in short circuit current 10% for monocrystalline silicon, 14% for polycrystalline and 16% for amorphous PV module with white glass and epoxy front sheets for a dust deposition of $10g/m^2$ are recorded by Jiang.et al. [34].

The average daily reduction in energy because of the dust settles on PV module for one year is approximate 4.4%; it may be increased to 20% in case of without rainfall for a long time [35]. Adinoyi et al. [36] stated that after the period of six months of exposure in Dhahran, KSA, reduction in output power was 50 %.

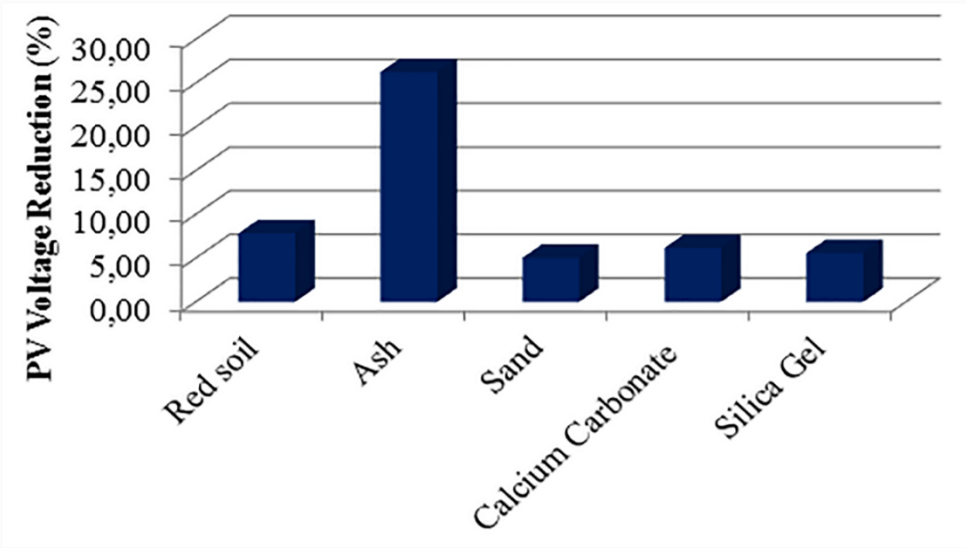

Fig. 2.4 PV output voltage reduction in percent owing to various dust particles [37]

Kazem et al. [37] studied the impact of ash, sand, silica, red soil and calcium carbonate dust elements on the PV module. The outcomes, shown in Fig. 2.4, demonstrate that the ash is the maximum influencing dirty element on the PV module voltage. The maximum loss in PV voltage (25%) is noted when the ash is gathered on the front sheet of the PV module. Rajput and Sudhakar [38] conducted an experimental study on the influence of dust settlement on the surface of PV modules and provided data on electrical performance. They conclude that the electrical characteristics of the solar panel are sensitive to the dust deposition rate.

Weber et al. [39] investigated the impact of dust in Mexico City. He observed that the dust settlement rate on flat surfaces fluctuated in the

vicinity of 24 and 102 $gm^{-2}d^{-1}$. Following 60 days of dust settlement on the PV modules without precipitation, the performance ratio is lessened by around 15%. But the yearly decline of generation because of the dust accumulation is low. Abhishek et al. [40] performed the indoor and outdoor experiments to determine the impact of dust settlement. On account of the outside test, the power loss because of $1.4g/m^2$ dust thickness was 5-6% of the greatest influence yield, though, on account of the indoor recreation setup where the dust thickness was 7.155 g/m^2, power loss was 45-55% of the most extreme conceivable influence yield. The study done by Mejia et al. [41] observed that the variations in the efficiency of an extensive PV business site (86.4 kWdc) from 7.2% to 5.6% amid a 108-day waterless period in the late spring because of the impact of dust. Ketjoy et al. [42] recorded the decrease in yield energy for the amorphous silicon PV module are 3.50 % with 260 mg dust and 7.28% with 425mg dust accumulation is, for monocrystalline silicon energy losses are 2.96 % with 260 mg tidy and 5.79 % 425 mg dust and for multi-crystalline silicon energy losses are 2.83% with 260 mg dust and 6.03% 427mg dust. They also gave the mathematical connection between the dust deposition and the PV module's output power. Klugmann et al. [43] conducted the experiment in Poland and observed that the average module efficiency drop is near to 25.5%/µm for naturally settled dust layer. The optimum everyday loss in efficiency in northern Poland for the 37° tilted silicon crystalline PV module was 0.8%. Chaichan et al. [44] completed an analysis to calculate the impact of air contamination and dust on the PV module and found that, in comparison to the perfect PV module, exposing the PV module to the outside environment for two months without cleaning reduced the yield energy to roughly 12%, while a normally cleaned PV module lost around 8% of its energy. Kumar and Sudhakar [45] clarified yearly execution in terms of power output losses

and performance ratio. They contrasted the consequences of PV system and the PV-SYST and PV-GIS programming apparatuses.

Dastoori et al. [46] investigated the influence of deposit dust element charge on PV module performance. The results indicate that dust settlement on the PV module relies upon the tilt angle as well as mainly relies upon the charge intensity of the dust.

Saidan et al. [10] researched the impact of dust on PV module execution in Bagdad City, Iraq. They observed that there was a decrease in both the short circuit current (I_{sc}) and the yield energy because of the dust deposition. The mean debasement rates of the efficiencies of the PV modules are 6.24%, 11.8% and 18.74% for the introduction times of one day, one week and one month individually. The energy production efficiency of panels decreases as dust deposition increases [47].

Abderrezel et al. [48] performed the experiment to analyze the impact of the dust settlement on the PV module in the form of electrical, optical and thermal characteristics. They observed that solar light is diffused for the uniform distribution of dust particles and in the case of randomly distributed dust, shadows are detected, which adds to the hotspot phenomenon. Recorded total losses in output power are from 10% to 16% when the dirt elements are settled on the bottommost edge of the PV module. The hot spot will be created on the PV module due to the overheating subjected to nature of dust and dust deposition. The temperature of the module is increased by dust particles such as "ash" and "soil". But for salt dust, the temperature of the dirty PV panel reduces.

Gholami et al. [49] carried out the experiment in Tehram, Iran to determine the influence of dust settlement on the PV module performance. The results revealed that after 70 days without rain, a 21.47% decline in the output power of PV module because of 6.0986 (g/m^2) dust settlement on the PV module.

The impact of carbon particles on PV performance is the largest. [50]. Natural dust deposition reduces PV module energy generation significantly [51]. According to another study, dust accumulation resulted in yield losses of 78.3%, 77%, and 70% for amorphous Si, cadmium telluride, and polycrystalline Si modules, and efficiency declines of 78%, 77%, and 71% for amorphous Si, cadmium telluride, and polycrystalline Si modules, respectively [52]. As indicated in Table 2.1, dust impacts on the electrical properties of PV modules have been observed in some studies.

Table 2.1 Summary of selected reported dust effects on Electrical parameters of PV module.

Author	Year	Location	Climate	Front Surface	Tilt angle (°)	Duration	Electrical Parameters	Max. Reduction (%)
Magg [53]	1977	Berkeley Springs,USA	Mild	Polycarbonate1 Polycarbonate1 Silicone	45	1 year	I_{SC}	10 12 7
Sayigh et al [54]	1979	Riyadh, Saudi Arabia	Desert	Polyethylene	25	I month	η	25
Nimmo and Said [55]	1979	Dhahran, Saudi Arabia	Urban	Glass	26	2 months	P_{out}	15
Hoffman and Maag [56]	1980	Cleveland OH	Suburban	Glass Silicon Rubber Silicon hard coat	40	83 days	I_{SC}	6 8 23
Khoshaim et al. [57]	1984	Riyadh, Saudi Arabia	Desert	Glass	Sun Tracker	30 months	I_{SC}	35
El-Shobokshy et al. [58]	1985	Riyadh, Saudi Arabia	Desert	Glass	Sun Tracker	1 month	I_{SC} P_{out} η	28.6 30.6 55
Al-Busairi & Al-Kandari [59]	1987	Kuwait	Desert	Glass	30	14 month	P_{out}	55
Salim et al [60]	1988	Riyadh, Saudi Arabia	Desert	Glass	24.6	1 year	η	28.6
Bajpai & Gupta [61]	1988	Sokoto, Nigeria	Semiarid	Glass	12.5	4 months	P_{max}	60
Ryan et. al [62]	1989	Eugene,OR	Urban	Glass	45	6 years	I_{SC}	8.4

Author	Year	Location	Climate	Front Surface	Tilt angle (°)	Duration	Electrical Parameters	Max. Reduction (%)
Said [63]	1990	Dhahran, Saudi Arabia	Urban	Glass	26	6 months	η	60
Yahya ans Sambo [64]	1991	Sokoto, Nigeria	Semiarid	Glass	13 0	2 weeks	I_{SC}	4.7 6
Pande [65]	1992	Isa Town, Bahrain	Urban	Glass	4-48	1 year	I_{SC}	2-17
Backer et al [66]	1997	Cologne, Germany	Urban	Glass	20	5 years	P_{out}	24
Townsend and Hutchinson [67]	2000	Davis, USA	Suburban	Glass	18.4	2 years	Isc	20
Asl-Soleimani [68]	2001	Tehran, Iran	Urban	Glass	45	8 days	P_{out}	43
Pang et al [69]	2006	Hong Kong, China	Urban	Glass	0	3 months	η	16.1
Boykin [70]	2011	Arava Valley, Isarel	Desert	Glass	30	2 weeks	η	8.7
Cano [71]	2011	Mesa,AZ,USA	Desert	Glass	23 33	3 months	I_{SC}	3.75 3.4
Ibrahim [72]	2011	Arar,Saudi Arabia	Urban	Glass	N/A	10 days	I_{SC} V_{OC}	27.8 8.6
Pavan et al [73]	2011	Puglia,Italy	Rural	Glass	25	8 weeks	P_{out}	6.9

Author	Year	Location	Climate	Front Surface	Tilt angle (°)	Duration	Electrical Parameters	Max. Reduction (%)
Rahman et al [74]	2012	Dhaka, Bangladesh	Urban	Glass	23.5	1 month	Isc P_{out}	33 34
Liqun et al [75]	2012	Taiyuan. China	Urban	Glass	0 45	2 weeks	P_{out}	32.6 18.2
Kalogirou et al [76]	2013	Limassol, Cyprus	Urban	Glass Tedlar	31	10 weeks	P_{out}	8 15
Adinoyi and said [36]	2013	Dhahran, Saudi Arabia	Desert	Glass	26	8 months	P_{max}	49
Piliougine et al [77]	2013	Malaga, Spain	Hot summer Mediterranean	Glass	21	10 months	I_{SC}	12.5
N.Ketjoy & M Konyu [79]	2014	Thailand	Rural	Glass	N/A	60 days	P_{out}	7.28
F. Mejia et al. [78]	2014	Santa calra,USA	Urban	Glass	16.4	108 days	η	7.2
Sulaiman et al [80]	2015	Kuala Lumpur, Malaysia	Rural	Glass	N/A	Hourly Daily Weekly Monthly	P_{out}	0.05 0.5 1.1 1.5
Dastoori et al [46]	2016	Dundee, UK	Lab	Glass	N/A	N/A	V_{out}	Reduce

Author	Year	Location	Climate	Front Surface	Tilt angle (°)	Duration	Electrical Parameters	Max. Reduction (%)
Kazem et al [81]	2016	Oman, Iraq	Desert	Glass	N/A	3 months	P_{out}	35
Saidan [10]	2016	Bagdad, Iraq	Desert	Glass	N/A	Daily Weekly Monthly	η	6.24 11.8 18.74
Abderrezek et al [48]	2017	Algeria	Lab	Glass	N/A	N/A	P_{max}	50
Guan et al [82]	2017	Chang'an, Xi,an, China	Rural	Glass	35	N/A	P_{out}	20.62
Golami [49]	2018	Tehran, Iran	Semiarid	Glass	N/A	70 Days	P_{out}	21.47

2.1.2 Influence on the Optical Characteristics

There are several studies related to transmittance loss caused by dust deposition in the form of scattering, absorption, and reflection of sunlight, which depends on the wavelength of solar radiation. Garg et al. [83] et al. carried out the experiment to calculate the impact of dust settlement on the transmittance of glass and plastic plates, utilized as a translucent cover of the flat-plate collector. They concluded that the dirt correction factor for the glass plates, tilted at 45°, is 0.92. Plastic plates have higher dirt correction factor because of their higher electrostatic behavior. Nahar and Gupta [84] examined the impact of dust settlement on the transmittance of the sun based irradiance on the glass surfaces presented to the outside condition in Thar desert, India. They revealed that the maximum transmittance reduction for the daily cleaned samples was 1.87% for a 90° tilt angle, 4.62% for a 45° tilt angle and 6.28% for a 0° tilt angle in the month of May due to dust storms. The maximum transmittance reduction of weekly cleaned samples is 5.67% for a 90° tilt angle, 13.81% for a 45° tilt angle and 19.17% for a 0° tilt angle in the duration of April-May. Hasan and Sayigh [85] performed the experiment to find the transmission loss due to the dust deposition with two wavelengths: 540 nm and 720 nm. They noticed that as the dust settlement density increased, light transmittance reduced at all detectable wavelengths. Al-Hasan et al. [86] examined the impact of dust deposition on light transmittance at the PV module with the wavelength range 190 to 900 nm. The transmittance of unpolluted and polluted PV modules was measured using a spectrophotometer at various dust deposition densities. The test information as shown in Fig. 2.5 (a), (b) & (c), demonstrating the variety of reflectance as a component of the wavelength can likewise be concluded in the type of transmission losses. They conclude that the transmittance was reduced as the dust deposition densities on the glass

sample increased with no wavelength dependence. They also found that the light transmittance reduced as the orientation angle improved.

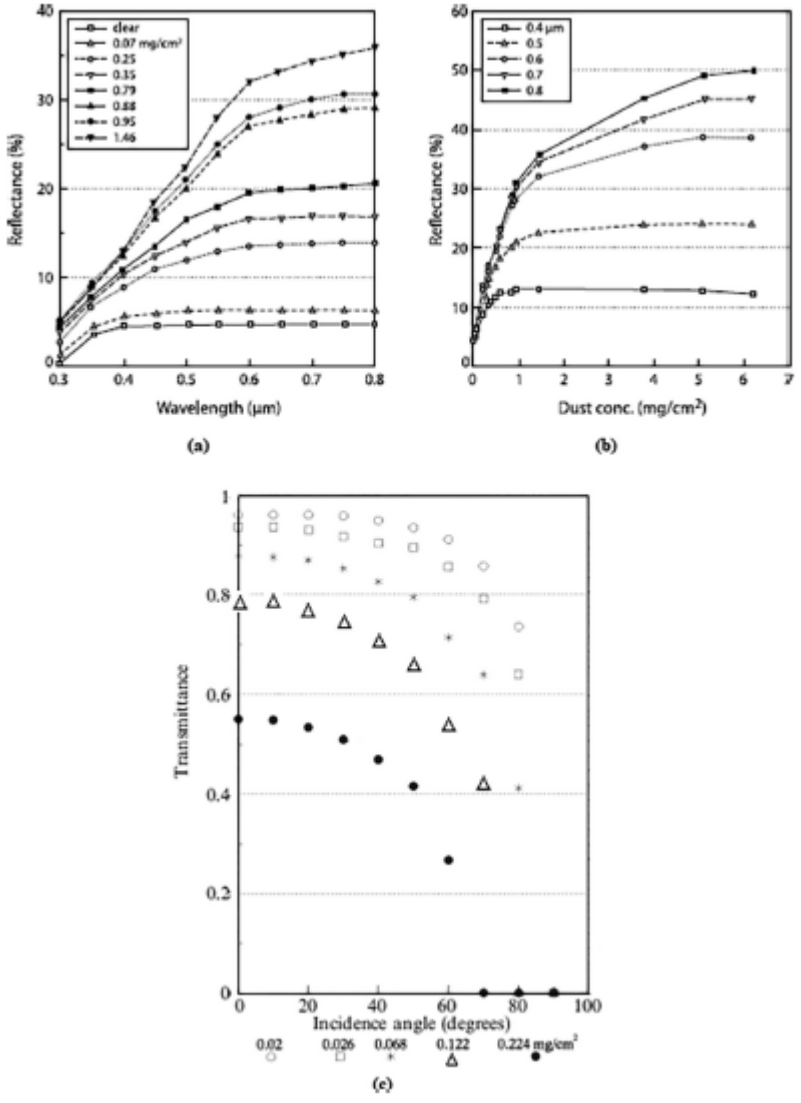

Fig. 2.5 (a) Variation in dusty glass reflectance with wavelengths; (b)Variation in dirty glass reflectance with dust densities; (c) Variation in transmittance with incidence angles for different amounts of sand dust particles [86]

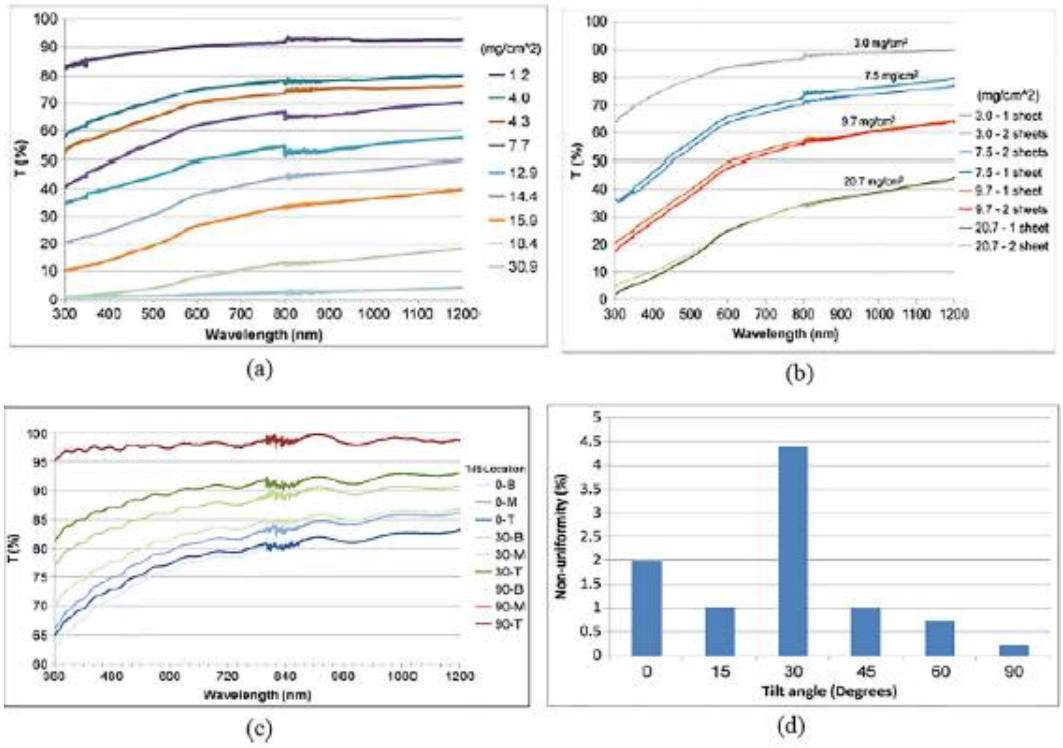

Fig. 2.6 (a) Spectral transmittance characteristics for various dust density; (b) Variation in transmittance with one and two dirty sheets of glass; (c) Spectral transmittance characteristics for different tilted panels (T = Top, B= Bottom and M= Middle). (d) Non-uniformity transmittance at different tilt angles (%) [87]

Qasem et al. [87] performed the experiments to determine the variation in transmittance between the topmost, central and bottommost of the samples collected at various inclination angles due to the dust deposition. It has been noted that the most pessimistic scenario was realized at a tilt point of 30^{o} with a non-consistency dust deposit of 4.4% on the examination with 0.2% for the 90^{o} tilt angle. The gathered information demonstrated a lessening in transmittance at wavelengths < 570 nm. It is also reported that at shorter wavelengths (300nm–570nm), transmission losses are considerable compared to those at longer wavelengths, as shown in Fig. 2.6. When the dimension of the dust element is equal to the light's wavelength, scattering losses rise. In the situation when size of dust

elements is less, every element carries on as a solitary dispersing object. At the point when the mass thickness rises to shape the thick layer, it behaves as numerous disseminated objects. In this situation, optical modelling can be utilized for analysing the transmission misfortunes.

Monto et al. [88] stated that the shading because of dust particles is divided into two types; soft shading refers to atmospheric concentrated dust, and hard shading refers to dust that settles on the PV module. Soft shading occurs when the atmospheric dust concentration is high or some dust elements settle on the PV module. The effect of soft shading is to reduce the PV module's current and keep the voltage constant. Hardening shading occurs when the heavy dust deposit and blocks the light to enter into the PV module. The impact of hard shading is proportional to the number of PV module shaded cells. If a few cells are shaded and other cells get solar light, there will be some yield energy with diminished yield voltage of the PV module. Some dust elements such as bird droppings, feathers, grass, leaves and dirt marks block the few cells of the PV module. In this condition, blocked cells behave like a resistance. Due to these reasons, blocked cells heat up and create the hot spot that threatens the PV module.

Gholami et al. [89] examined the parameters influencing the dust deposition and their effect on the transmission coefficient of the glass surface of the PV module for solar use. It has been observed that the transmission coefficient can be reduced by up to 25% by the dirt settlement on PV module after a period of 70-day. They also presented a correlation between dust density and transmission coefficient lost, Eq. (2.1).

$$\Delta\tau(\%) = -0.001335\rho_d^6 + 0.04398\rho_d^5 - 0.5427\rho_d^4 + 3.05\rho_d^3 - 7.703\rho_d^2 + 11.19\rho_d - 2.25 \quad \text{---------(2.1)}$$

Where $\Delta\tau$ (%) = Elimination in the Transmission coefficient,

ρ_d (g/m^2) = Surface density of dust settlement on the Surface

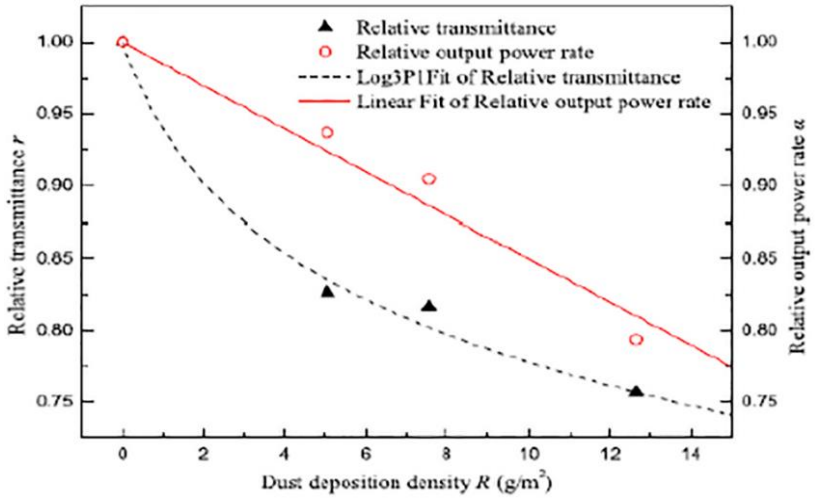

Fig. 2.7 Variation in comparative transmittance and the comparative output power rate with different dust density [82]

Gaun et al. [82] studied the effect of dust settlement on the PV module's temperature, the transmittance, and the yield energy of the PV module. The results revealed that dust statement not just lessened the transmittance of the top glass surface of PV modules, but in addition, decreased the module temperature, in this manner affecting the energy yield of the PV module. Additionally, the outcomes demonstrated that the relative transmission of a PV module declined by 20% in just 8 days because of dust settlement. The experiment results also revealed that the drop in the rate of generating power of a PV module because of the dust settlement was less as compared to the drop in the relative transmittance because, at the same time, due to dust deposition, module temperature decreases, which increases the efficiency of PV module. Fig. 2.7 shows the variation in comparative transmittance and the comparative rate of generating power with different dust densities. As indicated in Table 2.2, dust impacts on PV cover transmittance have been observed in some studies.

Table 2.2 Summary of selected reported dust effects on PV covers transmittance.

Author	Year	Location	Climate	Front surface	Tilt angle (°)	Duration	Type of PV device	Maximum Transmittance Loss (%)
Garg [83]	1974	Roorkee, India	Continental	Glass	60 40 20	30 days	Heat collector	10 16.7 50
Hoffman and Maag [90]	1980	Pasadena, USA	Continental	Polyvinyl, Glass, Acrylic, Silicone, soda lime, borosilicate, proprietary	45	150 Days	PV Module	37
Sayigh et al.[91]	1985	Kuwait	Desert	Glass	30	27 Days	Sheet	50
Nahar and Gupta [84]	1990	Thar, desert, India	Desert	Glass Acrylic PVC	45	20 Months	Sheet	14.1 18.9 44.5
Mastekbayeva and Kumar [92]	2000	Bangkok, Thailand	Urban	LDPE Plastic	15	30 Days	Air heater	24.2
Hegazy[93]	2001	Minia, Egypt	Urban	Glass	20 40 60	30 Days	PV Module	21 16 11
El-Nashar [94]	2003	Abu Dhabi, UAE	Desert	Glass	N/A	One year	Thermal collector	33.7

Author	Year	Location	Climate	Front surface	Tilt angle (°)	Duration	Type of PV device	Maximum Transmittance Loss (%)
El-Nashar [95]	2009	Abu Dhabi, UAE	Desert	Glass	24	One Month	PV Module	18
Apples et al. [96]	2012	Leuven, Belgium	Urban	Glass	60	4 Months	PV Module	3
Hee et al.[97]	2012	Singapore	Urban	Glass	0-90	33 Days	Sheet	10
Ghazi et al. [98]	2013	Brighton, UK	Urban	Glass	0	3 Weeks	Sheet	5
Qasem et al. [99]	2014	Kuwait	Desert	Glass	30	30 days	PV Module	2.8/10mg/m^2
Semaoui et al. [100]	2015	Algiea	Arid	Glass	32	One year	PV Module	8/day
Helen et al. [101]	2016	Kalkbult, SA	Semiarid	Glass			PV Module	0.11/10mg/m^2
Gholami et al.[89]	2017	Isfahan, Iran	Urban	Glass	15	70 Days	Sheet	24.83
Guan et al. [82]	2017	Xi’an, china	Continental	Glass	30	8 Days	PV Module	24.32

2.1.3 Influence on the Thermal Characteristic

Monto et al. [88] stated that some dust elements such as bird droppings, feathers, grass, leaves and dirt marks block the few cells of the PV module. In this condition, blocked cells behave like a resistance. Due to these reasons, blocked cells heat up and create the hot spot that threatens the PV module.

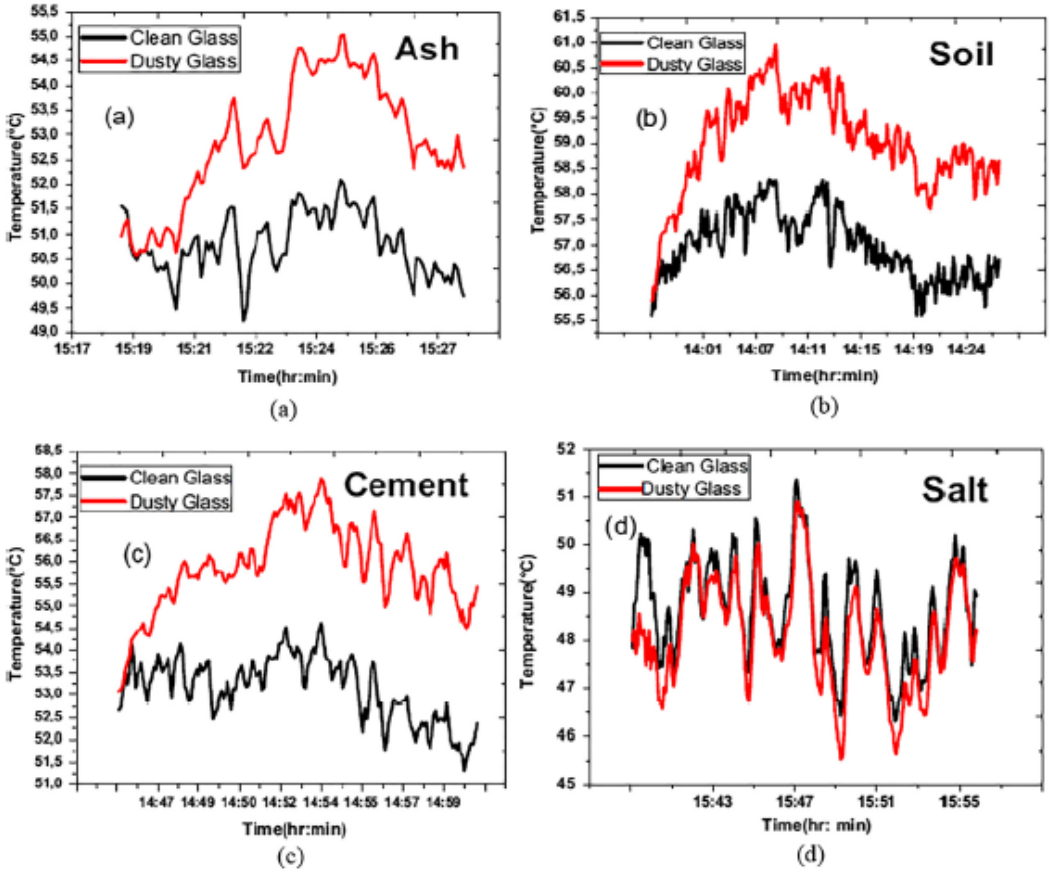

Fig. 2.8 Thermal effect of the dust on the glass, relative study (unsoiled and soiled glass) with: (a) Ash, (b) Soil, (c) Cement, (d) Salt. [48]

Abderrezel et al. [48] observed that randomly distributed dust adds to the hotspot, which increases the temperature. The temperature of the module is increased by dust particles such as "ash" and "soil", as shown in Fig.2.8. But for salt dust, the temperature of the dusty PV panel reduces.

Dorobantu et al. [102] examined the effect of surface impurities on the temperature of the PV module. It was observed that any dust deposit on the PV module leads to a heating of the affected region compared with the rest of the PV module. In the image taken with the thermos vision camera as shown in Fig. 2.9 (a) & (b), the dirty surface has 10 ºC more temperature as compared with the clean surface of PV.

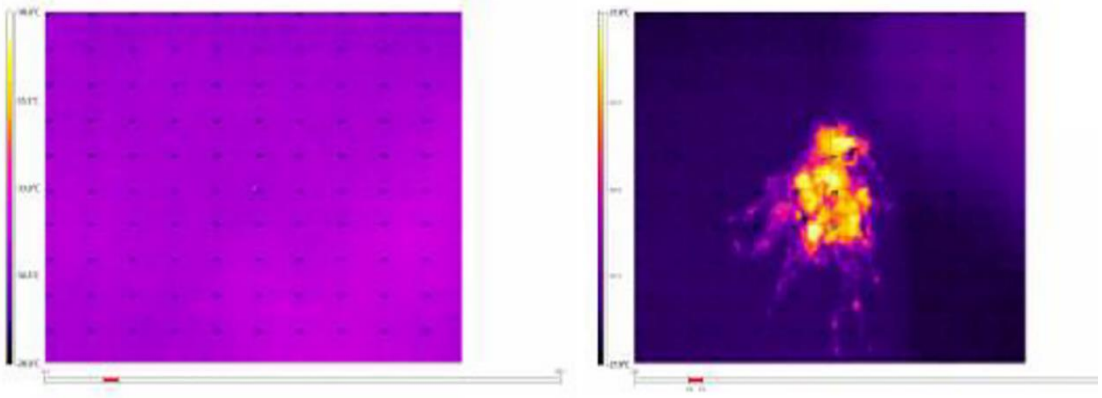

(a) (b)

Fig. 2.9 (a) Thermal Image of Clean PV Module; (b) Thermal Image of Dusty PV Module [102]

2.2 Factors affecting the dust deposition

The dust deposition density and the quality of dust differ from location to location around the world. The density of dust deposition is influenced by various of factors as shown in Fig. 2.10, but mainly by the ecological factors such as wind speed, wind direction, temperature, moisture, dust properties, humidity, rainfall, and installation factors such as incline angle, orientation, height, and top surface of PV module and location of the installation site.

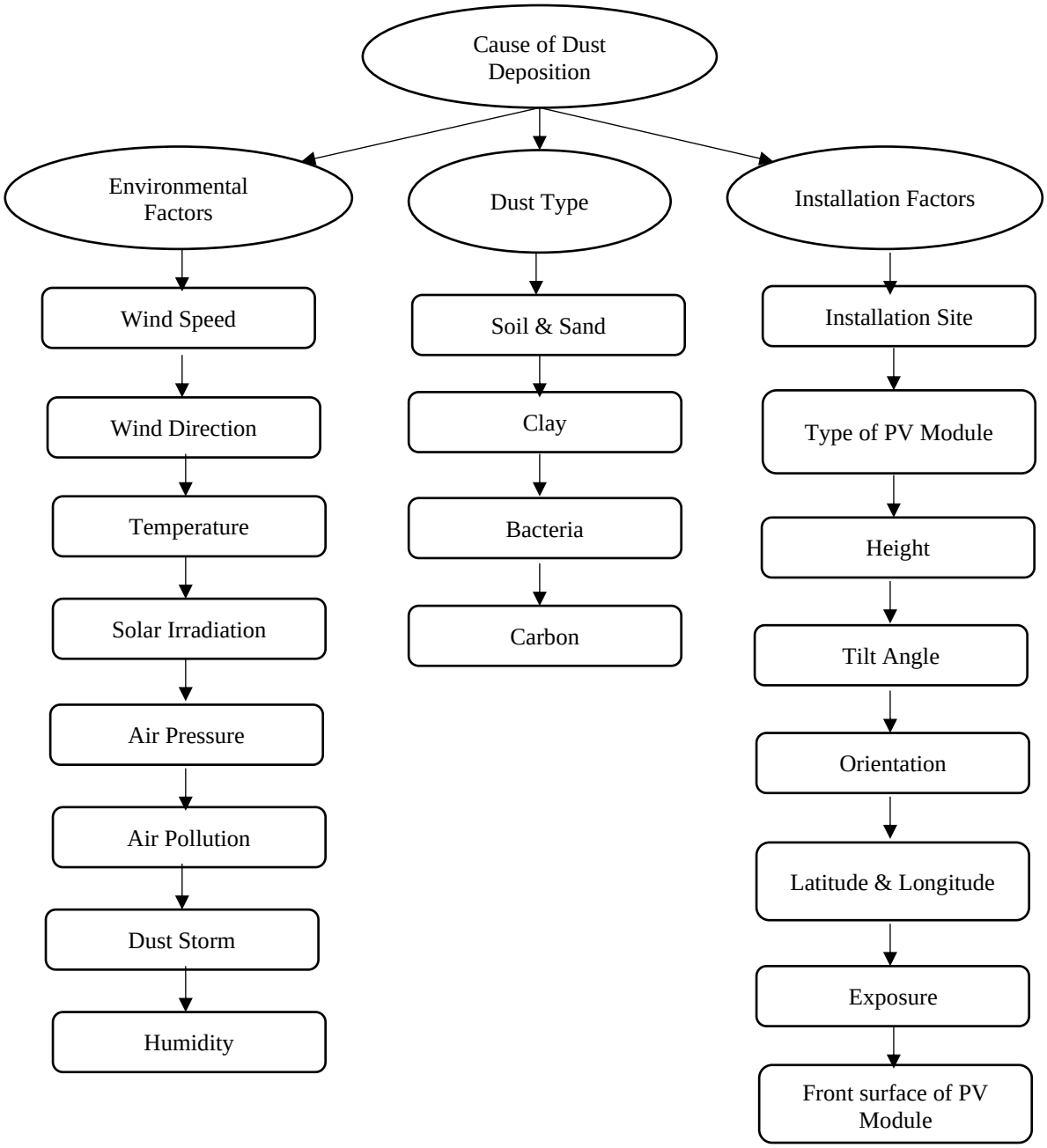

Fig.2.10 Factors affecting the dust deposition on the PV module

2.2.1 Environmental Factors

2.2.1.1 Wind velocity and Wind direction

The wind has a significant influence on the dust deposition and removal from the solar PV module's surface. Dust is carried by the wind. Slow breezes can deposit dust on the PV module, whereas strong wind can remove it. The airborne dust density is determined by the concentration of airborne dust carried by air as well as its speed. With a high concentration of airborne dust, the rate of dust deposition will be higher, and vice versa [104].

The settlement of dust on PV module surfaces is influenced by the wind in two ways [103]. The wind, on the one hand, removes some of the pollution from the photovoltaic surface (for wind-facing surfaces) [105]. When the PV surface does not face the wind, more pollution is collected, and more dust is produced [49]. Some particles deposited on a photovoltaic cell are removed by the wind. The direction and speed of the wind are governed by the circumstances [106]. The dust particle size and the microscopic structure of the deposition layer also depend upon [107]. According to studies, even when wind speeds exceed 50m/s, it is impossible to clean the fine dust particles that accumulate on a horizontally installed PV panel [6].

Goossens et al. [103,104,108] performed experiments related to wind tunnel simulations to find out the impact of the wind velocity and direction on the settlement mechanics of airborne dust on PV collectors. Their results have shown that the impact of the wind direction on the dust settled and distribution is more related to the impact of the wind speed. Clarke et al. discovered that the rise in average monthly wind velocity was mostly responsible for the increase in dust settlement and that the minimum wind speed for lifting dust in Libya was 6.5 m/s [109]. According to Elminir et al., dust deposition is affected by wind direction

and surface orientation [110]. According to Kohil et al., dust elements from the surface are charged as a result of wind attrition. These dust particles land on a surface that has already been charged by previously charged dust particles. The coulomb force is activated, and depending on the polarity of dust elements and the distribution of surface charge, it can be either attractive or repelling. The attracting force will enhance the density of the dust deposition, whereas particles of the same polarity will be re-suspended in the air [111]. The efficacy of dust element removal is dependent on particle size and wind velocity, according to Schneider et al. [112], as shown in Fig. 2.11.

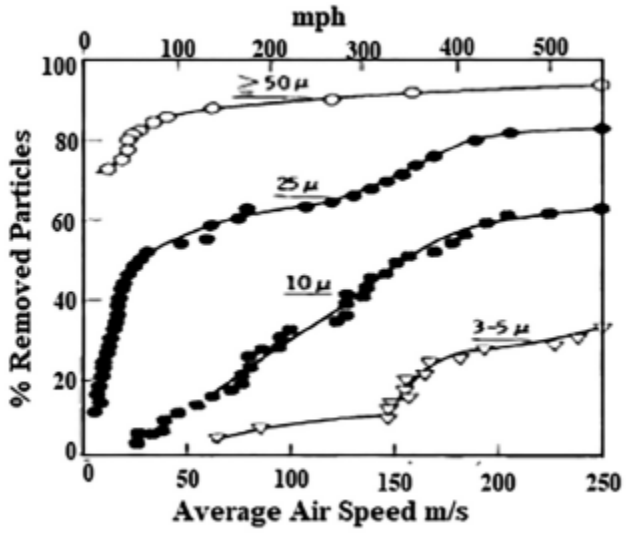

Fig.2.11 Effectiveness of wind removal of dust particles [112]

2.2.1.2 Temperature and Moisture

The dust deposition process is influenced by temperature variations in two ways: ambient temperature and the temperature of the PV module's front surface. When the ambient temperature is high, the moisture in the area around the installation site decreases, and the local climate becomes dry. The wind can readily pick up dust [113]. In desert and semi-arid environments with high temperatures, the rate of dust deposition remains

high. When the temperature is low near the sea, high vapour will condense into water droplets on the PV panel, causing the surface of the PV panel to become more adhesive and stickier, attracting more dust particles from the air [114,115].

Jiang et al. [34] revealed that when the temperature of the glass surface of the PV module equals the nearby air temperature, dust deposition density is the utmost as shown in Fig. 2.12. They also stated that the dust settlement densities are diminished with the increase in temperature of the PV module's surface. This is because a force known as the thermophoresis force, which is created by temperature differences between the surrounding air and the PV module's surface, influenced the dust settlement process. This force is exerted from a higher to a lower temperature zone.

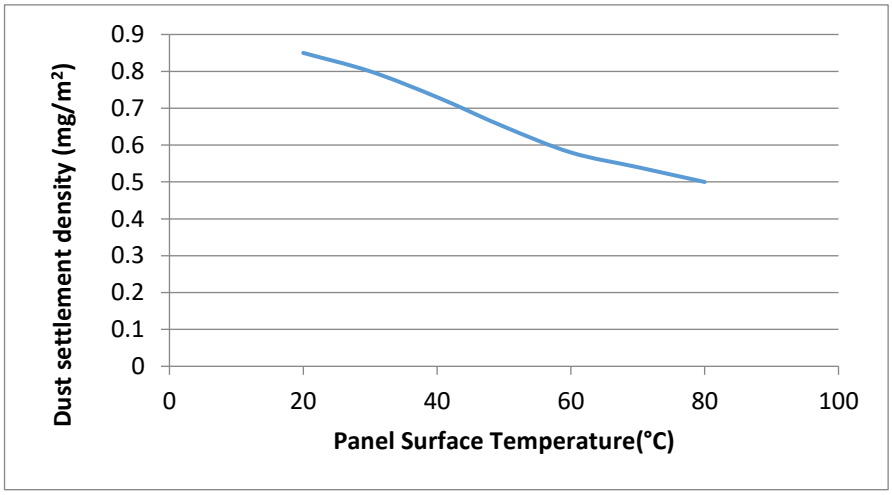

Fig.2.12 Dust settlement density under various surface temperature [34]

2.2.1.3 Humidity

Humidity has a significant impact on the adhesive force between dust elements and the PV module surface, according to Mekhilef et al. [113]. They observed that countries near the ocean have high humidity, which promotes the stickiness of dust particles on PV panels. It has also been

observed that increasing relative dampness from 40% to 80% results in an increase of about 80% in adhesion. Apart from this, high relative humidity creates the development of adhesive and reinforcing dust layers on the PV module. The bond powers of dust elements on level surfaces, mainly depend on the touching territory between dust elements and the top glass surface, so they increment with the expansion of the dust element's size. Because of the capillary forces created between the dust elements and the glass surface, humidity promotes dust element adherence [9]. Sayed et al. performed the experiment to comprehend the impact of moisture and water vapour concentration on the level of attraction forces between dust elements and a surface; a proficient bond power estimation between silica bead and silica planar surface has been completed under different humidity intensities. Fig. 2.13 demonstrates that the bonding force improves as the humidity level rises because there is condensed water in the gap between the dust element and the surface, which produces a water capillary bond between the bead and the surface. [9].

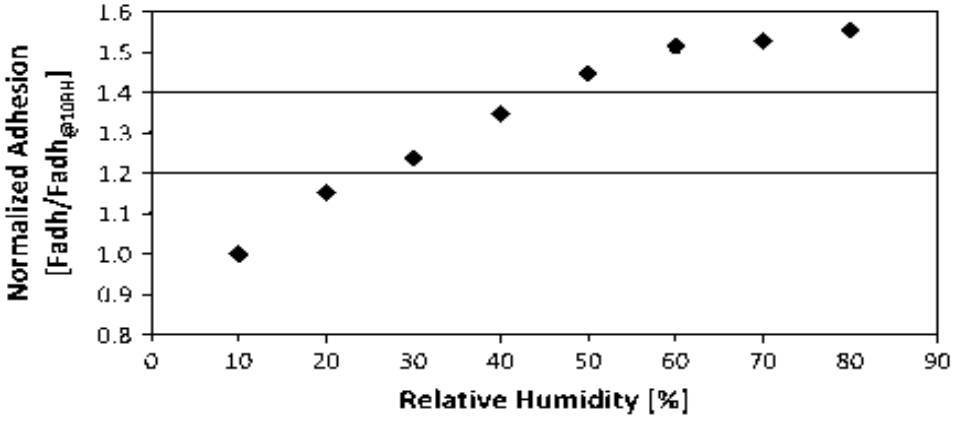

Fig 2.13 Impact of humidity on adhesion force [9]

Kim et al. [116] carried out the experiment to estimate the re-suspension rates of hydrophobic PE spheres and hydrophobic PE spheres of clean glass, CARC covered gold, and aluminium covered glass surfaces in a wind tunnel. They revealed that rates of re-suspension of dust particles

from the surface were influenced both by relative humidity and surface properties. Rates of re-suspension of hydrophilic elements on hydrophilic surfaces were more influenced by RH in comparison with those of hydrophobic elements on hydrophobic surfaces. Fig. 2.14 shows that the re-suspension rates of glass depend on the relative humidity.

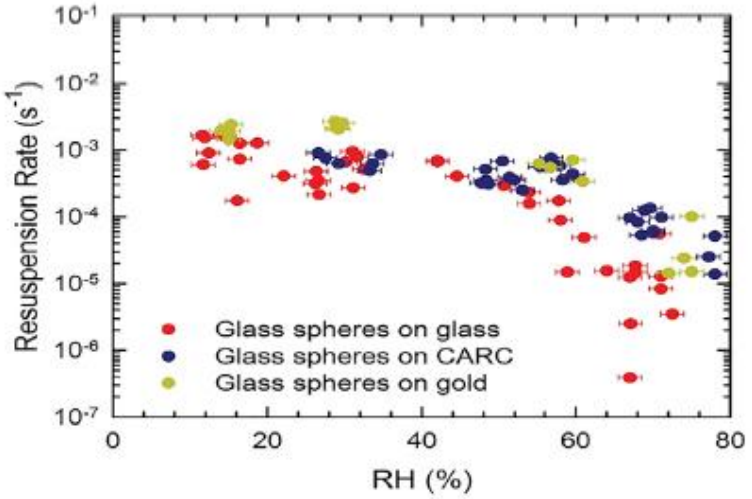

Fig.2.14 Re-suspension rates of glass depends on the relative humidity RH [116]

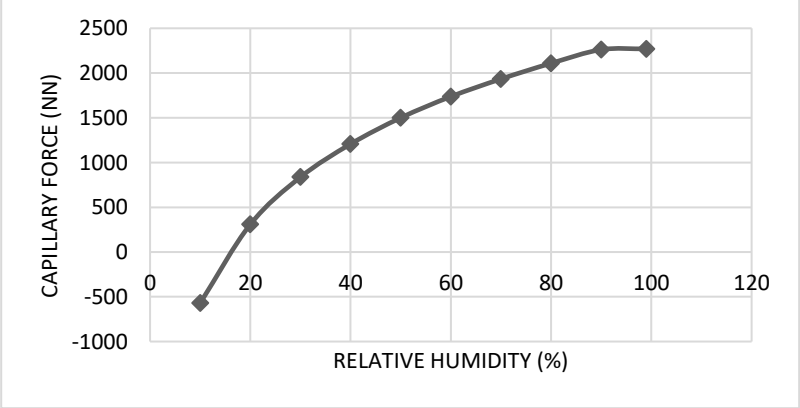

Fig.2.15 Capillary force depends on the relative humidity RH [117]

Isaifan et al. [117] performed the experimental analysis to understand the mechanism of the adhesion force between dust elements and PV surfaces. Four key bonding forces were assessed: gravitational forces, capillary,

electrostatic and van der Waal. In high relative humidity, capillary force dominates the bonding process between dust elements and PV module surfaces, accounting for approximately 98% of total forces, whereas van der Waal force controls in dry conditions. Fig.2.15 shows the relation between relative humidity and capillary force. The impact of surface irregularity over the coated vs clean glass did not demonstrate a critical decline in the bonding force as estimated in the lab.

2.2.1.4 Rain falls

The rainfall significantly affects the dust deposition process. Dust deposition may be increased by light rain with a shorter duration. Water drops can collect with airborne particles in light rain, causing the module's surface to become dusty. Heavy rain can unsoil the PV module's front surface. Kimber et al. [118] investigated the impact of dusting on enormous grid-connected PV modules in California, the United States. He concluded that to unsoiled the PV module's front surface., minimum of 20 mm of rainfall is required. Bethea et al. [119] found that low rainfall encourages stronger dust adhesion to the module, resulting in dust being converted into mud. It cannot be removed easily and needs a mechanical cleaning method. Amid long dry periods in the interims between rainfalls, a rain-resistance, dust layer is developed which cannot be removed by natural cleaning [19]. Fig.2.16 shows the development of layers of dust deposition, Layer A is a rain-resistant layer that has formed as a result of the prolonged dry spell. Layer B is a dust layer that forms as a result of the light rainfall and dry climate. It can be cleaned using washing and scrubbing procedures. The loose layer, Layer C, can be washed by rain [120]. Fig. 2.17 shows the dust accumulation and precipitation from Nov. 2010 to March 2012 in the Southern Central Valley [121].

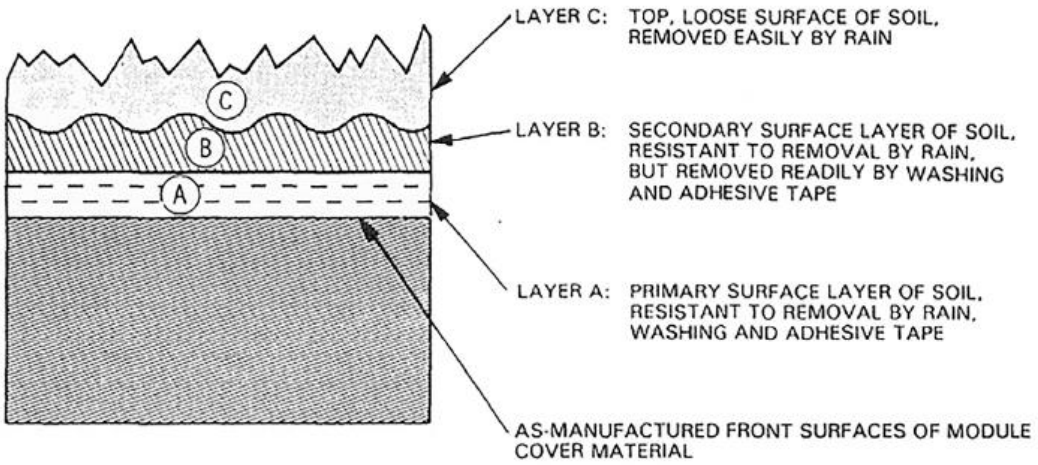

Fig. 2.16 Dust Deposition Layers [120]

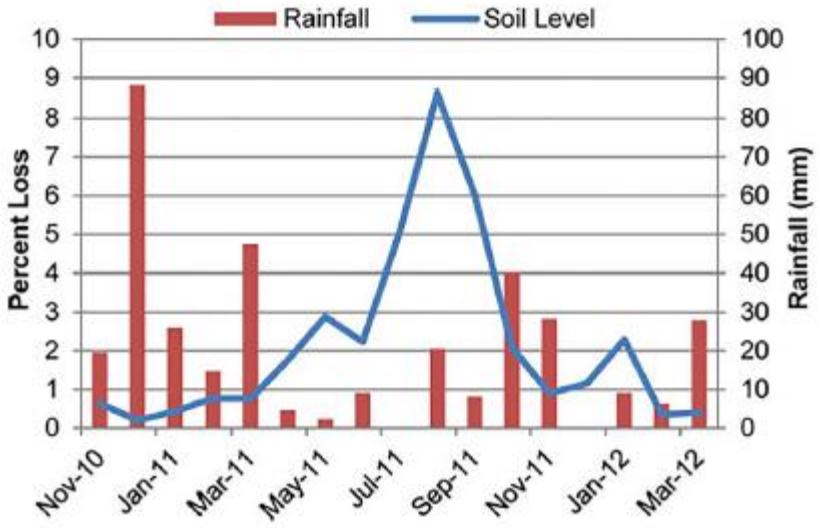

Fig. 2.17. Dust accumulation and rainfall for Southern Central valley period from Nov 2010 to March 2012 [121]

2.2.1.5 Dust Properties

The characteristics of the dust vary from location to location throughout the world. The physical and chemical properties of dust elements have a significant impact on the dust deposition process. El-shobokshy and Hussein [28] found that when compared to fine dust particles, coarser dust particles can be easily eliminated with high wind speed. They also found that due to gravity, the accumulation rate of small dust particles (less than

5 micron in diameter) was 5%, whereas the accumulation rate of large dust particles was 75%.

Large dust elements attach to smaller dust particles due to the electrostatic charges of the smaller dust particles [122]. Brown et al. [123] & Corn et al. [124] exhibited that their adhesion force improved considerably with the particle size, as shown in Fig.2.18. They additionally found that the contact region between particles and rough surface assumes a key part in the attachment between particles and surface. According to Penney et al., dipole moments in an electrical field created by contact potential differences cause each dust particle to follow a certain route [125]. The Coulomb forces between the dust particle layers generate great bonding (adhesive) forces by the dipoles. Kazmerski et al. [126–127] revealed that the grip force between particles and module glass surfaces is lower than the inter-particle grip force.

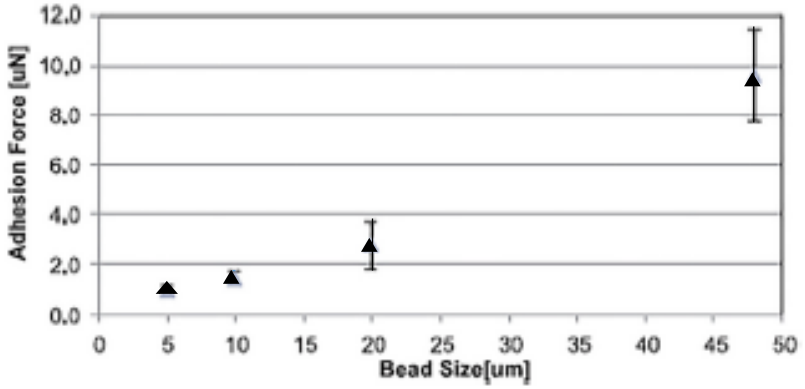

Fig.2.18 Impact of dust particle size on bonding (adhesive) force [123,33]

2.2.1.6 Bird Droppings

The dust accumulation on the PV module's surface is enhanced by bird droppings. Bird droppings not only prevent solar radiation from entering the cell but also provide an adhesive for dust particles. The influence of bird droppings on the performance of PV modules was investigated by Hammond et al. [128] & Al-Ammri et al. [129]. They found that the effect of bird droppings was more severe than the effect of dust deposition. It's not only a temporary defect, but also permanently damages the affected area of the solar cell. Fig. 2.19 illustrates the temperature distribution due to bird droppings on the PV module.

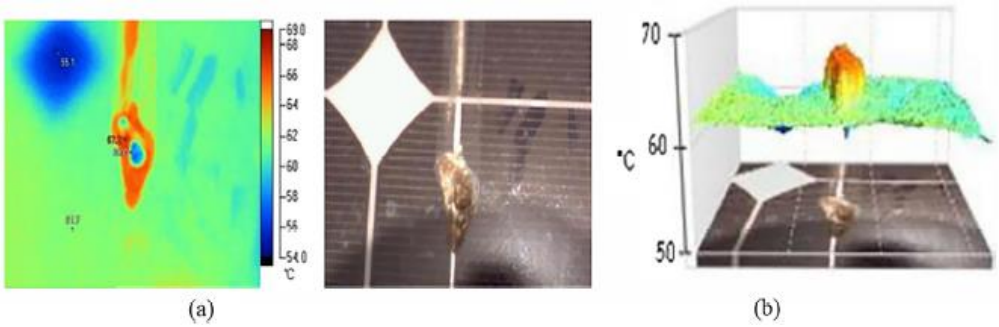

Fig.2.19 The impact of birds' dropping on the surface temperature of PV module: a -JR Visible Light, 3D image of a birds' dropping on surface of PV module, b- JR, Visible Light, 3D of the two halves of the PV module surface [129]

2.2.2 Installation Factors:

2.2.2.1 Tilt angle and Orientation

Another important component that influences the dust settlement on the PV module is the tilt angle. The rate of dust settlement is higher on the horizontal surface (tilt angle 0) than on the vertical surface (tilt angle 90) due to gravitational attraction. The enormous number of particles

deposited on the horizontal surface would be bigger than those deposited on the vertical surface [71,130-134]. Hegazy et al. [93] observed that surface dust density was higher on the high tilted PV module with small particles (less than 1 micro m.), while surface dust density was higher on the low tilted PV module with larger dust particles (mean diameter of 3 micro m.). The direction of the PV module is critical for determining the rate of dust deposition. In comparison to a PV module that is less exposed to the breeze, the PV module that faces the breeze directly will contract the most dirt deposition [11,103,135-136]. Fig. 2.20 shows the variation of dust density with tilt angle and exposure time [93]. Elminir et al. [110] related the orientations to the inclination angles. Fig. 2.21 shows the variation of dust settlement with orientation angle. With the influence of the gravitational forces, a few of the bigger dirt elements may move from the upper portion of the PV module to the lower portion of the PV module as the tilt angle increases. It has been reported that the quality of dirt deposited on the glass at various orientations with the same inclination angle was about equal. He also found that glass samples oriented NE with a 15° tilt angle deposited more dust (8.02g/m^2) than other orientations due to the impact of NE winds, which carry the discharges from the nearby cement industries. The impact of inclination is strongly linked with the amount of dirt settlement rate on the PV module. The 90° tilt angle demonstrated the minimal variety of dust deposition of 0.1 mg/cm^2 because gravity influences it and helps the procedure of dust elimination after some time. The PV module inclined at 30°, the ideal inclined angle in Kuwait in regard to sun locus, demonstrated the most noteworthy variation of dust deposition of 1.4 mg/cm^2, with the vast majority of the dust deposition towards the base of the sample PV module. The experiment was carried out by Nahar et al. [84] to assess the influence of dust collection on the transmittance of various glazing materials, e.g. glass acrylic & PVC sheet, with different tilt angles in the Thar desert. They

observed that the reduction in transmittance diminishes as the tilt angle increases because less dust settles as the tilt angle from the horizontal axis increases.

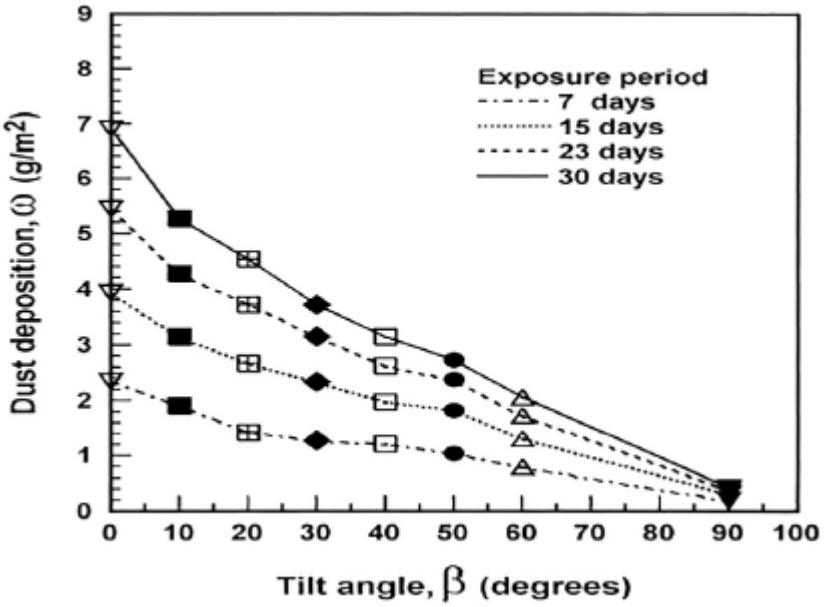

Fig.2.20 Variation of dust density with tilt angle and exposure time [93]

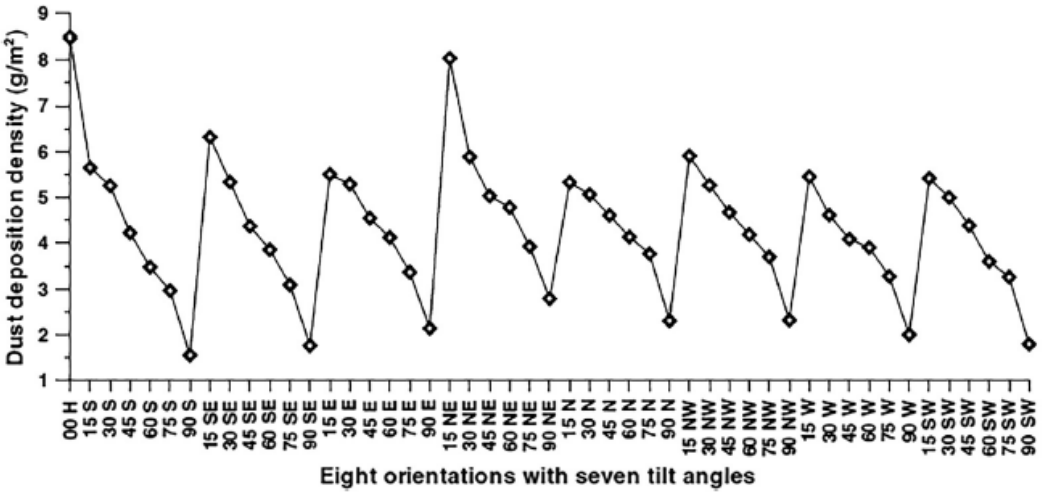

Fig.2.21 Variation of dust deposition with tilt angle [110]

Barbon et al. evaluated the energy losses caused by deviations from the installation's tilt angle and orientation in relation to the ideal position. A

photovoltaic system installed in a South orientation with deviations of up to 10° from the optimum tilt angle has a negligible effect on energy losses [137].

2.2.2.2 Height

The air-dust density decreases exponentially with altitude in a normal situation. The PV module should be mounted at a height to avoid dust deposition. Because wind speed rises with height, the influence of the wind on PV modules deployed at a higher level than the ground is more pronounced [71]. Neil et al. [138] performed the experiment in a lab environment under controlled conditions to simulate the dust deposition on the PV module. They found that dust element deposition has a non-linear effect on the height at which the elements are deposited. 2.22 shows the change in the dust density on the glass with the height from which it was accumulated. It is also observed that increasing the height decreases the dust density on the surface.

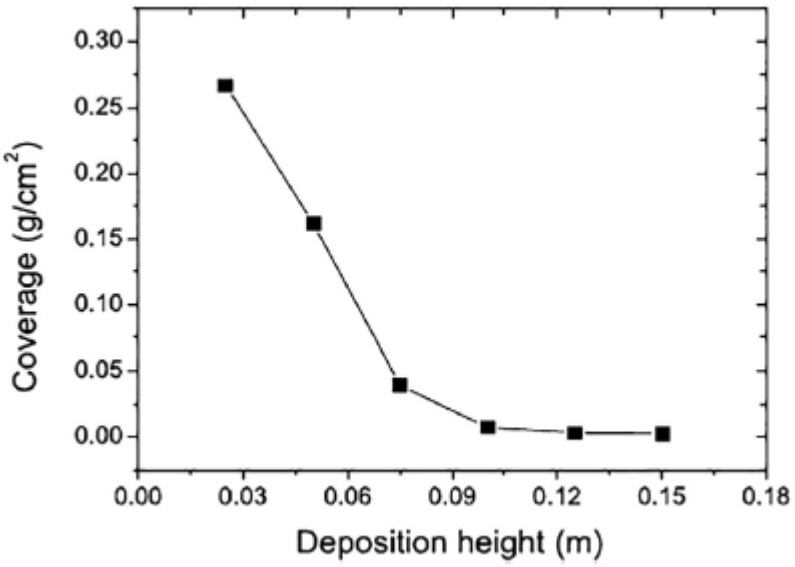

Fig.2.22 Variation of dust density with height [138]

2.2.2.3 Front surface of PV Module

The texture of the PV module's front surface, as well as the extra coating, have a significant impact on the dust deposition process [73]. The studies done by Garg et al. [83] and Nahar and Gupta [84] revealed that in comparison to polyvinyl chloride (PVC) and acrylic surfaces, dust deposition was found to be reduced on glass surfaces, as shown in Fig 2.23. In comparison to the Tedlar cover, Kalogirou et al. [76] found that the PV module's glass cover is less affected by dust accumulation. Front surface glazed with the super hydrophobic or hydrophilic coating is less deposited by dust particles in comparison to the unglazed surface [139,140].

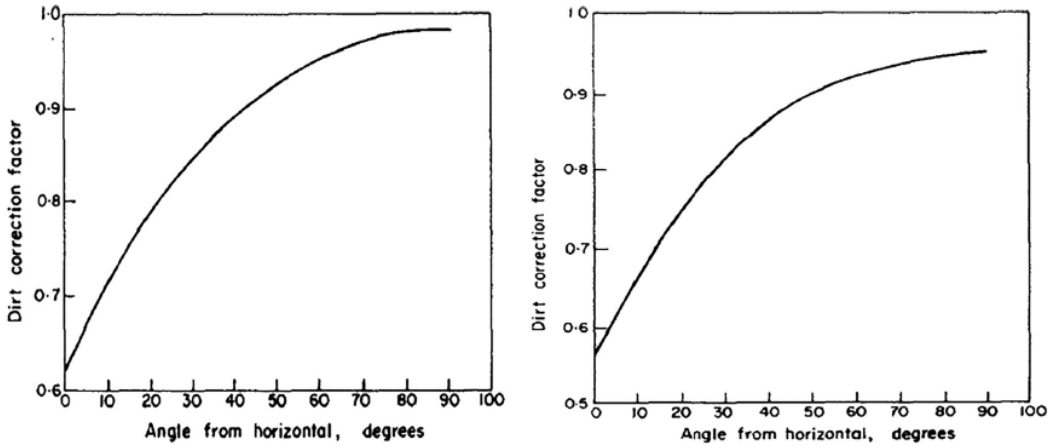

(a) (b)

Fig.2.23 Dirt correction factor with various inclinations (a) for Glass (b) for Plastic [83]

2.2.2.4 Installation site & Exposure time

The amount of dust deposited is mostly determined by the installation site. The installation site is located in a desert environment with a high rate of dust deposition. If PV modules are installed in city and countryside areas, the dust accumulation rate in both locations differs because of differences in ambient temperatures and wind speed in urban and rural zones, as illustrated in Fig.2.24 [141].

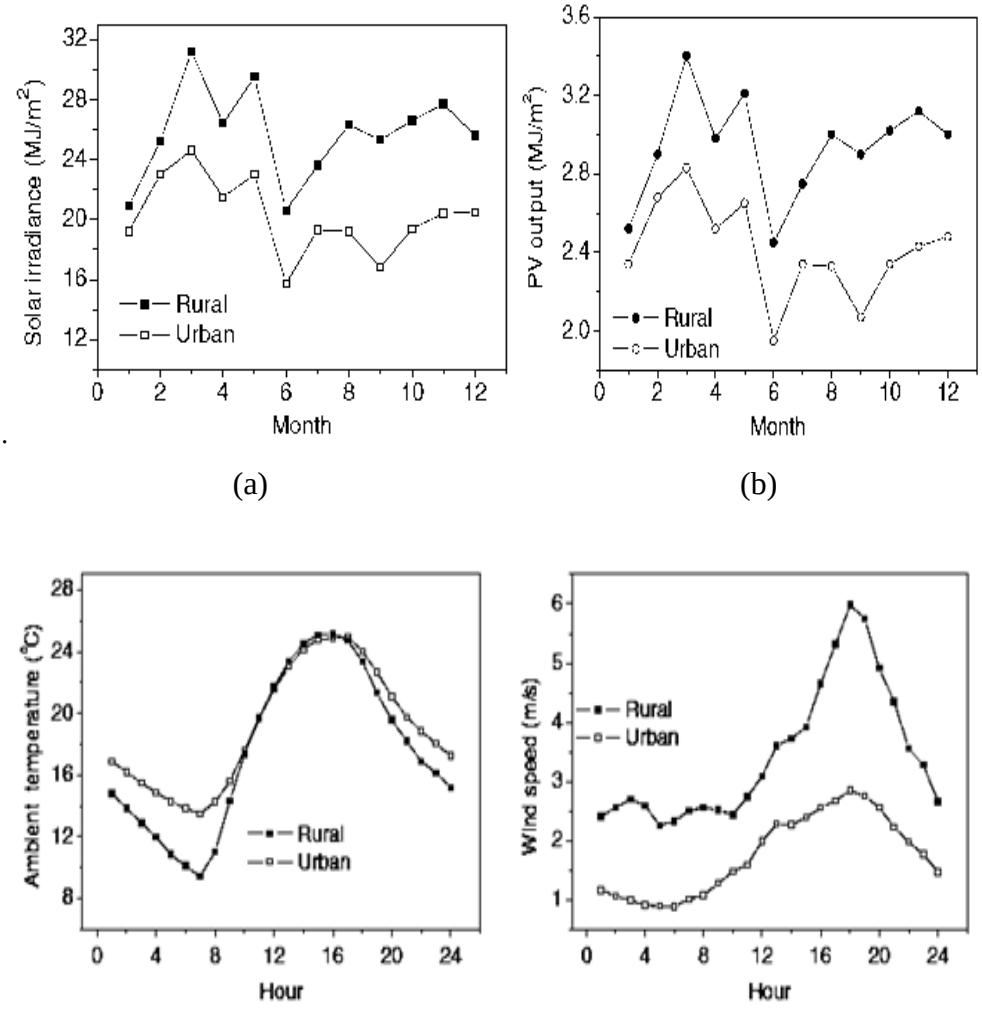

(a) (b)

(c) (d)

Fig.2.24 (a). Variation of solar radiation; (b)Variation in PV output Power; (c) Variation in Temperature; & (d) Variation in wind speed in Urban & Rural are of Maxico city for 2003 [141]

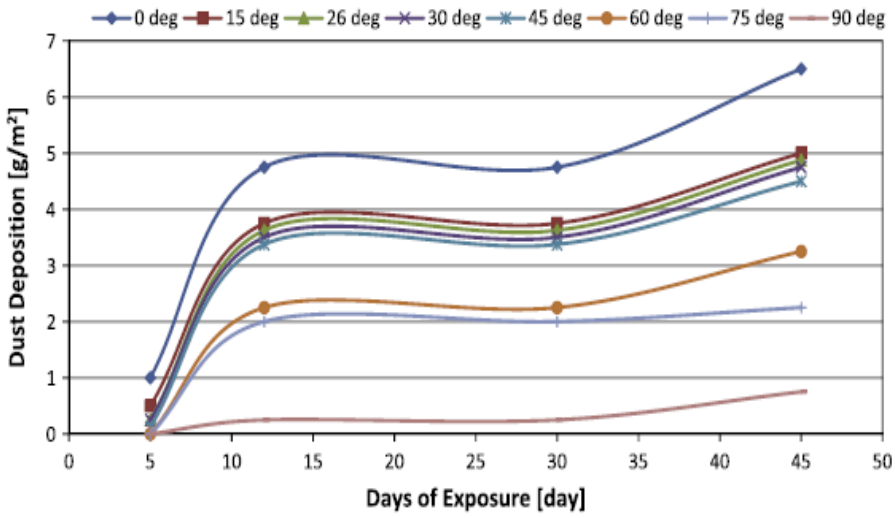

Fig. 2.25 Variation of dust deposition on surface with no. of days [9]

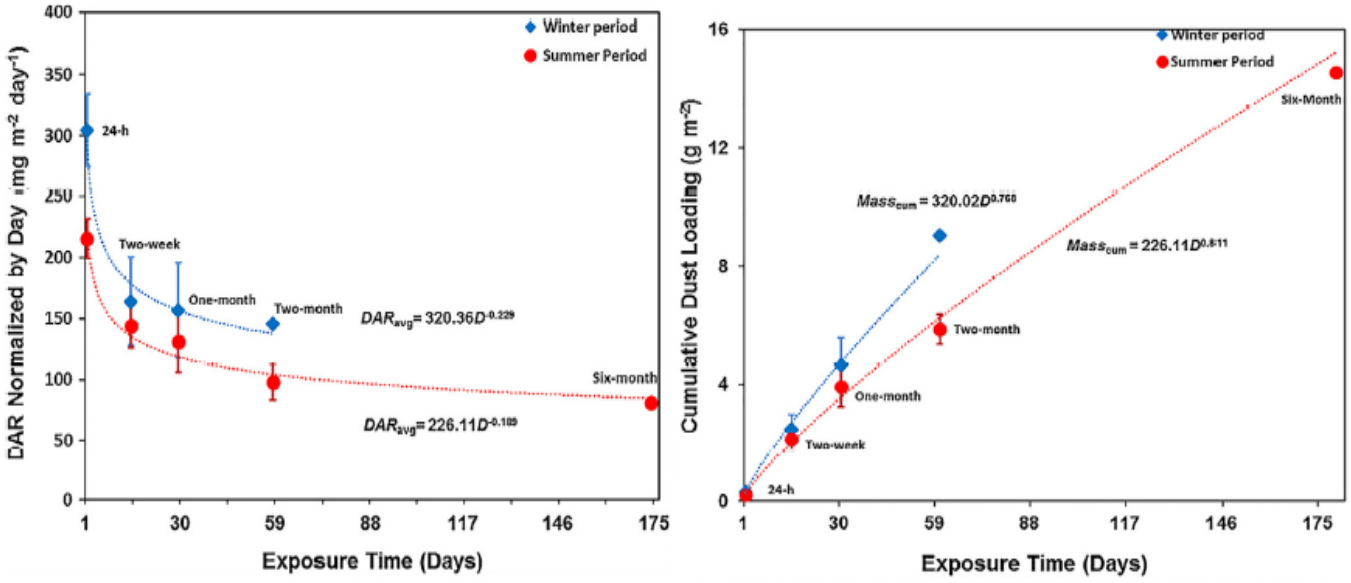

(a) (b)

Fig. 2.26 (a) Variation of dust density per day with exposure time;
(b) Cumulative dust density with exposure time [5]

The rate of dust accumulation on the PV module's surface is shown in Fig. 2.25 as a function of the time of exposure to outside environmental conditions [9]. Javed et al. [5] found that the dust deposition rate was more in the initial phases of dust deposition and fixed as exposure time

increased. It was also detected that cleaned PV module surfaces retain more dust compared to unclean PV modules. The deposited dust concentration improved with increasing exposure duration, which can be seen in Fig. 2.26 (a) and (b). After a month of exposure, the average deposited dust density was 5 g m^{-2}, increasing to 15 g m^{-2} after six months. The rate of dust deposition is proportional to the time of exposure [92].

2.3 Hail formation, Characteristics and damage potential

Hail is a strong solidified type of precipitation that causes extensive damage to the PV system. Summer is the best time for hailstorms to form because the weather is hot and humid. Hailstorms occur in many locations of the world, but they are more common and intense in mild and mid-latitude areas [142,143].

Hailstorm is a mesoscale framework with space, size of a couple of kilometers to a few 100 kilometers and time, size of not as much as an hour to a few hours. It causes torrential rain, lightning, thunder, hailstorms, dust storms, squalls of surface breeze, down-blasts, and tornadoes. Hail is frequently linked to thunderstorms and shifting weather fronts. This is shaped in tremendous cumulonimbus mists, ordinarily known as thunderheads [144,145].

Hailstorms are caused by four different atmospheric factors, which are characterized as:

- Strong convective unsteadiness making solid updrafts.
- Plentiful dampness at low levels nursing into the updrafts.
- Solid breeze shear, high up, as a rule veering with stature, upgrading updrafts.
- Certain dynamic systems, such as air flow over mountain ridges, can aid in the arrival of flimsiness [146,147].

The procedure of hail development in a thunderstorm is shown in Fig. 2.27. When the sun warms the earth during the day, the air around it

warms up as well. Hot air rises and cools because it is less dense and lighter than chilly air. Its ability to retain moisture decreases as it cools. When rising, warm air cools to the point that it can no longer carry the majority of its moisture, water vapour condenses, forming puffy-looking mists. The gathering dampness discharges warmth of its own into the encompassing air, making the air rise quicker and surrender significantly more dampness [148].

The volume of hail that reaches the ground falls at a rate of around 40 metres per second, and is often less than 10% of the total amount of rain produced by a hailstorm [149]. Hail from multiple rainstorms never reaches the earth because it liquefies into droplets when it dives into warmer air near the ground. That is why tempests in hotter atmospheric zones only produce hail on the ground on rare occasions. Hailstorm damage, on the other hand, is more prevalent and severe in mid-latitude and temperate countries due to its higher frequency and intensity [149].

Hailstorms can be as little as pellets or as huge as golf balls or even larger, as shown in table 2.3 and Fig.2.28. These are rarely totally circular, usually oblate in shape, and some have ice knobs projecting outwards, as well as a layered structure on the inside. The diverse atmospheric conditions in which they were formed result in unusual shapes such as pyramids and discs, as well as size variances. Studies inferred that most thing harm starts when hailstone widths are 20 mm or more prominent. The bigger the stones, ordinarily, the more prominent the property harm [151]. The size ranges and quantity of hail that fall per unit area during a hail fall, wind forces during the event, and the property of the target are all taken into account when calculating hail damage.

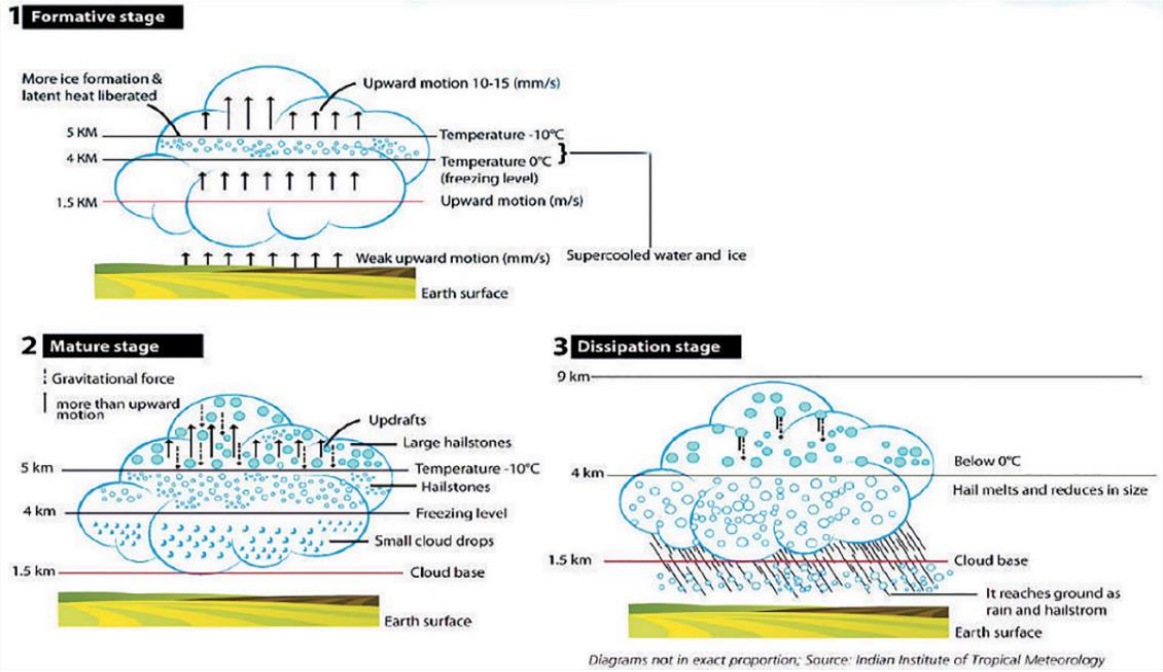

Fig.2.27 Formation of thunderstorm [148]

Fig.2.28 Hail stones produced under varying intensities of hailstorm [150]

Table 2.3. Hailstorm intensity scale [150]

Size Code	Hail Diameter (mm)	Shape of Hail	Intensity	Impacts
H0	<8.4	Pea	Hard hail	No damage
H1	8.4 to 15.2	Marble	Potentially Damaging	Slight damage to plants, crops.
H2	15.2 to 20.3	Coin or grape	Potentially Damaging	Substantial destruction to fruit, vegetation.
H3	20.3 to 30.5	Nickel to quarter	Severe	Severe harm to fruit and yields, harm to glass and plastic structure.
H4	30.5 to 40.6	Golf ball	Severe	Extensive glass damage, Vehicle frame destruction.
H5	40.6 to 50.8	Tennis ball	Destructive	Extensive demolition of glass, destruction to tiled roofs, substantial risk of injuries.
H6	50.8 to 61.0	Baseball	Destructive	Aircraft body spoilt; walls rutted.
H7	61.0 to 76.2	Grapefruit	Very destructive	Severe roof destruction, risk of severe injuries.
H8	76.2 to 88.9	Softball	Very destructive	Severe destruction to aircraft bodywork.
H9	88.9 to 101.6	Softball	Super hailstorms	Extensive structured destruction, Risk of severe or even fatal injuries to persons caught in the open.
H10	>101.6	Softball and Up	Super hailstorms	Extensive structured damage, Risk of severe or even fatal injuries to persons caught in the open

2.3.1 Effect of hailstorm on the Performance of the PV Module

The dense hailstorm may harm the front glass surface and breakage solar cell. When cracks show up in a solar cell, the parts isolated from the cell likely won't be totally separated, but the distance between the cell sections and the number of cycles for which the module is distorted affect the series resistance across the crack.

Fig.2.29 Hailstorm

Fig2.30 Hailstorm affected PV module

The drop in current is proportional to the detached area when a cell section is completely separated [15, 152-153]. Hailstorm not only reduces the total output power generation of PV modules but also reduces the life of PV modules, as revealed in Fig. 2.29 and Fig. 2.30.

Donald & Abraham performed the experiments to determine the effect of hailstorm on the PV Module's performance. In this test they used steel balls, hail stones (frozen ice spheres) and three loading methods, namely: pneumatic gun, gravity drop and static loading. Results are introduced that dropped steel ball test display little connection with high-speed ice-ball tests, though statically stacked steel balls demonstrate a to some degree better adjustment with the ice ball test. In this test eight of the sixteen outlines tried, utilize glass as a major aspect of the superstrate framework. Two of the outlines, type EII and sort H4, utilize the glass superstrate as the sole methods for cell bolster in spite of the fact that an aluminum casing and elastic gasket are utilized to help the glass board around its fringe.

The results demonstrate that the influence of the hailstorm on the PV module is mostly dependent on the PV module's front layer material. No panel configuration utilizing a clear silicone potting as the front layer demonstrated fit for withstanding 1-inch width simulated hailstones without cell breaking. Two types utilizing annealed glass as the front layer were fit for withstanding up to 1-inch width simulated hailstones, however the glass was broken under the effect of 1-1/4-inch width hailstones; one type utilizing annealed glass survived 1-1/4-inch width hailstones. Three other configurations, one including 0.10-inch-thick acrylic and the other two 0.125-inch-thick tempered glass, withstood 1-1/4-inch, however not 1-1/2-inch, width simulated hailstones. Three other configurations, two using 0.125-inch-thick tempered glass and the third utilizing 0.19-inch-thick tempered glass, withstood 1-1/2-inch breadth ice balls yet broke under the effect of 2-inch ice balls [154].

Fig.2.31 demonstrates the harm to a Type AI PV module at the effector site of a 1.61-inch width shaped ice balls going at 70 mph. Note that the outermost acrylic sheet has been totally damaged, and that underlying cell is broken. Fig.2.32 demonstrates the harm to a Type BI PV module at the effector site of a 1.28-inch breadth formed ice balls going at 61 mph.

The harm indicated is fairly characteristic of those modules that utilize a silicone elastic front surface encapsulate. The cell is widely broken, however the silicone encapsulate is unbroken and adherent. Fig.2.33 illustrates the harm to a Type EII solar panel at the impact of a 1.61-inch width simulated hailstone moving at 70 mph. Again, this kind of destruction is typical of panel types integrating annealed glass as the top surface (Types EI, EII, and 64). Note that the focal point of effect is close to the edge of the panel. The glass panels were observed to be substantially more likely to fail when affected close to the edge. Fig.2.34 illustrates that the failure of types BIIK, F42, and F43, which integrated a

tempered glass, is indistinguishable to the annealed glass types, with the exception of that the glass breaks over the whole surface of the PV panel.

Table.2.4 Effect of Simulated Hailstones on the PV Module [154]

Panel Type	Front Surface	Hail size (inches) at velocity mph					
		0.49 at 33	**0.77 at 44**	**1.05 at 55**	**1.28 at 61**	**1.61 at 70**	**2.07 at 79**
AI	Acrylic Sheet			No damage	No damage	Punctured Acrylic sheet	
BI	Silicon Potting		Slight cell Breaking	Appreciable cells Breaking	Extensive cells Breaking	Extensive cells Breaking	
BII	Silicon Potting	Slight cells Breaking 2 of 9 hits	Appreciable cells Breaking	Extensive cells Breaking	Extensive cells Breaking, Dents aluminium Pan	Extensive cells Breaking, Dents aluminium Pan	
CI	Silicon Potting			Slight cells Breaking	Appreciable cells Breaking 3 to 5 hits		
CII	Silicon Potting		No damage	Slight cells Breaking	Appreciable cells Breaking	Extensive cells Breaking	Extensive cells Breaking, Punctured Fibre glass
DI	Silicon Potting		No damage	Slight cells Breaking 3 to 5 hits			
DII	Silicon Potting		Dents in silicon, slight cells Breaking	Dents in silicon, Appreciable cells Breaking	Dents in silicon Extensive cells Breaking	Dents in silicon Extensive cells Breaking	Dents in silicon Extensive cells Breaking, punctured Fibre Glass

Panel Type	Front Surface	Hail size (inches) at velocity mph					
		0.49 at 33	**0.77 at 44**	**1.05 at 55**	**1.28 at 61**	**1.61 at 70**	**2.07 at 79**
BIIK	Tempered Glass			No damage	No damage	No Damage 2 hits shattered Glass, 1 hit near edge	
EI	Annealed Glass			No damage	No damage	Broke the Glass 2 of 3 hits	
EII	Annealed Glass		No damage	No damage	No damage	Broke Glass	
F41	Tedlar Film			No damage	No damage		
F42	Tempered Glass					No damage	Shattered Glass, 1 hit near edge
F43	Tempered Glass				No damage	No damage 3 hits Shattered Glass	
G4	Annealed Glass			No damage	No damage	No damage	
H4	Tempered Glass		No damage	No damage	No damage	No damage	No damage 13 hit shattered Glass, 1 hit near edge
J4	Tempered Glass			No damage	No damage	No damage	No damage 13 hit shattered Glass, 1 hit near edge

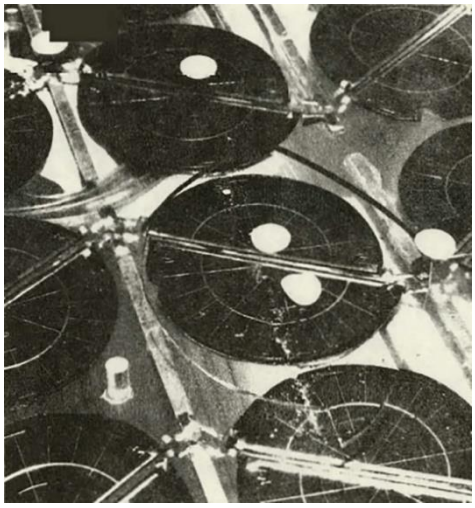

Fig.2.31 Acrylic Sheet front Surface (Panel Type AI) – Impact Site of 1.61-inch Dia.170 mph excited Hailstone [154]

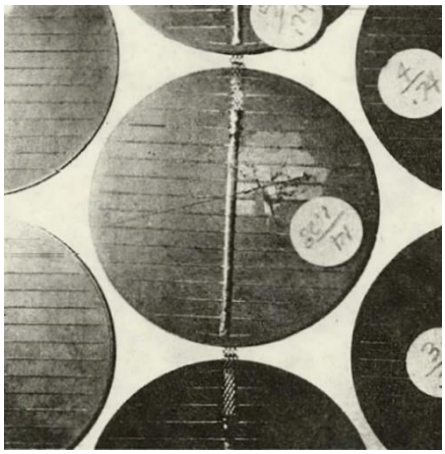

Fig.2.32 Silicon rubber front Surface (Panel Type BI) – Impact Site of 1.28-inch Dia.161 mph excited Hailstone [154]

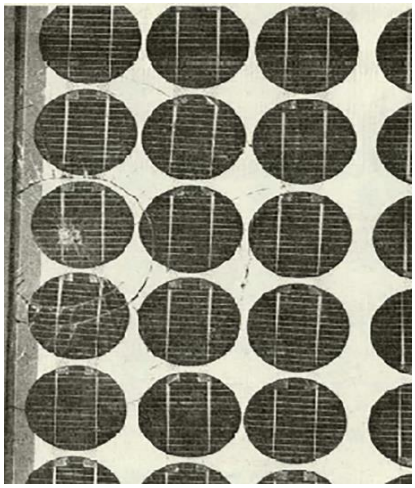

Fig2.33 Annealed Glass front Surface (Panel Type EII) – Impact Site of 1.61-inch Dia.170 mph excited Hailstone [154]

Fig 2.34 Tempered Glass front Surface (Panel Type BIIK) – Impact Site of 1.61-inch Dia.170 mph excited Hailstone [154]

Besides the hail affect testing and the subjective comments recorded above relating to the observed damage, quantitative electrical power estimations were made on four of the panel types before and after hail affect testing. In these tests, the electrical output power of the panel is recorded when the panel is exposed to a standard light source. The results of these tests appear in Table 2.5.

Table.2.5 Impact of a hailstorm on the PV panel's output power [154]

Panel	**Panel Area (Hit/ft^2)**	**Output Power (W)**		**Power Degradation (%)**
		Before Hailstorm	**After Hailstorm**	
BII	15	11.0	2.7	75
CII	10	19.6	11.7	40
DII	6	34.8	21.3	39
EII	5	24.8	23.5	5

When cracks appear on the front glass surface, the solar insolation that reaches the solar cell is reduced. When cracks appear in a solar cell, the cell is fully isolated as a result of current decreasing. Thus, a precise technique for shielding the PV module from hailstorms is expected to be created. Glass splits and cell parts appear on the PV module surface in the midst of hailstorms, which may provoke obstruction of cell parts and, consequently, a misfortune in the overall yield impact made by the PV modules [155-160,15,152,153]. There are various crack detection

techniques such as the thermography technique, electroluminescence imaging method, and resonance ultrasonic vibration technique [161-163]. In the PV module, there are a few kinds of breaks: diagonal breaks, perpendicular to bus bar breaks, parallel to busbar breaks, and multiple direction breaks, as shown in Fig. 2.35. Diagonal breaks and multiple direction breaks create a noteworthy decrease in the yield intensity of PV modules [156].

Table.2.6 Specification of both PV systems [15]

Solar panel's Specification	**1st PV system: SMT 6 (60) P**	**2nd PV system: KC130 GHT-2**
Maximum Power	220 W	130W
Voltage at MPPT (V_{mp})	28.7 V	17.6 V
Current at MPPT (I_{mp})	7.67 A	7.39 A
Open circuit voltage (V_{OC})	36.74 V	21.9 V
Short circuit current (I_{sc})	8.24 A	8.02 v
No. of Series Connected cells	60	36
No. of Parallel Connected cells	1	1
Tilt angle and azimuth angle (North-South)	42°,185°	42°,180°
Davis pyranometer sensor tilt angle and azimuth angles(North-South)	42°,185°	42°,180°

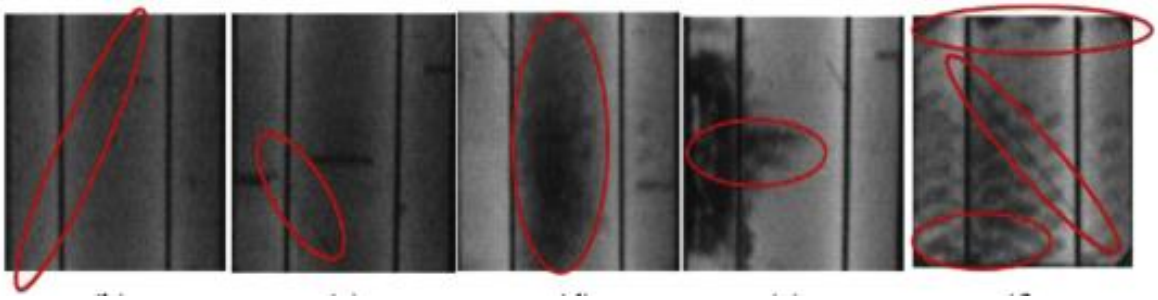

(a) (b) (c) (d) (e)

Fig.2.35 (a) diagonal Breaks (+45°); (b) diagonal Breaks (-45°); (c) Parallel to bus bars; (d) perpendicular to bus bar Breaks; (e) Multiple direction Breaks [15]

Dimish executed an experiment to determine the effect of the cracks on the overall amount of energy produced by the PV modules. For this experiment, two different PV plants are used as shown in Table.2.6. The first system has 10 polycrystalline PV modules with a peak power of 220Wp and the second system has 35 polycrystalline with 130Wp each. Results are shown in tables 2.7–2.10 and Fig. 2.36-2.37.

Table.2.7 Performance indicators for Diagonal breaks [15]

Nature of Crack	**No. of affected Solar Cells**	**Damaged Area (mm^2)**	**Effect on the Output Power**
Short +45 Or Short -45	1	1-83	Insignificant
Long +45	2	85.85-169.7	Significant
Or	3	172.7-256.6	Significant
Long-45	4	257.5-344.4	Significant
	5	345.1-424.3	Significant

Table.2.8 Performance indicators for Parallel to bus bar breaks [15]

Nature of Crack	**No. of affected Solar Cells**	**Damaged Area (mm^2)**	**Effect on the Output Power**
Short	1	1-59.2	Not Significant
Long	2	63-81	Not Significant
		82-121	Significant
	3	122-177	Significant
	4	177.3-239.7	Significant

Table.2.9 Performance indicators for Perpendicular to bus bar breaks [15]

Nature of Crack	**No. of affected Solar Cells**	**Nos. of busbars affected**	**Damaged Area (mm^2)**	**Effect on the Output Power**
Short	1	1	1-16.2	Insignificant
	2	2	16.3-60	Insignificant
Long	3	3	61.3-78.5	Insignificant
	4	4	79.4-120	Significant
		5	120.5-137.4	Significant
		6	138-179.8	Significant
		7	181.5-195	Significant
		8	196.2-240.2	Significant

Table.2.10 Performance indicators for multiple breaks [15]

No. of affected Solar Cells	Damaged Area (mm^2)	Effect on the Output Power
1	1-45	Insignificant
	46.2-1000	Significant
2	100-3700	Significant
3	170-5000	Significant
4	223-8200	Significant

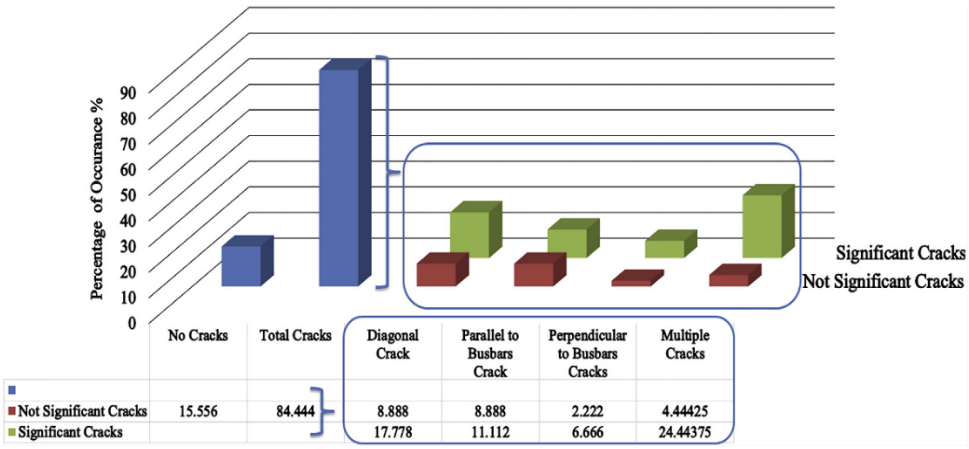

Fig 2.36. Percentage of breaks in the inspected PV modules, overall substantial Breaks equal to 60% out of 84.44% [15]

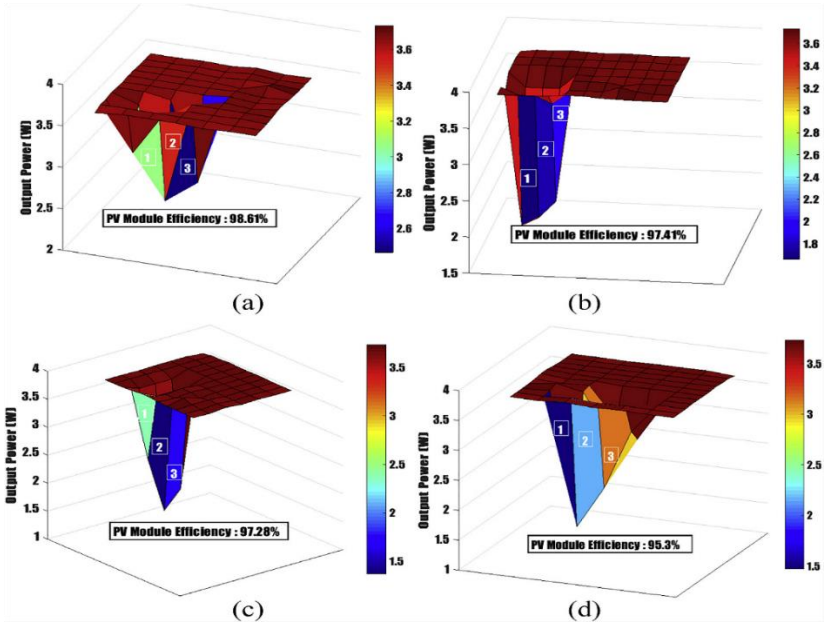

Fig. 2.37. (a) Surface nature for a diagonal (45) break effect 3 cells; (b) Surface nature for a parallel to busbars break effect 3 cells (c) Surface nature for a perpendicular to busbars break effect 3 cells, 6 busbars; (d) Surface nature for multiple directions breaks effect 3 cells [15]

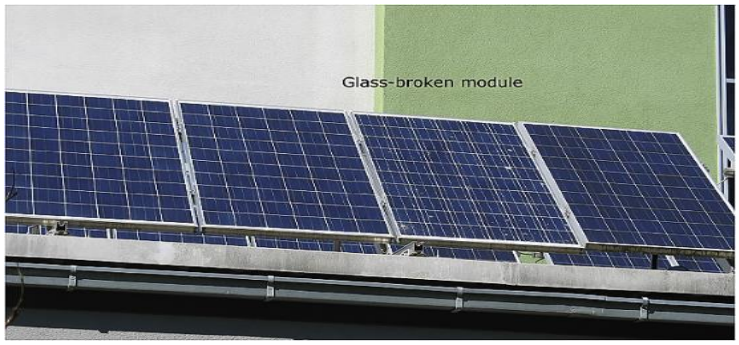

Fig.2.38 Module with broken glass after hailstorm (plant 3) [164]

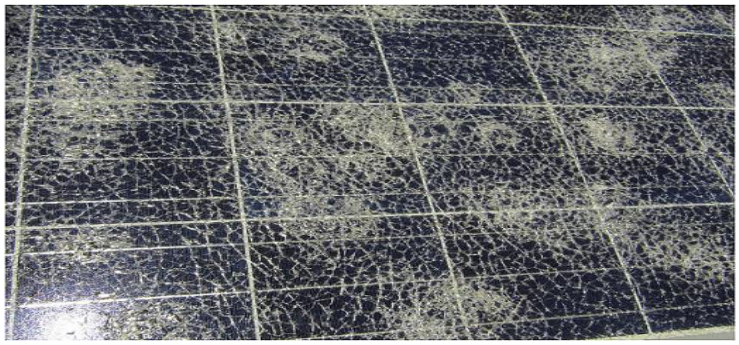

Fig.2.39 Module with broken glass after heavy hailstorm (plant 1) [164]

Muehleisen et al. [164] investigated the effect of hailstorms on the PV module. In the case of a heavy hailstorm, there is a possibility of damaging the front glass surface and breaking the solar cell also, resulting in efficiency losses. Three photovoltaic plants which were affected by the hailstorm in the south of Austria were investigated. The effect of hailstorms on PV modules has been shown in Fig. 2.38–2.39. Some glass-broken modules: 4 panels out of 80 for Plant 1, 3 panels out of 510 for Plant 2, and 1 panel out of 32 for Plant 3 were affected. This damage has a serious influence on the PV plant's output. After the hailstorm, a loss in the PR of plant 1 of approximately 10–20% could be detected. The effect of the hailstorm on plants 2 and 3 is modest in the PR, as shown in Fig 2.40–2.42.

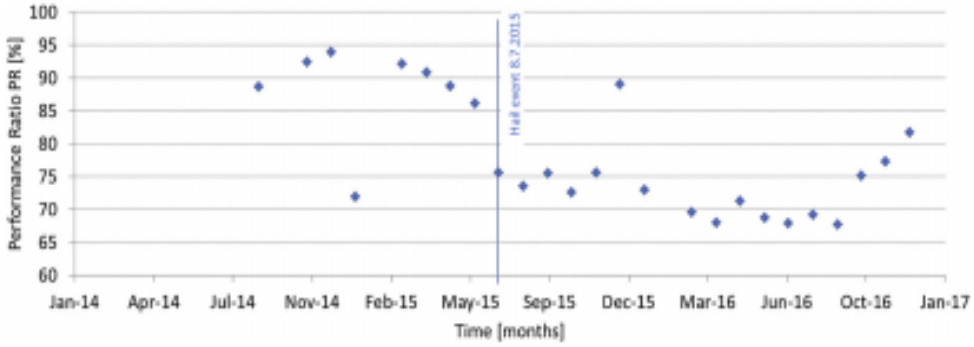

Fig.2.40 After hailstorm Performance ratio of Plant1 [164]

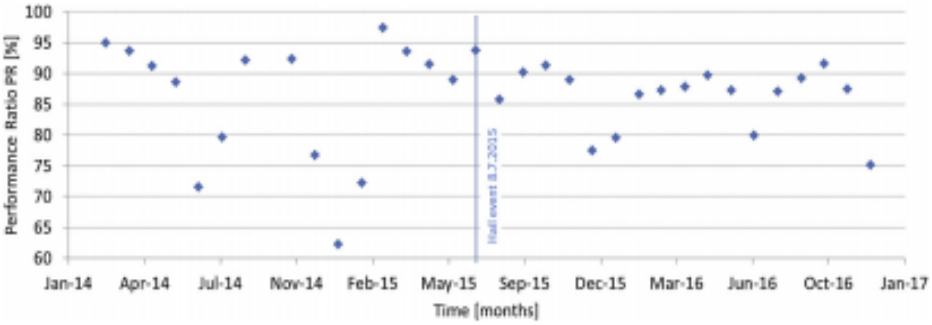

Fig.2.41 After hailstorm Performance ratio of Plant2 [164]

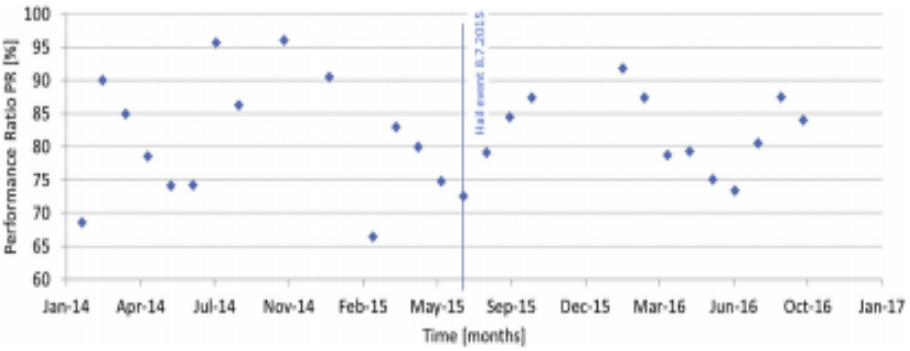

Fig.2.42 After hailstorm Performance ratio of Plant3 [164]

2.4 Methods of reducing dust deposition

Dust deposition on the PV module surface not only reduces the module performance but also decreases the lifespan. So, cleaning of PV modules has become very essential. Mani and Pillai recommended mitigation and cleaning methods based on three climate zones: the low latitude zone, the mid-latitude zone, and the high-latitude zone [11]. Fig. 2.43 shows the four zones with different dust intensities. Zone 4 shows the greater level of dust. There are various cleaning methods for reducing the effect of dust

settlement on the PV module depending upon the dust deposition densities as shown in Fig. 2.44.

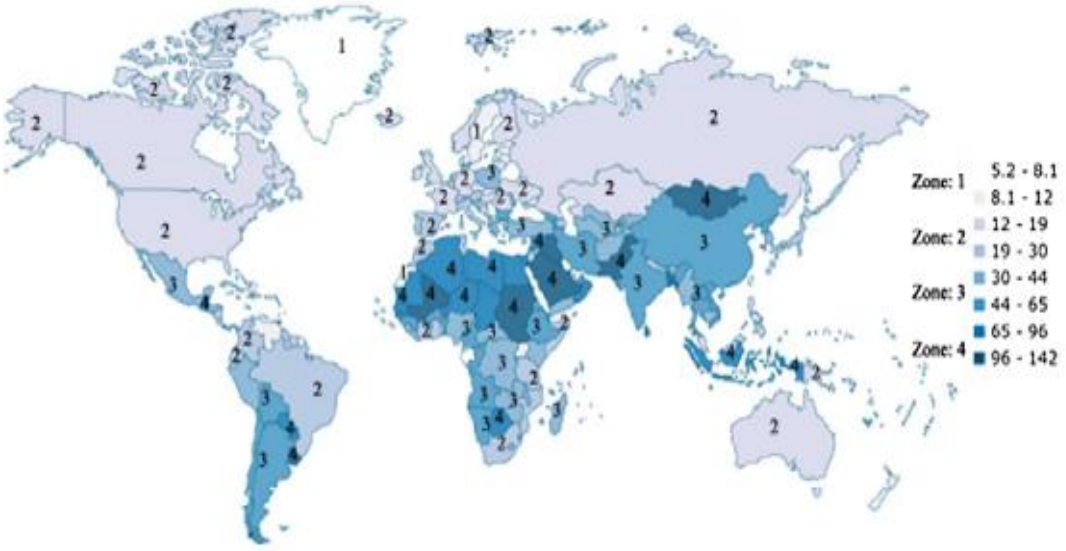

Fig.2.43. PM10 world map [mg/m^3] [165]

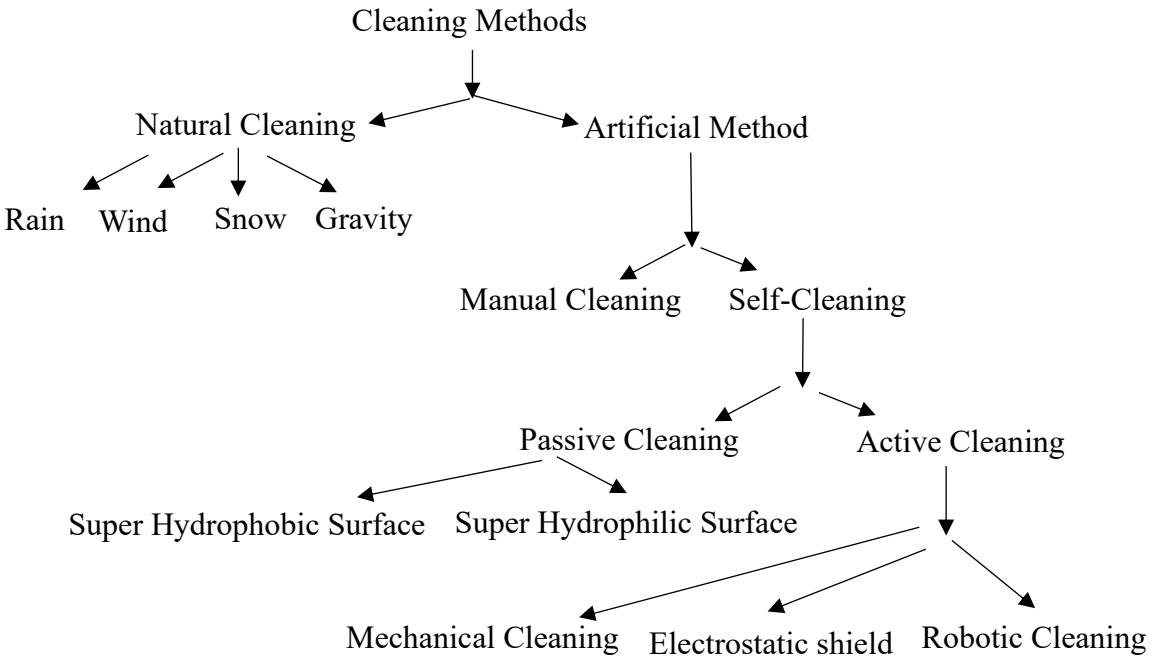

Fig. 2.44 Different types of Cleaning Methods

2.4.1 Natural Cleaning Method

The area with low dust deposition such as the United States and Europe, natural cleaning by rain, wind, and snow are more effective to restore to original capacities. The area where dust is one of the most important elements, such as the Middle East and North Africa, affecting PV module performances significantly, it is imperative to accomplish artificial cleaning methods to recover the PV module performance. Haeberlin and Graf [12] and Appels et al. [96] carried out the experiments in Switzerland and Belgium respectively to find the effect of the rainfall on the cleaning of the PV module. Results demonstrated that rainfall restores the PV module performance sufficiently, no need for manual cleaning. Bethea et al. [120] found that low rainfall encourages dust adhesion to the module, resulting in dust being converted to mud. It cannot be removed easily and needs a mechanical cleaning method. The tilt angles play an important role in the natural cleaning of PV modules because the horizontal surface is not easy to clean by rainfall. The higher tilt angle makes dust fall effortlessly because of the gravitational force [166]. Smith et al. [167] observed that cleaning by precipitation was competent to re-establish the yield energy by 1% of a physically cleaned PV module after a loss of 4% because of dust deposition.

The wind can reduce the dust deposition by removing the bigger dust particles from the PV module. Cuddihy et al. [168] stated that the wind cleaning is not extremely powerful for smaller particles (less than 50μm) due to adhesive force. At high installations, wind speed is greater compared to ground level, so for PV systems placed at a high level, wind cleaning is more effective.

2.4.2 Manual Cleaning Method

The manual cleaning method requires a person, water, and soft cloth to clean the PV module. This strategy is amongst the best cleaning techniques for cleaning the PV modules in small-scale solar PV plants [169]. In case of extensive PV power, pressured jets and brushing are used

[170-171]. Maharram et al. [172] stated that using some kind of detergent improves the cleaning performance for the hard soiling. The importance of brushing after water cleaning has been revealed by Pavan et al. [73]. In this experiment, the water cleaning method was utilized to clean the two extensive PV plants using pressured water. After washing, the panels of one power plant were brushed. The results showed that after cleaning, the output power of PV plants was increased by 1.1% without brushing and 6.9% with brushing. Brushing removes the highly adhered fine particles, which cannot be removed by water cleaning alone. Freese et al. [173] stated that excessive brushing creates scratches on the surface of PV panel, which degrades the performance of the PV panel. He concluded that brushing must be used with extreme care. For large PV plants, this cleaning method becomes very tedious and challenging as the solar power plants consist of a number of PV modules installed at a height of 8 to 15 feet or more from the ground. The time is required, and the safety of the person and the panel is threatened.

2.4.3 Self- Cleaning Method

There are various self-cleaning methods to reduce the effect of dust deposition. In the self-cleaning method, the usage of humans can be replaced or removed by using the automation auxiliary system for cleaning in order to save water and maintain PV module effectiveness.

2.4.3.1 Active Cleaning

Active cleaning methods can be considered as those methods that continuously consume power in order to clean the PV module.

2.4.3.1.1 Mechanical Cleaning Method

Mechanical cleaning methods are equipped with wiping, blowing and brushes. This system can be controlled electrically and electronically. The single-axis solar tracker, which features a self-cleaning system, was created by Tejwani and Solanki [174]. This self-cleaning system comprises a stepper motor, microcontroller, and gearbox as shown in Fig. 2.45. The initial position of the PV panel is perpendicular to the ground in the morning. The system rotates in such a way to maintain the solar

radiation normal to the PV panel. When the stepper motor rotates 180° angle, the PV panel becomes vertical to the earth. At these times, a brush rotates because of gravitational force and cleans the surface of the PV module. After 360° rotation of the stepper motor, again PV module gets back into the vertical position with respect to the ground. The brush cleans the PV module. The PV module is cleaned two times a day in this manner.

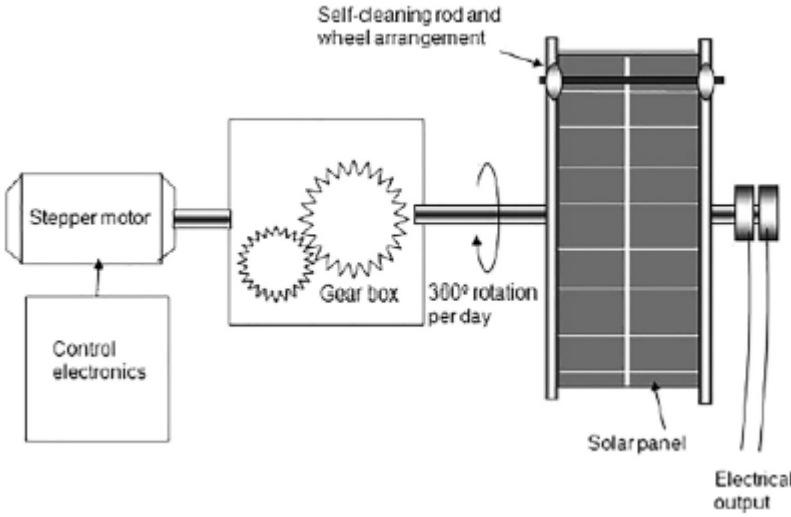

Fig. 2.45 Self-cleaning mechanical system with sun-tracking [174]

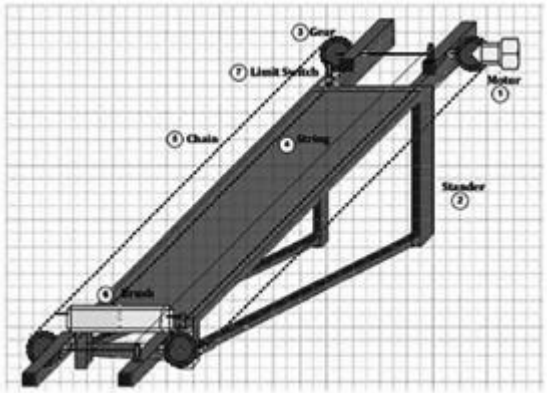

Fig.2.46 Electro-mechanical cleaning system [175]

Lamount and EI Chaar [175] introduced two cleaning structures using the PLC and PIC that are effectively used for eliminating the dust deposition and bird droppings on the PV module. The first structure consists of wipers, a dark-activated sensor, and a movement sensor and is controlled

by the PLC device. Whereas the second structure consists of a roller brush, alarms and is controlled by PIC as shown in Fig 2.46. Willians et al. [176] stated that 95% of the output power can be achieved by using mechanical vibration to eliminate dust accumulation on the PV module.

2.4.3.1.2 Electrostatic Dust-removal Method

Masuda et al. [177] and Masuda and Matsumoto [178] stated that a travelling wave of the electric field can carry charged air dust elements in a transverse way. This concept is used in developing the electrostatic dust removal method. The EDS system consists of a parallel electrode which is made of transparent indium tin oxide, on a transparent plastic sheet, made of polyethylene terephthalate. A three-phase AC voltage supply range of 750 to 1250 V at the frequency between 4 and 20 HZ is connected to the electrodes to generate an electromagnetic field on the surface, which repels the dust elements due to the electrostatic reaction. The negative electrode induces the negative charge on the dust elements that are present on the surface of the PV panel. The dust elements are accumulated at the positive electrode after being attracted. In this way, a contact-less dust-removal technique helps in improving the efficiency of the PV module. EDS showed about 80% dust can be removed and performance of PV module increases up to 90% [179,181]. The efficiency of EDS depends on many factors, such as the rate of dust deposition rate, type of dust, and applied voltage. The dust elimination ability of the transparent electrodynamics surface is sensitive to changes in magnitude, wave shape, and frequency of the applied voltage. In areas where water is scarce, electrostatic cleaning systems are recommended [182].

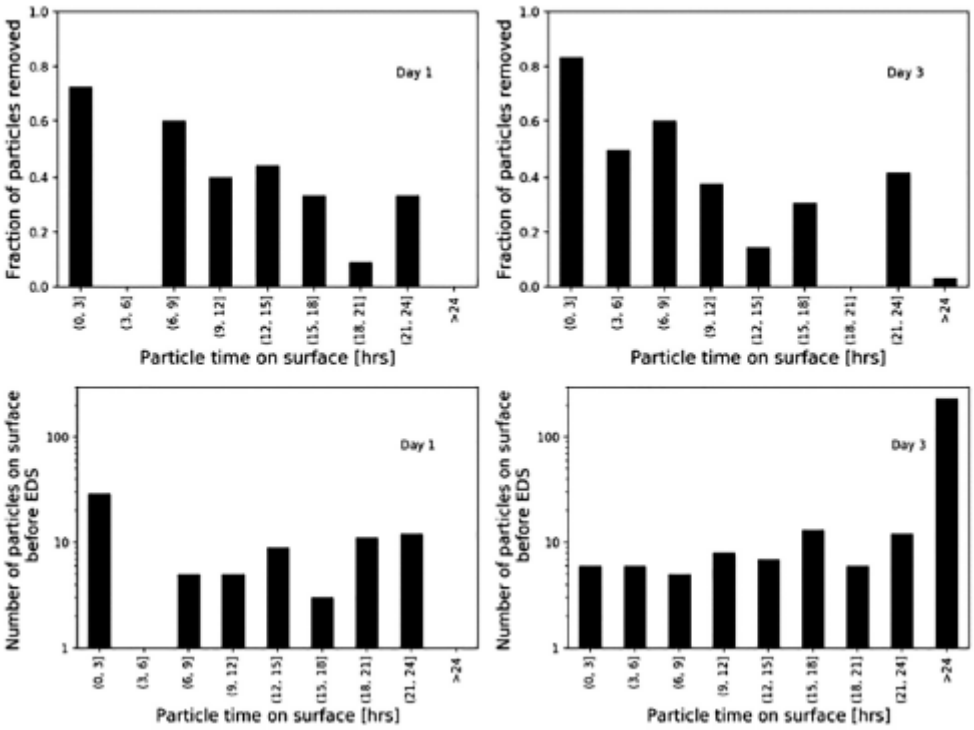

Fig.2.47 Day 1 (left) and Day 3 (right) of the field test EDS efficiency as a function of dust age (top row) and particle amount in various age groups (bottom row). [180]

Guo et al. [180] performed the experiment to find the cleaning efficiency of EDS in the outdoor environment. Dust settlement on the EDS prototypes happened constantly in the outdoor environment, and over the course of two stages of testing, the EDS was stimulated once every 24 hours, with each stage lasting four days. EDS efficiency decreased from 40% to 14% over a four-day period. It was also revealed that removal efficiency diminishes as dust elements remain longer on the EDS surface. Also, remaining dust from past cycles is generally not removable in the following cycle. Therefore, stimulating the EDS at shorter time intervals should result in higher overall dust removal efficiency. The removal efficiency of EDS depends on the distance from an electrode at the start of field exposure but becomes less dependent on it as the number of EDS cycles increases. Fig. 2.47 demonstrates that the dust that was saved inside for the previous 24 h was expelled at the same efficiency upon EDS stimulation on Day 1 or Day 3. However, the cleaning efficiency from past cycles was very low.

2.4.3.1.3 Robotic Cleaning

JU and Fu [183] stated that robotic cleaning increases the installation and maintenance costs but reduces water usage. They carried out the experiment with two identical monocrystalline PV modules. One PV module has a cleaning system that consists of an electrical motor and brush using a spray, whereas the other PV module has a natural cleaning system. The PV module with a cleaning system generated greater power compared to the naturally- cleaned PV module. But the functioning cost of the cleaning system was more over the same test duration. Fig 2.48 (a) & (b) show the robotic cleaning methods.

2.4.3.2 Passive Cleaning

2.4.3.2.1 Super hydrophobic surface

Super hydrophobic surface is defined as the surface which has the properties of low wettability and high water droplet mobility. Modifying the PV module's surface property by using super hydrophobic characteristics can improve the cleaning effect. Dust deposition can be easily removed using rainfall or a water cleaning system on a surface with a super hydrophobic characteristic. This increases the probability of recovery of the surface cleanliness of PV modules and, furthermore, expands the daylight retention capacity by having the largest effective module area to catch the sunlight. There are a number of research papers which have verified that hydrophobic surfaces reduce dust deposition [184-187]. Fig 2.48 (c) shows the self-cleaning hydrophobic coating.

Cuddihy [184] gives the most punctual guide to structure and selection of coatings or surfaces to resist dust deposition. He presents two methods to accomplish the desired chemical characteristics: Hydrophobicity and Hydrophilic. Dew has a significant influence on soiling, which can be beneficial or detrimental depending on the installation area [188].

(a) (b) (c)

Fig 2.48 Types of cleaning devices :(a) water spray cleaning device [202]; (b) self-cleaning robot [203]; (c) self- cleaning hydrophobic coatings [204]

To develop the self- cleaning surfaces, micro and nanostructure are required. The rough structure of the surface with micro and nanostructures not only reduce the stickiness of water droplets but also increases the hydrophobicity property. There are a numbers of studies which reveal that hydrophobic surfaces reduce dust deposition.

Checco [189] indicated that when the contact angle is greater than 150° and the hysteresis is less than 5°, a surface can be described as super hydrophobic. Verma et al. [190] developed the super hydrophobicity glass with nanostructured for improving the solar module to provide the self-cleaning nature of the surface and increase in gross optical transmission.

It's still unclear if super hydrophobic surfaces can effectively combat dust accumulation. Mittal and Jelle [191] expressed that the cleaning, impact utilizing the super hydrophobic layer isn't strong enough to keep going for 3-4 years. Yong et al. [192] found that only 71.8% of the PV modules effectiveness ready to recuperate from debasement because of dust deposition utilizing the super hydrophobic layer. Apart from that, the super hydrophobic layer made from polymer [139,140, 193-195], they added more dust because of the high surface energies of the polymer [196].

Yusuf et al. [197] conducted experiments to determine the efficacy of various cleaning techniques and discovered that self-cleaning with a

hydrophobic coating has 99% optical efficiency during the wet season and 95% during the dry season.

2.4.3.2.2 Super hydrophilic surface

The super hydrophilic surface is defined as the surface that has a property of strong attraction to water. When the contact angle is close to 0°, a super-hydrophilic surface can be achieved. [198,192]. This can be obtained by utilizing nano-film covering of titanium oxide on the nanostructured glass surface. Water dew on the super-hydrophilic surface is levelled and broadly spread onto the surface and carries dust particles away.

The difference between the super hydrophobic and super hydrophilic surfaces, as shown in Fig. 2.49, is that water dews on the hydrophilic surface are flattened and widely spread, but water dews on the hydrophobic surface are mostly circular moulded and do not spread.

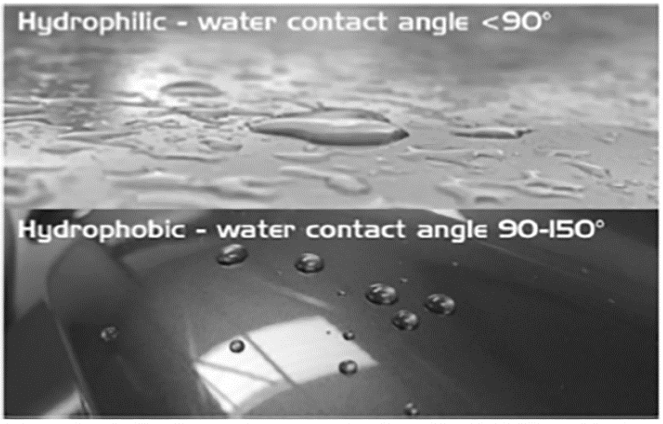

Fig.2.49 Water drops of the hydrophilic surface against hydrophobic surface [200]

He et al. [187] stated that the super-hydrophilic layer is not suitable for solar PV modules in the arid region because this surface needs rain to acquire its cleaning effect. This type of cleaning method may be applicable in medium and high rainfall regions. Son et al. [199] investigated that only 1.39% of efficiency was the drop, utilizing nanostructured super hydrophilic glass without synthetic treatment, which was 1.23% more than the super hydrophobic layer.

It has been investigated that the effect of the hybrid hydrophobic and hydrophilic coating on the surface of PV module. The studies reveal that this hybrid coating provides excellent anti-reflective and anti-soiling properties. When a layer of hybrid hydrophobic and hydrophilic coating is applied to the PV module's surface, the water collection rates increase by 95% when compared to an uncoated glass surface and by 51% when compared to evenly coated hydrophobic low-iron glass. Fig. 2.50 depicts a hybrid hydrophobic–hydrophilic surface preparation concept. Once dew drops reach a critical mass, they slide-off, absorbing and carrying away the dust particles that have been accumulating on the surface. The hybrid coating decreases reflections by more than 75% due to its low index of refraction. Usually, PV panel losses due to reflections from the top glass surface are roughly 4%; losses due to dust collection are much larger, reaching up to 50% of the energy produced. Anti-soiling qualities are obtained by a mix of mechanisms, including preferred nucleation and development of liquid water droplets on hydrophilic parts during natural condensation (i.e., dew), as well as high droplet mobility on the hydrophobic surface [204-207]. Fig. 2.51 shows the water condensation on (a) hydrophobic and (b) hybrid hydrophobic–hydrophilic surfaces with time.

Rate of water collection as function of number of rows of hydrophilic features is shown in Fig. 2.52(a). For this assessment, every single hydrophilic ring has a breadth of 2 mm with an edge-to-edge partition separation of 4 mm. On a hydrophobic surface without hydrophilic rings, the highest water gathering rate was 36% higher, and on hydrophilic (bare) glass, it was more than twice as high. Expending the number of rows further brought about a continuous reduction in water collection rates. The reliance of water collection rates on the distance across of the hydrophilic rings is shown in Fig. 2.52(b). The separation between features was held at 4 mm, with two rows of features for all examples. For hydrophilic rings with a diameter of 2 mm, water collection rates were reduced by 19% and 8%, respectively; for lesser (1 mm) and larger (3

mm) ring diameters, water collection rates were reduced by 19% and 8%, respectively.

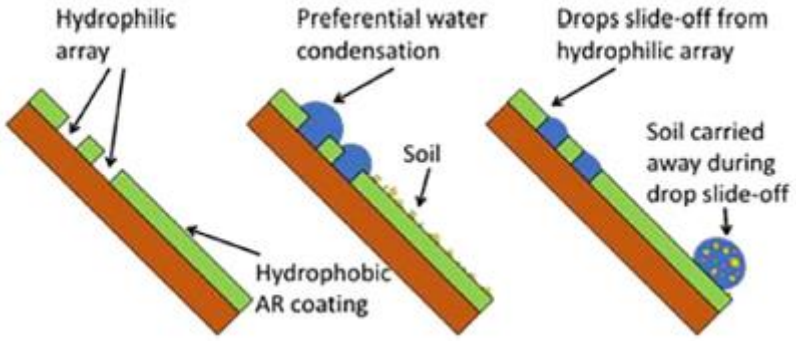

Fig. 2.50 Hybrid hydrophobic–hydrophilic surface preparation schematic. [208]

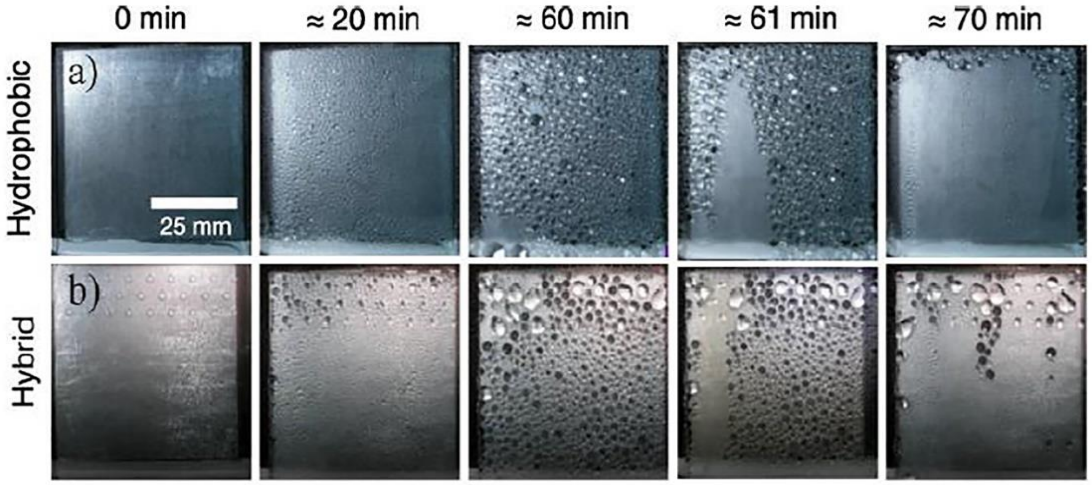

Fig. 2.51 Water condensation on (a) hydrophobic and (b) hybrid hydrophobic–hydrophilic surface with time [204]

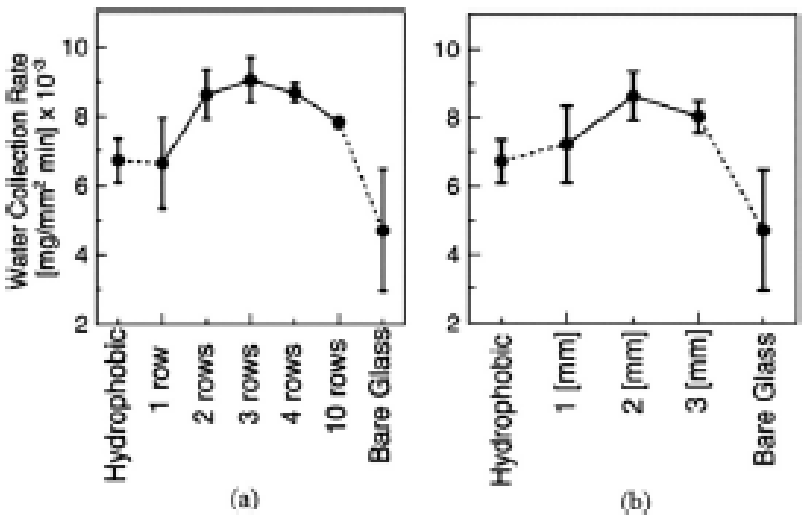

Fig.2.52 Rate of water collection depends on (a) the number of rows of the hydrophilic ring features (b) the diameter of two rows of hydrophilic features. [204]

Table.2.11 Comparison between different mitigating Techniques [174-179,209]

Mitigating Techniques	**Requirements /Components**	**Benefits**	**Drawback**	**Maximum Efficiency**	**Controlling Techniques**
Natural Cleaning	Rainfall, Wind, Snow, Gravity, Tilted Panel	• No cost	• Weather Dependent • Site Dependent • Not effective for small dust particles		N/A
Manual Cleaning	Manpower, Water, Brushes, Cloths, Detergent, Ladder	• Efficient to recover PV Performance • Performed whenever required	• High cost • Limited Water in arid area • Scratches may be produced	100%	N/A
Mechanical Cleaning	Wipers, Blower, Brushes, Motors, Gears, Chains, Sensors	• Reduces labour cost • Automatic Activation • Both Cleaning & scrubbing.	• Maintance required • Power Consumption • High capital cost	95%	PLC, PIC Microcontroller

Mitigating Techniques	**Requirements /Components**	**Benefits**	**Drawback**	**Maximum Efficiency**	**Controlling Techniques**
Electrodynamics Screen	High Voltage, Transparent front screen Sensors	• Very effective & fast • Waterless • Auto or Manually • No mechanical component • Less energy uses	• High capital cost • Ineffective for small particles • Less durability of transparent screen • Performance depends on relative humidity	90%	PLC Microcontroller
Robotic Cleaning	Motor, Sensors, Brushes, Spray, Filter,	• Auto cleaning & brushing • Requires less water	• High cost • Slow operation • Filter has to be changed periodically	-	Microcontroller Arduino
Passive Cleaning	Forming hydrophobic / hydrophilic surface Chemical coating	• No power requires • Improve the natural cleaning	• Lifetime is limited • Reduced the optical performance	71.8%	N/A

2.5 Wired and wireless data acquisition system

The literature survey revealed that numerous wired and wireless data acquisitions were developed for usage in measuring, acquiring, and monitoring of the PV system and environmental parameters. Mukaro and Careise developed a data collection technique for monitoring solar irradiance that used a microcontroller and SolData silicon-cell pyranometers as the solar irradiance sensor, with the obtained data saved in a serial I2C EEPROM. The data can then be sent to a computer for analysis [210]. Koutroulis and Kalaitzakis have developed the hi-tech system using LabVIEW to observe and analyse the information of renewable energy system [211]. The suggested observing system utilizes a lot of sensors to quantify environmental and soil conditions. Additionally, it can screen the electrical output variables of hybrid PV/wind system. Such variables incorporate, PV system voltage and current, the wind speed. The gathered information is additionally handled, shown on the screen, and put away on the PC [211].

Anwari et al. [212] introduced a portrayal of monitoring system for 5 kW PV system, which contains sensors, remote passageway and PC. It empowers managers for getting to PV variables by means of a wireless link. For measuring voltage and current, a voltage divider and three current sensors with 50A rating have been utilized. For detecting solar irradiance and temperature of the PV module, LDR and LM35 temperature sensor have been utilized. Forero et al. [213] built up an observing system using LabVIEW which can gather and show the parameters of a solar PV system.

Zou et al. proposed the observing system for gathering information and estimating the performance of grid-linked PV system [214]. Balan et al. [215] & Thomas et al. [216] suggested DAQS based on a microcontroller for observing solar irradiance. The proposed system contains two pyranometers for measuring the global solar irradiance and the diffuse irradiance due to shading. The collected information is constantly stored and transferred into PC by serial interface RS-232.

Aristizabal et al. [217] proposed an observing system using virtual instrumentation (VI). The proposed system is fit for gathering information about the performance of PV system parameters and furthermore estimating surrounding factors which contains solar radiation and temperature. Alex et al. [218] proposed a model comprised of DAQS, PC, battery, and a test system for PV modules so as to gather information and test the exhibition of the PV plant. Belmili et al. [219] constructed a data acquisition system using microcontroller for receiving the parameters of PV module under outdoor conditions. This system is intended to procure temperature and solar radiation. After that, it records the I-V and P-V attributes of the PV module.

Benghanem et al. suggested a wireless data acquisition system that estimates the solar radiation considering the remote locale's energy necessity [220]. Gagliarducci et al. has described a monitoring and controlling system for complex photovoltaic system [221]. This monitoring system stored and occasionally reports the whole performance of PV system. If there should be an occurrence of erroneous conduct, the system will quickly inform the administrator. A few analysts likewise build up an observing system for current-voltage curves of PV system. Van et al. prepared a system for constantly observing the I-V qualities of seven PV modules. Additionally, [222] has built up a PC based monitoring system for PV system that permits sketch of the I-V qualities of a PV system in genuine climatic test conditions. The solar radiation and temperature are the basic variables seen by observing systems [220-223]. Dragan proposed an open-source adaptive system for customising low-cost IED interactions between IoT and electrical applications. This IED can be used to monitor a low-voltage intelligent electronic device (IED) system with an infinite number of sensors, and it is available on the Internet of Things (IoT) [224].

The existing data acquisition systems are still expensive and need at times for an unpredictable design or limitations on their connection, even those called economic circuits if they are utilized for lower levels of power production. Different innovations depend on the on-board web server to

process the information through Ethernet. These systems are compelled by lower memory to store a lot of information, and the customers just view constrained information Many existing wired and wireless data acquisition systems rely on the expensive and complicated LABVIEW license software [21]. The wired DAQ systems are only accessible close to the PV systems, and wireless data acquisition systems can monitor and record the limited number of parameters at a high cost. There are only a few open-access wireless data acquisition systems that can monitor and record low voltage and low current. [22]. Table 2.12 shows the comparison between the proposed IoT enabled data acquisition system and some exiting data acquisition systems.

Table 2.12 Some exiting data acquisition systems for the PV system.

Author	Network	Hardware	Software	Cost ($)	Parameter	Function
Koutroulis et al. 2003 [211]	Wired	NI DAQ	LabView	Not mention	T_A, G_I, RH, S_{WC}, T_S, S_{HF}, S_{Dir}, , S_v, BP, $V_{A,mod,}$ I_A, V_S, I_S, W/GV, W/GC	Observing PV, temperature and wind generator parameters.
Forero et al. 2006 [213]	Wired	NI modules	LabView	Not mention	I_{AC}, V_{AC}, I_A, $V_{A,MOD}$, T_A, G_I	Observing the impact of solar irradiance and ambient temperature on PV performance.
Ulieru et al., 2010 [225]	Wired	PCI 6023 E Automatic variable resistor (AVR)	LabView	Not mention	$V_{A,MOD}$, I_A	Observing stability and reliability of PV system
Torres et al., 2012 [226]	Wired	DAQ, MORNING STAR charge controller	LabView	Not mention	$V_{A,MOD}$, $V_{A,REG}$, V_S, $V_{L,}$ I_A, I_S, I_L, T_{MOD}, G_I,	Observing the impact of solar irradiance and module temperature on PV performance.
Chouder et al., 2013 [227]	Wired	Agilent 34902A	LabView	Not mention	$V_{A,MOD}$, V_{AC}, I_A, I_{AC}, $G_{I,}$ T_A	Observing the impact of solar irradiance and ambient temperature on PV performance.
Congedo et al., 2013 [228]	Wired	PLC Siemens inverter (330.0.TL-IT) and scada WINCC	Not mention	Not mention	$V_{A,MOD}$, V_{AC}, I_A, I_{AC}, G_I, T_A, P_A, T_{MOD}	Observing the impact of ambient temperature, relative humidity, module temperature and wind speed on PV performance
Fuentes et al., 2014 [229]	Wired	Arduino UNO	Arduino IDE	Not mention	$V_{A,MOD}$, V_u, V_S, V_L, V_{BU}, I_A, I_L, I_{BU}, P_{BU}, P_A, $P_{L,}$ I_{TU}, I_{FU}, P_{TU}, P_{FU}, I_{Ts}, I_{Fs}, P_{Ts}, P_{Fs}, T_A, G_I, S_W, T_{MOD},	Observing the impact of irradiance, ambient temperature, humidity, wind speed and relative on PV performance

Ferdoush and Li, 2014 [230]	Wireless	Arduino UNO	Arduino IDE	Not mention	T_A, RH	Monitoring air temperature and relative humidity
Touat et al., 2016 [22]	Wireless	Microcontroller, DC-DC converter, Sensors	Arduino IDE	1000	Dust, T_A, T_{MOD}, RH, G_I, S_W, $V_{A,MOD}$, I_A	Observing the impact of dust on PV performance
Rezk et al 2017 [231]	Wired	DAQ NI6009, MPPT Charge Controller	LabView	Not mention	$V_{A,MOD}$, I_M, P_M	Collecting and displaying the electrical output parameters of stand-alone PV system
Pachauri et al. 2021 [21]	Wired	Arduino UNO	Arduino IDE	Not mention	$V_{A,MOD}$, I_A	Collecting PV panel voltage and current

CHAPTER 3

REAL-TIME IoT ENABLED DATA ACQUISITION SYSTEM

This chapter discusses all the design steps of the real-time IoT enabled data acquisition (DAQ) system and also tests the developed IoT enabled DAQ system's viability in severe environments.

3.1 Requirement of IoT based data acquisition system

The literature review revealed that using a PV module in an outside application according to the manufacturer's specifications resulted in errors and may lead to system dissatisfaction later on. Solar PV systems have a major fault in that they lose performance due to external factors, making them unsuitable for desert or remote locations. In a remote PV system, real-time monitoring systems are essential for gathering all the variables necessary for predicting system performance and optimization. A literature survey reveals that many existing research uses expensive and difficult-to-access wired data gathering equipment that uses LABVIEW licensing software [21]. The wired DAQ systems are only accessible close to the PV systems. There are some wireless data acquisition systems that can monitor and record a limited number of parameters at a high cost. There are only a few open-access wireless data acquisition systems that can monitor and record low voltage and low current. [22]. Existing data acquisition systems, which are either continuously connected to the power supply or manually managed, necessitate the presence of humans to operate the system near the PV plant. The existing data acquisition systems are still expensive and need at times for an unpredictable design or limitations on their connection, even those called economic circuits if they are utilized for lower levels of power production. Different innovations depend on the on-board web server to process the information

through Ethernet. These systems are compelled by lower memory to store a lot of information, and the customers just view constrained information.

3.2 Essential parts of developed data acquisition system

The developed internet of things (IoT) based data acquisition system can overcome the aforesaid challenges. Open-access software and cloud services were used to construct the suggested IoT-enabled data acquisition system. The developed DAQ system can be turned on and off using a Wi-Fi enabled switch, depending on the requirements. We can not only conserve energy but also extend the life of sensors in this way. The suggested DAQ system's information can be viewed from any location. The proposed IoT DAQ system has been planned for long-term data collection of the PV system's variables. Fig. 3.1 shows the block diagram of a suggested IoT based data acquisition system. The system consists of an ESP8266 Wi-Fi module, a temperature and humidity sensor DHT 22, an anemometer, a dust sensor, LM35 temperature sensor, INA219 sensor, and the cloud platform ThingSpeak. ThingSpeak displays variables such as generated power, voltage, current, panel temperature, humidity, ambient temperature, solar radiation, air dust density, and wind speed. This information can be accessed by mobile phones, tablets, and workstations linked to the internet via Thing Speak APIs from anywhere in the world. The proposed wireless data acquisition system can be remotely switched on and off. Table 3.1 shows the parts of proposed wireless DAQ and Table 3.2 shows the technical specifications of components of the proposed IoT enabled DAQ system. Fig. 3.2 shows the flow chart of the developed data acquisition system.

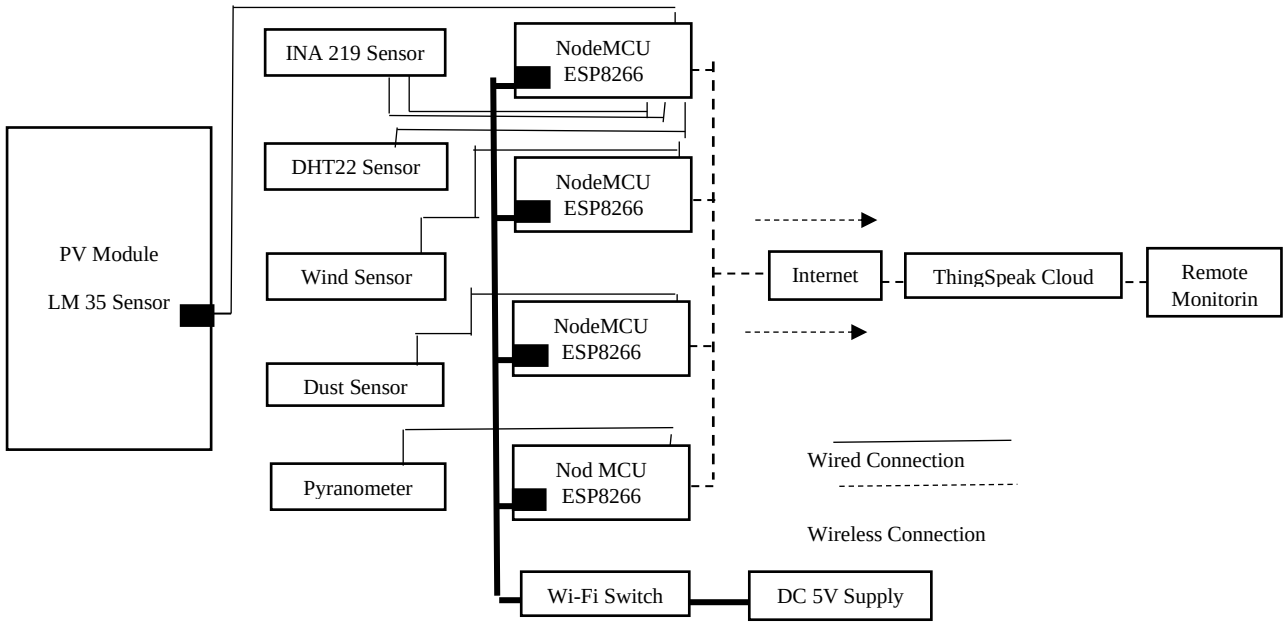

Fig.3.1 Block diagram of Proposed IoT based Data acquisition system for PV module

Table.3.1 Components of Proposed IoT DAQ

Components	**Quantity**	**Hardware /Software**	**Remark**
Node MCU ESP 8266	5	Hardware	Wi-Fi module
INA 219 Sensor	1	Hardware	To sense Voltage, Current
DHT 22 Sensor	1	Hardware	To sense Temperature, Humidity
LM 35 Sensor	1	Hardware	To sense panel Temperature
Anemometer	1	Hardware	To sense wind speed
Dust Sensor	1	Hardware	To detect ait dust particles
Pyranometer PYRA300	1	Hardware	To detect solar irradiance
Battery/Variable resistance	1	Hardware	Load
Relay Module	1	Hardware	To Control the switch
ThingSpeak	-	-	Cloud Platform
Blynk	-	Software	To Control hardware remotely
Arduino IDE	-	Software	For Node MCU/ESP32

Table.3.2 Technical Characteristics of Components used in proposed Data Acquisition System

Name of Component	Parameters	Specification
	Operating voltage	3.3 V or 5V
	Available GPIO Pins	10
Node MCU ESP8266	RAM	36 kb
Wi-Fi Module	Clock speed	80 MHZ/160MHZ
	MCU	32 bit TenSillica L 106
	Supply Voltage	3.3V to 5.5V DC
	Measure voltage	0 to 26V DC
INA 219 Sensor	Measure Current Range	-3.2A to 3.2A
	Operating Temperature	-40℃ to 125℃
	Accuracy	± 0.5%
	Supply Voltage	7 to 24V DC
	Output voltage	0 to 3V DC
	Range	0 to 1800 W/m^2
Pyranometer PYRA300	Operating Temperature	-40℃ to 65℃
	Accuracy	± 5%
	Transducer	Silicon photodiode
	Operating voltage	3.3 or 5V
	Measurement range	0-100%RH；-40℃-80℃
DHT 22 Sensor	Resolution	16bit（temperature), 16bit（humidity）
	Operating Current	0.3mA
	Accuracy	±0.5℃ and ± 1%
	Operating voltage	4 to 30V
	Output Voltage	up to 6V
LM 35	Output Current	up to 10mA
Temperature Sensor	Accuracy	±0.5ºC
	Temperature Range	-55 ºC-150 ºC
	Supply Voltage	7-24 V
	Max wind Speed	70m/s
Wind Sensor	Accuracy	1m/s
	Resolution	0.1m/s
	Output Voltage	0.4-2 V
	Module	GP2Y1010AU0F
	Type	Optical
Dust sensor	Supply Voltage	3-5 V
	Measurement Range	500µg/m^3
	Sensitivity	0.5V/(100µg/m^3)
	Operating Temperature	-10ºC-65ºC

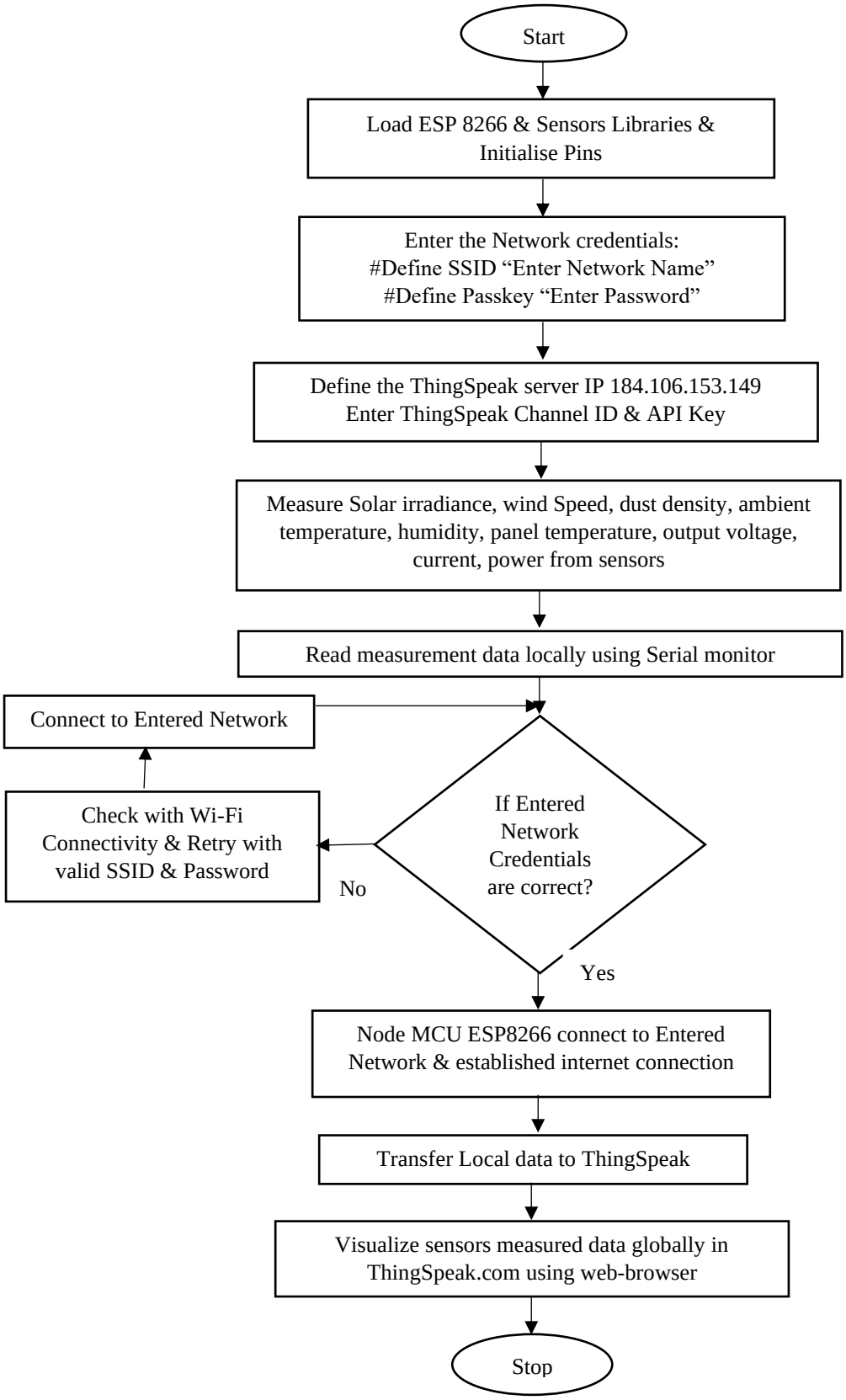

Fig. 3.2 Flow chart of Proposed Data acquisition system

3.3 Calibration Process

Before mounting the overall system, all sensors were verified and calibrated precisely. The values of current, and voltage, read by the INA219 sensor, can be displayed, and compared with the reading of a standard multimeter (Aplab VC97) at the same time. The HTC HD-304 humidity and temperature meter is used to calibrate the DHT22 sensor and LM35 sensor. The DHT22 sensor was calibrated using a vapour produced inside an encapsulated container where both the DTH22 humidity sensor along with the HTC HD-304 was placed. The readings of both the HTC HD-304 meter and the DHT22 sensor are recoded simultaneously. The LM35 sensor was mounting at the rear side of the PV panel using a highly thermal conductive adhesive. The commercially INSPEED VORTEX wind speed sensor was used to measure the wind speed. we used the firm calibration curve for the calibration of dust sensor. we perform the experiments on the sensing element of the GP2Y1010AU0F sensor with different dust levels, which are found to be within the limit of this sensor. Entire calibration results were repeatable.

3.4 Experimental setup

To determine the validity and accuracy of the proposed IoT based data acquisition system, we conducted a small test on a 53 watt polycrystalline solar panel, and the position of the solar PV module was selected so that the PV panel could gather optimum solar radiation as much as possible during the day. The specifications of the test field and the PV panel are given in Table 3.3 & Table 3.4. All the sensors are mounted and attached to the four ESP8266 modules for plotting P-V and I-V characteristics as well as accumulating various information regarding PV system and environmental parameters. Fig.3.3 shows the actual experiment setup of the developed IoT based data acquisition system.

For gathering maximum output power through the year from static PV modules, they must be inclined at an angle equal to the latitude angle of

the location towards the south facing. The PV module will be vertical to the sun every equinox when inclined by the site latitude angle.

Table.3.3 Test location details

Description	**Value**
Place	Academic Block 1, Manipal University Jaipur
Latitude	26.84
Longitude	75.56
Tilt angle	27°
Facing	South

Table.3.4 Technical Characteristics of PV Module

Parameters	**Value**
Type	Poly Crystalline
Short Circuit Current (I_{sc})	2.986 A
Peak Current (I_{mpp})	2.8 A
Open Circuit Voltage (V_o)	22.905 V
Peak Voltage (V_{mpp})	19.1 V
Peak Power (P_{mpp})	53.48 W

3.5 Validation and the performance of the developed IoT Based data acquisition system

Obtaining accurate I-V and P-V attributes has become a necessary part of optimum designing of any PV system. To determine the I-V & P-V curves of the PV module, the variable resistance has been connected with the PV module and gradually increased and recorded the value of voltage and current by the proposed IoT DAQ and standard multimeter at the same time. We found that I-V & P-V curves are almost the same in both methods. Fig. 3.4 and Fig. 3.5 demonstrate I-V and P-V characteristics for the photovoltaic panel by using the proposed IoT enabled DAQ system and standard measuring instrument.

By observing the above, I-V and P-V characteristics for the photovoltaic panel, it can be determined that the developed IoT data acquisition system is accurate and reliable when compared to the traditional method of measurement. Fig. 3.6 represents the real-time information for nine parameters of the PV module and the surrounding climate on the ThingSpeak webpage. The ThingSpeak is an IoT cloud service provider that acts as a host for the assortment of sensors to monitor the detected information at the cloud level and composite a unique element of porting the detected information to the MATLAB R2016a utilizing a channel ID and read API key that is allotted by administrations and ready to follow information at the particular sample at particular intervals.

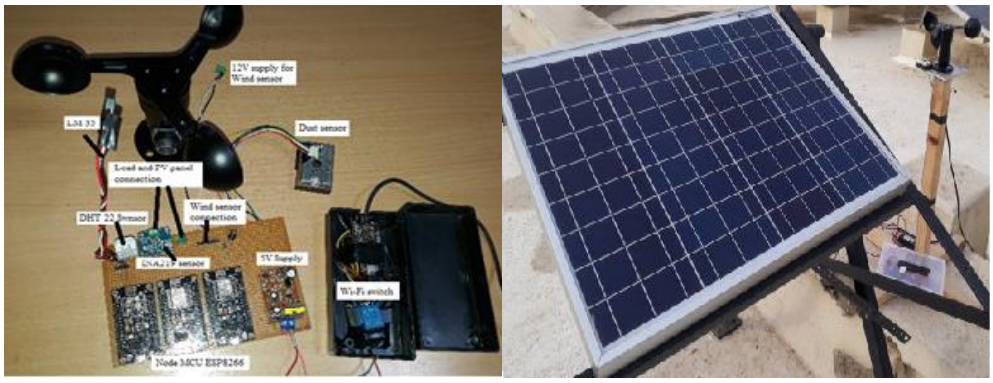

Fig.3.3 Proposed IoT based DAQ system with experimental setup

The existing PV data acquisition systems, which are either continuously connected to the power supply or manually managed, necessitate the presence of humans to operate the system near the PV plant. The developed IoT-enabled DAQ system, which can be turned on and off using a Wi-Fi enabled switch, can save energy while also extending the life of sensors. This method can save 58% of energy (assuming a daily operation time of 10 hours). The voltage and current sensors are used for measuring voltage and current respectively in existing data acquisition systems, only one INA 219 sensor has been utilized for voltage, current, and power measurement in the proposed IoT based DAQ system.

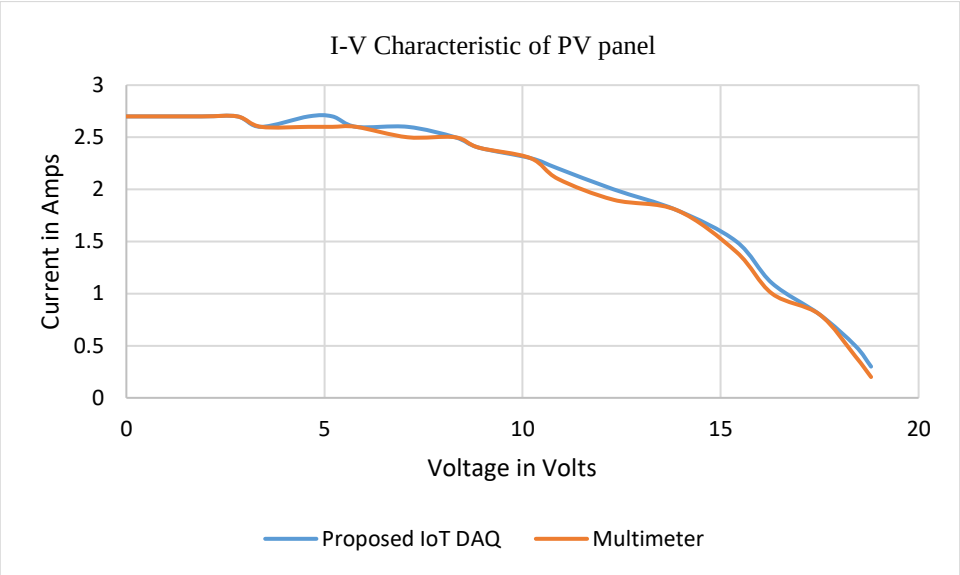

Fig.3.4 I-V characteristics of the PV panel using proposed DAQ and standard multimeter

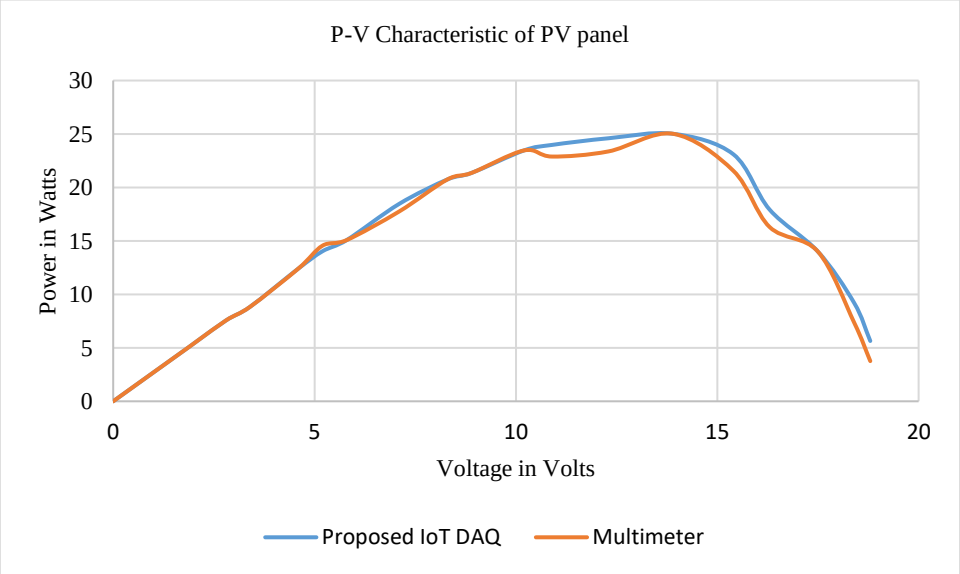

Fig.3.5 P-V characteristics of the PV panel using proposed DAQ and standard multimeter

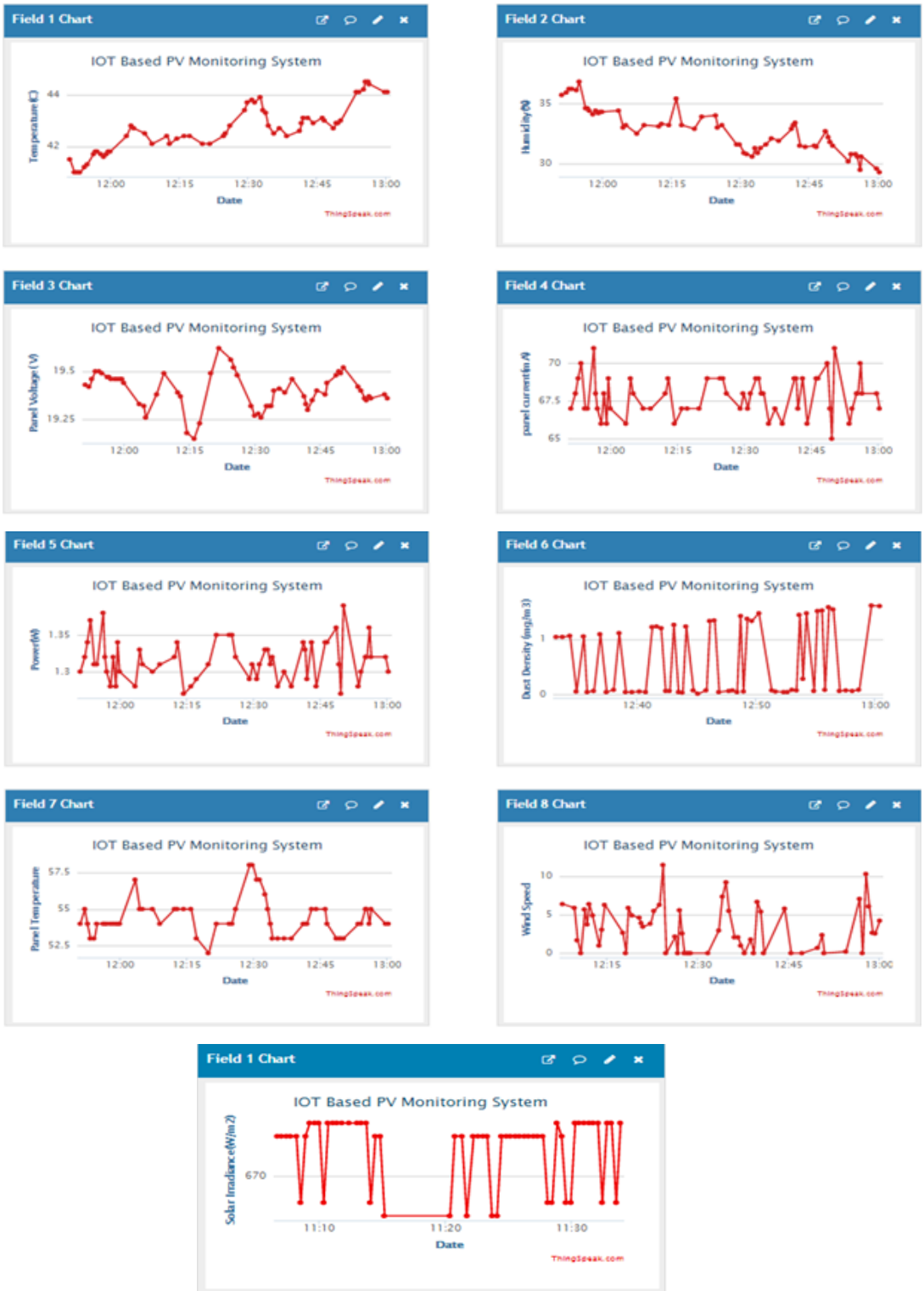

Fig 3.6 Results on ThingSpeak IoT Clouds

Table 3.5 shows the comparison of energy consumption of the proposed IoT enabled data acquisition system with and without a Wi-Fi switch, and Table 3.6 demonstrates the cost estimation of the proposed IoT based data acquisition system that seems very amicable for researche. The technical specifications of the proposed IoT enabled data acquisition system are shown in Table 3.7. Table 3.8 shows the comparison between the existing DAQ with the proposed DAQ system of the PV system.

Table 3.5 Comparison of Energy Consumption of proposed IoT based DAQ with & without Wi-Fi switch.

Period	**Energy Consumption without Wi-Fi switch (kWh)**	**Energy Consumption with Wi-Fi switch (kWh)***	**Energy Saving (kWh)**
One Day	0.12	0.05	0.07
One Month	3.6	1.5	2.1
One year	43.8	18.25	25.55
	Annually percentage saving of Energy		**58 %**

Table 3.6 Cost Estimation of Proposed IoT Based DAQ

Components	**Quantity**	**Rate ($)**	**Total Cost ($)**
Node MCU ESP 8266/ESP32	5	6	30
INA219 sensor	1	6	6
DHT 22 Sensor	1	4	4
LM 35 sensor	1	1	1
Dust Sensor	1	7	7
Anemometer	1	70	70
Pyranometer	1	150	150
Relay Module	1	1	1
Blynk App	-	Open Accesses	-
Arduino IDE	-	Open Accesses	-
ThingSpeak	-	Open Accesses	-

Table 3.7 Technical Characteristics of proposed IoT Based DAQ

Specification	**Value**
Supply Voltage	5-12 V DC
Measure Voltage Range	0-36 V DC
Measure Current Range	0-15 A
Operating Temperature	0℃ to 80℃
Accuracy	± 1%
Nos of Parameters	09

Table 3.8 Comparison between existing DAQ with proposed DAQ system of PV system

Author	**Year**	**Software**	**Network**	**Component**
Ulieru et al. [225]	2010	LabView	Wired	PCI 6023 E Automatic variable resistor (AVR)
Torres et al. [226]	2012	LabView	Wired	DAQ, MORNING STAR charge controller
Chouder et al. [227]	2013	LabView	Wired	Agilent 34902A
Ferdoush et al [230]	2014	Arduino IDE	Wireless	Arduino UNO
Touat et al. [22]	2016	Arduino IDE	Wireless	Microcontroller, DC-DC Converter, Sensors
Rezk et al. [231]	2017	LabView	Wired	DAQ NI6009, MPPT Charge controller
Parra et al. [232]	2018	Arduino IDE	Wired	ATmega328, Raspberry- Pi, RTC
Jiang et al. [233]	2019	Arduino IDE	Wireless	Arduino UNO, RS-232 interface
Motahhir et al. [234]	2019	Arduino IDE	Wired	Arduino UNO, Servo motor, LDR
Pachauri et al. [21]	2021	Arduino IDE	Wired	Arduino UNO, Sensors
Proposed DAQ System	**2022**	**Arduino IDE**	**Wireless**	**ESP8266/ESP32, Sensors**

3.6 Discussion

Real-time tests revealed that the acquired monitoring information is acceptable, economical, and reliable. The developed IoT enabled data acquisition system can record nine parameters with a voltage range of 0-36V and a current range of 15A. This system can save 58% of energy (assuming a daily operation time of 10 hours). The future of MATLAB in ThingSpeak and the other way around gives an even more profound investigation and examination of detected information at a basic level that is to deal with the encompassing condition where the parameters are imperative to measure. This research shows a one-of-a-kind stage interface for the solar PV monitoring system to catch estimation from numerous parameters and investigate outwardly progressively and synchronize mode, which is the crucial aspect for fast fluctuating information streams. This work offers esteemed endeavours towards the choice of a progressively proficient and easy-to- use monitoring system in the solar PV module. The designed device is valuable to the analysts for comprehending the conduct of various photovoltaic technologies in normal conditions and for the investigation of degradations in PV modules concerning age and natural impacts.

CHAPTER 4

PERFORMANCE ANALYSIS OF PV SYSTEM IN DIFFERENT CLIMATE CONDITIONS

This chapter discusses the investigation of the performance of a 106W PV system under Jaipur weather conditions over a one-year period using an IoT enabled monitoring system. The performance of installed PV systems at different places depends on the atmosphere and local conditions. The performance and energy production potential of a site without a thorough examination is difficult to forecast. It becomes critical to conduct field experiments and scientific data analysis at the location. In this chapter, the authors present details on the behaviour of PV panels in various seasons in the Jaipur (semi-arid) region. The study period is split into four seasons: post-monsoon, winter, summer, and monsoon.

4.1 Site Selection

There are six major climatic subtypes in India: hot and dry, hot and humid, mild, cool and clouded, cool and sunshine, and composite. The meteorological department of India follows the international standard of four seasons: winter, summer, monsoon (rainy) season, and a post-monsoon period. The primary goal of these studies is to investigate the behaviour of solar modules in the various seasons and climatic conditions of Jaipur, as well as the effectiveness of the proposed self-cleaning using developed IoT based data acquisition system.

Rajasthan, India's largest state, accounts for approximately 10.4% of the country's geographical area. Desert land covers around 2,08,110 km^2 in Rajasthan, which receives the highest solar radiation, i.e., 6.0-7.0 kWh/m^2 in the country, as shown in Fig.4.1. Table.4.1 shows the installed solar power capacity in India. For these studies, we chose Jaipur, the capital of Rajasthan, because its climate conditions almost meet India's common climate conditions. The summers in Jaipur are extremely hot, while the

winters are extremely cold. The maximum temperature in May is between 44°C and 45°C.

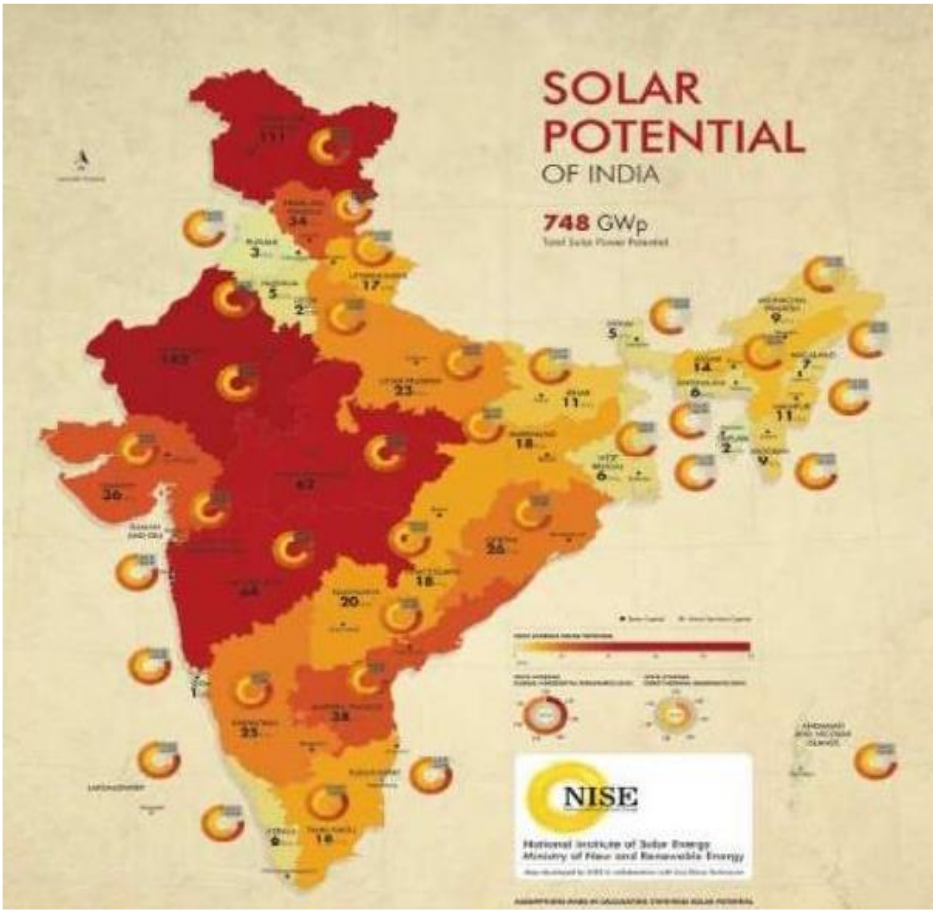

Fig. 4.1 Solar potential of India [137]

Table.4.1 Installed Solar Power Capacity in India [137]

State	MW
Rajasthan	14454.70
Gujarat	7806.80
Karnataka	7597.92
Tamil Nadu	5690.79
Telangana	4621.07
Andhra Pradesh	4390.48
Maharashtra	2753.3
Madhya Pradesh	2746.27

In the summer season, when the daytime temperature rises to 4-6°C above the normal ambient temperature, a heatwave prevails. The maximum temperature rise begins in mid-March and peaks in May. The precipitation increases as the thundering activity begins in mid-June, and the rainiest months are July and August. In October and November, the rainfall drops sharply. The precipitation has drastically decreased from October to March. In June, the rainfall started to gradually and in August it reached its peak. The downward trend in minimum temperatures starts in the middle of September and runs until January. The coldest month is December. From mid-December to mid-March, temperatures are low. Minimum winter temperatures range between 9 and 10°C. In the morning, dung and fog are present.

4.2 Experimental Setup

To examine the performance of solar panels in various seasons and Jaipur's weather conditions, we installed two polycrystalline silicon PV panels of 53W each on the roof of Manipal University Jaipur. The solar panels were connected in parallel, and the output terminals of the PV system were connected to the resistive load. The PV solar panels have an inclination of 27^{o} to the south and are located at a latitude. During the study, two commercial PV panels were used with the specifications shown in Table 4.2. Table 4.3 shows the specification of the test location.

Table.4.2 Specifics about the test location

Description	**Value**
Place	Academic Block 1, Manipal University Jaipur
Latitude	26.84
Longitude	75.56
Tilt angle	27°
Facing	South

Table.4.3 Specifications of solar panels used in the experiment at standard testing conditions

Parameters	**Value**
No.	2
Type	Poly Crystalline
Short Circuit Current (I_{sc})	2.986 A
Peak Current (I_{mpp})	2.8 A
Open Circuit Voltage (V_o)	22.905 V
Peak Voltage (V_{mpp})	19.1 V
Peak Power (P_{mpp})	53.48 W

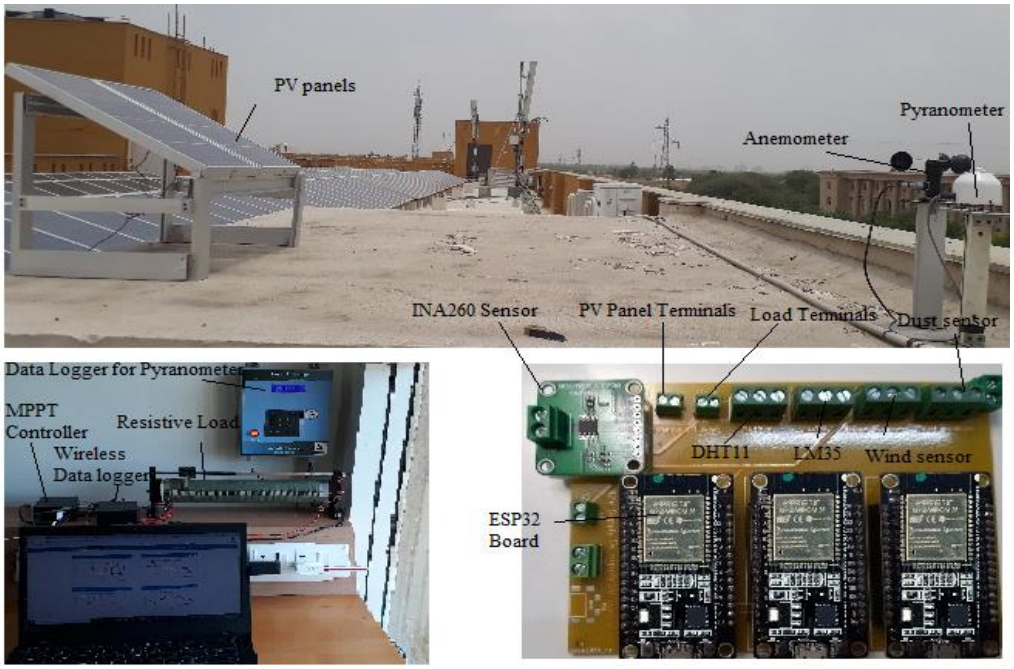

Fig.4.2 Experiment setup along with IoT data logger and load

The PV modules' position was chosen to allow them to capture as much sunlight as possible during the day. An IoT based monitoring system has been used, which collects real-time information and sends it to the ThinkSpeak cloud server. The system comprises of three ESP32 modules, the DHT11 temperature and humidity sensor module, the INA 260 sensor

module, the LM35 temperature sensor, anemometer, and ThingSpeak. For solar radiation, an EKO MS40M pyranometer is used. Fig. 4.2 shows the experimental setup for investigating the performance of the PV system in different climate conditions.

4.3 Data Collection

The developed wireless monitoring system has been used which collects real-time information and sends it to the ThinkSpeak cloud server as shown in Fig. 4.3. This monitoring system has a remote access facility. Before mounting the overall system, all sensors were verified and calibrated precisely. All sensors are then connected and installed to the IoT enabled data acquisition system for gathering various parameters such as wind speed, dust level, relative humidity, ambient and PV surface temperatures, power output. The calibration process was repeated every month.

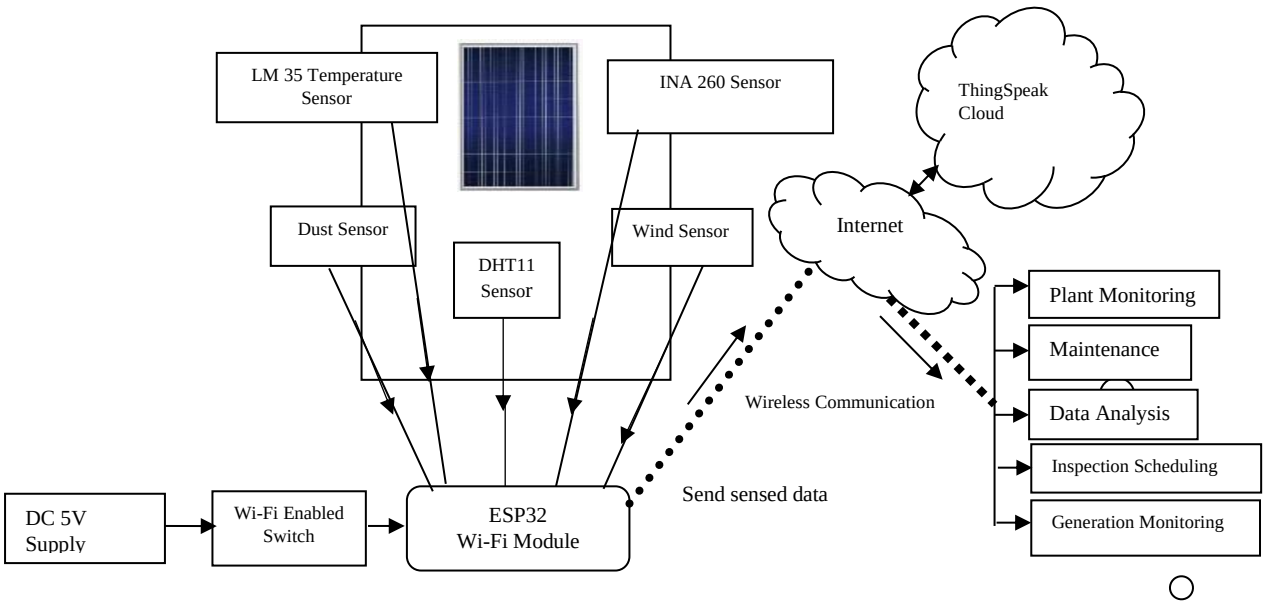

Fig.4.3 The architecture of wireless DAQ system for monitoring of PV System

The period of investigate is split into four seasons for better understanding, such as post-monsoon (From the middle of September to

the middle of December), winter (From the middle of December to the middle of March), summer (From the middle of March to the middle of June), and monsoon (From the middle of June to the middle of September). To investigate the performance of the PV panel in different seasons, two 53W PV panels, connected in parallel, were cleaned on the first day of the start of each season, and noted the values of voltage, current, power, and surface temperature of the panel, and environmental parameters for the entire season. On the last day of the season, the PV & VI curves for dirty and cleaned PV panels were drawn. First, we collected the data from VI and PV curves of a dusty solar panel, then cleaned the solar PV panel and collected the data from VI and PV curves. Data is taken for dusty panels and cleaned with the same solar radiation, ambient temperature, and relative humidity.

Measurements were recorded at an interval of 5 minutes from 7.00 am to 6.00 pm for a period of one year (Sept. 2019 to Sept. 2020). The values have been collected from 7:00 am to 6:00 pm, as the solar radiation appears to be within these times. We calculated the operating efficiency based on average solar radiation, average output power and PV system's area during the time periods or seasons [261,262] and compared the average efficiency of PV panels on the first and last days of the seasons at STC conditions. The average efficiency of the first day of each season was used as a reference in this study. The uncertainties of the measuring sensors INA260 (U_1), anemometer (U_2), pyranometer (U_3), DHT11 sensor (U_4), LM35(U_5) sensor and multimeter (U_6) used in this experiment are shown in Table 4.4.

Table 4.4 Standard uncertainties for the components

U_1(%)	**U_2(m/s)**	**U_3(W/m^2)**	**U_4**	**U_5(°C)**	**U_6(%)**
0.5	1	1.5	0.5°C for Temperature 1% for Humidity	0.5	0.5 for Voltage 1.0 for Current

4.4 Results and Discussion

The study was performed on a 106 W solar photovoltaic (PV) system setup on the rooftop of Manipal University in Jaipur, Rajasthan, India. From Sept. 2019, PV modules have been installed and subjected to soil and floating dust particles until Sept. 2020. as said above. We cleaned the PV panels on the first day of the start of each season. The primary objective of the PV system was to investigate the behavior of solar modules in Jaipur's various seasons and climatic conditions.

Season, latitude, cloudiness, and air dust density are just a few of the site-specific factors that influence PV system performance. A thorough examination of the behavior of the PV systems will provide useful data to predict future performance to improve the planning and management of power system requirements.

The behavior of PV panels varies, corresponding to variations in temperature and irradiance. The panel temperature (T_P) and dust accumulation play a considerable part in the degradation of the generation of energy from the PV system. The actual output power is observed to be higher in summer and the monsoon because of good radiation availability compared to post-monsoon and winter. Fig. 4.4 shows the average values of ambient temperature, relative humidity, wind speed, solar radiation, air dust density, and panel temperature of all four seasons from 7.00 am to 6.00 pm for a duration of one year (Sept.2019 to Sept.2020). Fig.4.4 reveals that the solar radiation, ambient temperature, wind speed, air dust density, panel temperature, and humidity are different during different periods of the study, and therefore the PV output power is the corresponding.

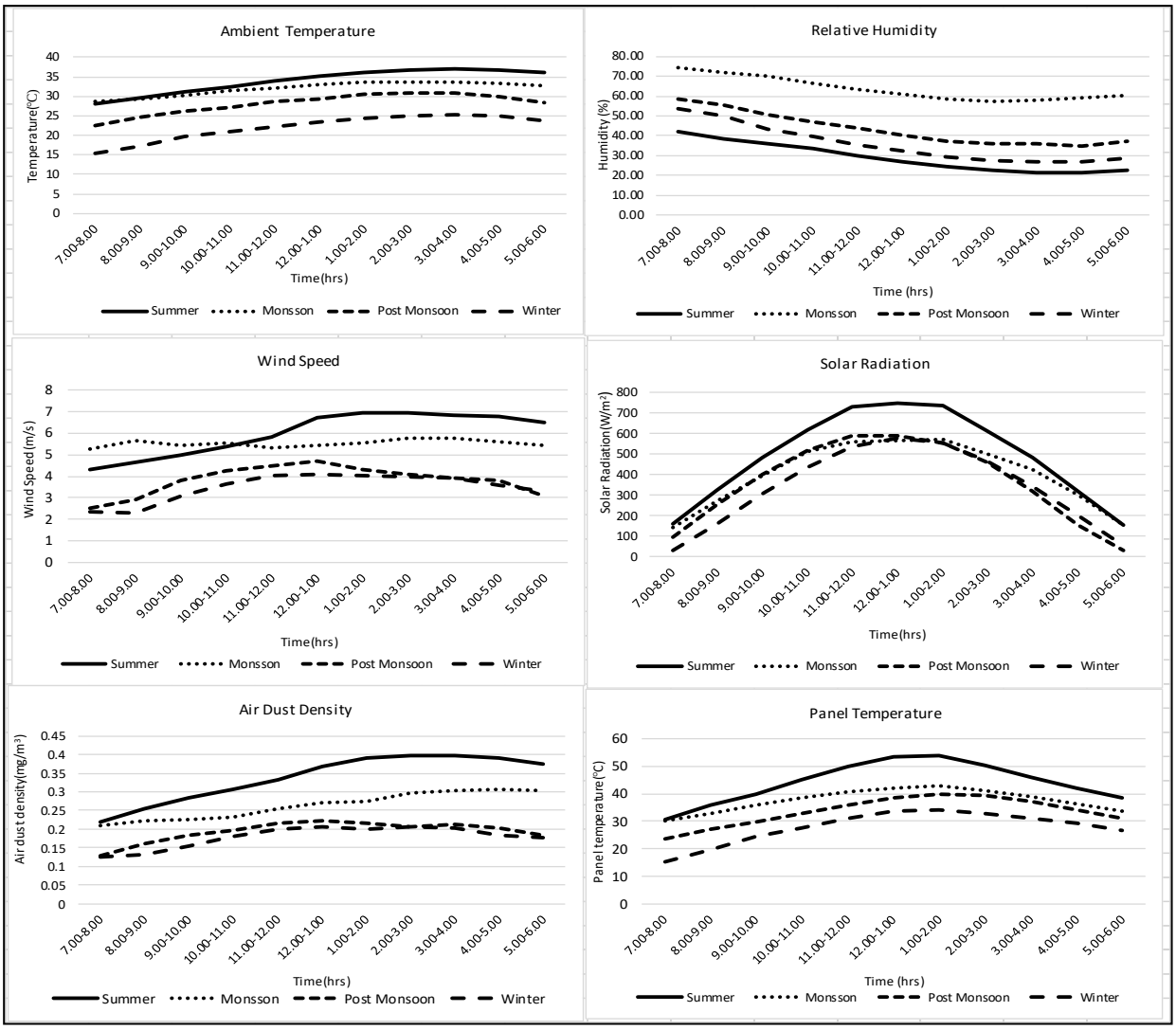

Fig.4.4 Average values of Ambient temperature, Relative Humidity, Wind Speed, Solar Radiation, Dust density, Panel temperature of all four seasons from 7.00 am to 6.00 pm duration of one year (Sept. 2019 to Sept. 2020).

At various stages of the study, the PV panels' panel temperatures (T_P) and the formation of dust on the panel surface are important sources of variable panel efficiency patterns, which affect the PV system output. In summer, the panels operate near maximum output between 10:00 a.m. and 2:00 p.m., and in monsoon, post-monsoon, and winter, the panels operate near maximum output between 11.00 a.m. and 2.00 p.m., 1.00-3.00 p.m.,

and 12.00-1.00 p.m., respectively. Because of the increasing sun intensity, the maximum power is always about 12:00 between September 2019 and September 2020. The maximum solar radiation of 1112 W/m^2 was noted in August. The maximum solar radiation measured during the summer was 1098 W/m^2. Solar radiation in the post-monsoon and winter seasons was measured at 908 W/m^2 and 835 W/m^2, respectively. During the research period, the annual average solar radiation was 388.25 W/m^2. Summer, monsoon, post-monsoon, and winter solar radiation averaged 485 W/m^2, 404 W/m^2, 360 W/m^2, and 334 W/m^2, respectively. April was the month of the highest average solar radiation with a value of 521 W/m^2, whereas the second highest value of average solar radiation was 509 W/m^2, which was recorded in the month of October. The sunshine period was lower during July and August because of the monsoon season and the winter sunshine period is also lower because of the axial shift of the Earth.

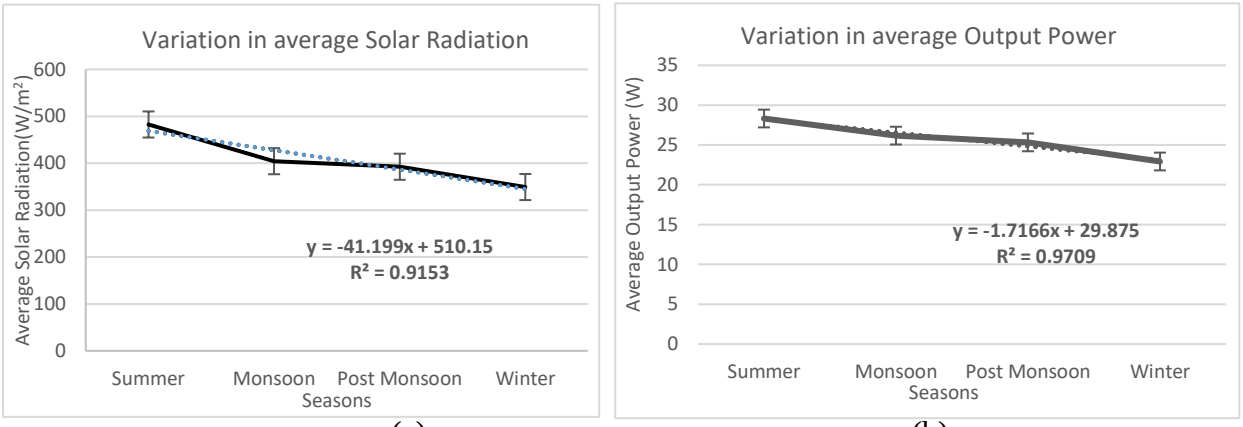

(a) (b)

Fig.4.5 (a) Variation in Solar Radiation with seasons (b) Variation in Output Power with seasons (dotted lines represent linear regression lines and bars represent standard errors.

Fig. 4.5 shows that the average solar radiation and average output power vary linearly with the seasons with nearly a unity correlation (r^2=0.915) and (r^2=0.970) respectively. The average solar radiation and average output power of 28.32 W & 485.05 W/m^2 in summer, 26.17 W & 404

W/m^2 in the monsoon, 25.31 W & 359 W/m^2 in the post-monsoon and 22.92 W & 333.76 W/m^2 in winter have been noted.

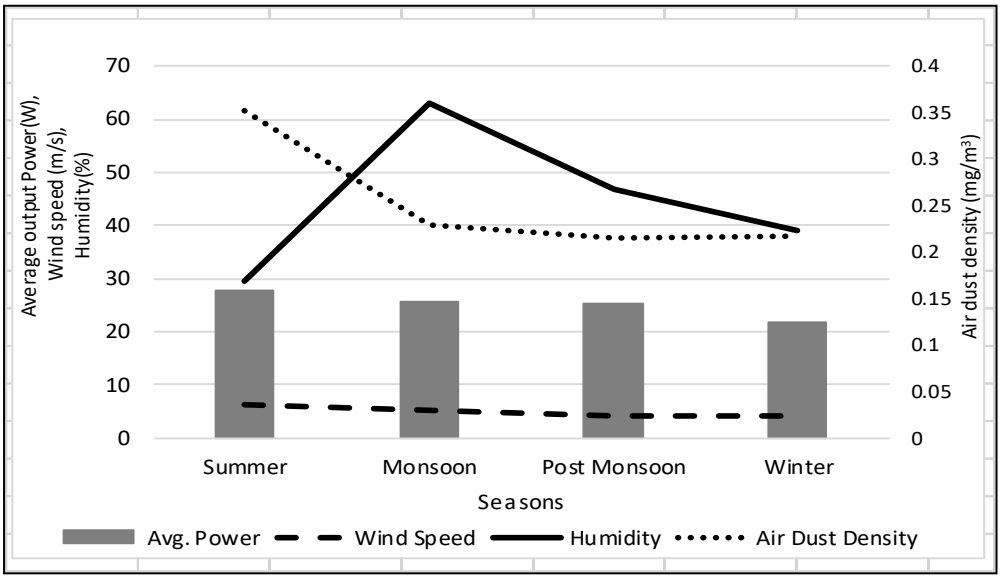

Fig.4.6 Variation in airborne dust density in different seasons

The average values of air dust density and wind speed have been recorded at 0.35 mg/m^3 and 6.08 m/s respectively in summer, which is the maximum as shown in Fig. 4.6. Fig.4.4 shows that air dust density is very high during summer, especially in the afternoon, because of high wind velocity and low relative humidity. The average airborne dust density of 0.352 mg/m^3 in the summer season, 0.235 mg/m^3 in the monsoon season, 0.215 mg/m^3 in the post monsoon and 0.217 mg/m^3 has been recorded as shown in Fig.4.6. We noticed that the dust accumulation on the PV panels, which mainly depends on air dust density, plays a considerable part in degradation of the generation of output energy of the PV system. In the summer, the average air dust density was 0.35 mg/m^3, reducing efficiency by 24.5% over four months. Despite the decrease in air dust density in winter, especially in the month of January, the reduction in efficiency of the panel is high, because bird-droppings are more in this period. In the summer, rising ambient temperature reduces relative humidity, as shown

in Fig.4.4. During the summer, a minimum relative humidity of 6.61% was recorded. During the monsoon season, humidity reached a peak of 98.17%. The dust deposition on the PV panel's surface also depends on the wind velocity and humidity.

It is observed that in the monsoon season, humidity aids in the reduction of air dust density by making it damp and unable to float in the atmosphere. But in the case of PV modules, it gives dust a sticky character, which prevents it from moving around and increases the dust deposition rate on the PV modules. The wind has a considerable impact on the accumulation of dust on the panel's surface as well as its removal. The wind functions as a dust-carrying agent. Low-speed wind can deposit dust on the solar module surface, whereas high-speed wind can clean it [55,56]. In the month of August, the maximum average humidity of 72.7% and the minimum average airborne dust density of 0.12 mg/m^3 have been recorded.

The panel efficiency varies differently in different seasons. The average maximum efficiency value is 10.55%, which takes place during the summer between 9:00 a.m. and 10:00 am, 11.03% during the monsoon between 12:00 and 1.00 p.m., 12.42% during post-monsoon between 1.00 p.m. and 3.00 p.m. and 12.16% during the winter between 12.00 and 1.00 p.m. as shown in Fig.4.7.

The ambient temperature and panel temperature in summer remain high. On the 4th of June 20, the extreme ambient temperature was 44.3°C. We found that the rear surface temperatures that directly affect the efficiency of the PV panel are significantly higher than the environmental temperature, especially in summer, where 6.08 m/s is the average speed of the wind, which converts into a heatwave, plays a significant role in boosting the temperature of the solar panel apart from ambient temperature and solar radiation as shown in Fig.4.7. The output current increases exponentially as the temperature of the solar panel rises, whereas the voltage output decreases linearly. The generated power

obviously decreases as we move from March to June due to the increase in panel temperature and the accumulation of dust on the panel's surface. Summer, monsoon, post-monsoon, and winter maximum panel temperatures were 71°C, 66°C, 55°C, and 48°C, respectively.

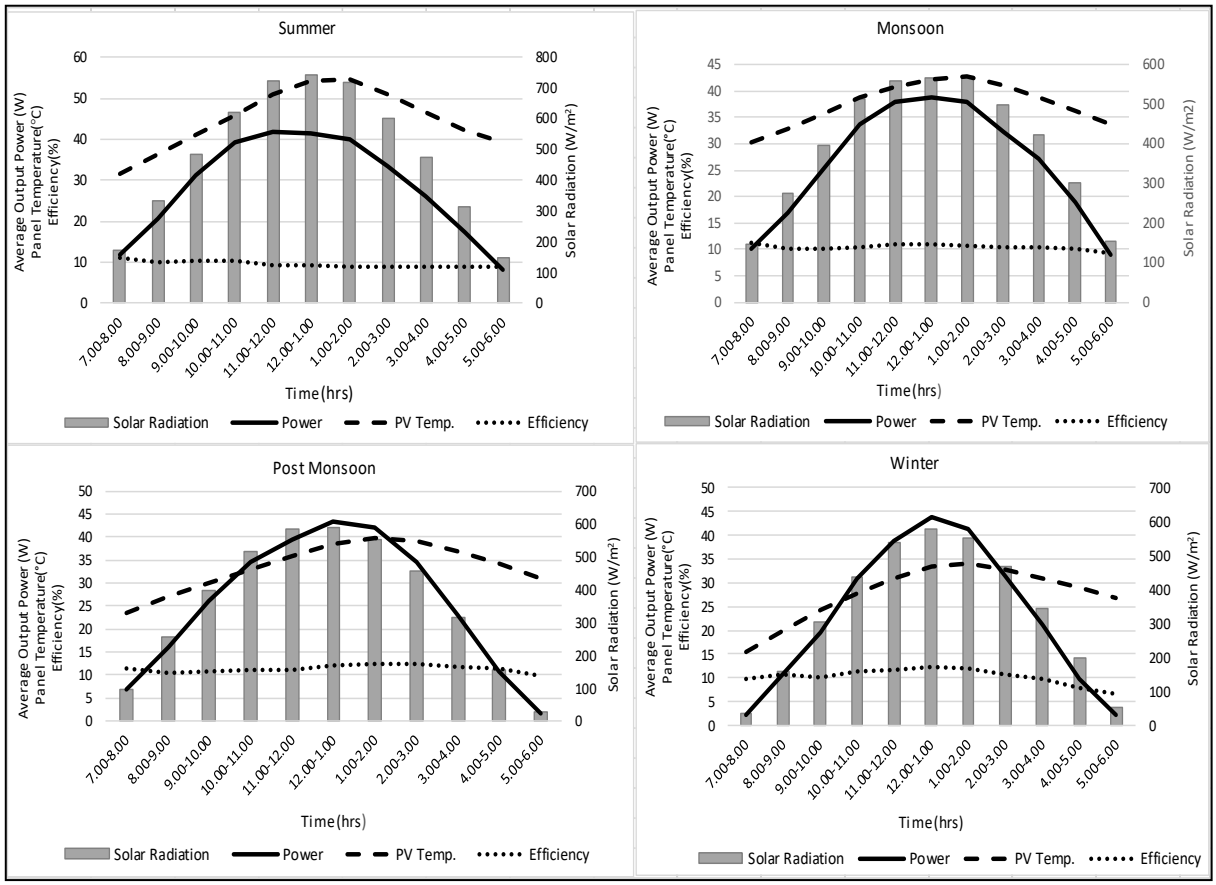

Fig.4.7 Average values of Solar Radiation, Output Power, Panel temperature, Efficiency of all four seasons from 7.00 am to 6.00 pm duration of one year (Sept. 2019 to Sept. 2020).

It was also observed that there was a difference between the front panel temperature and the back panel temperature. When the temperature of the back panel and the front surface were measured simultaneously, the back panel temperature was 62.9°C and the front surface temperature was 58°C. Fig.4.8 shows the thermal images of the front glass surface and back panel surface measured by the Bosch Professional Thermal imaging camera GTC400 C.

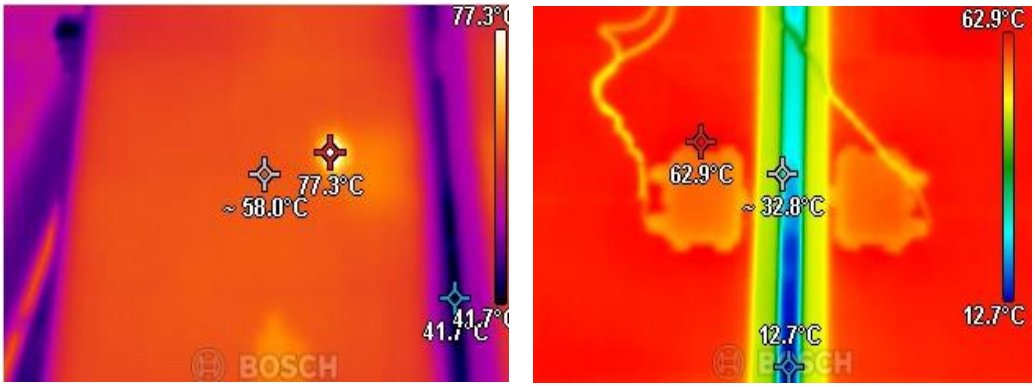

(a) Front surface of the PV panel (b) Back surface of the PV panel

Fig.4.8 Thermal images of front glass surface & back surface of the PV panel

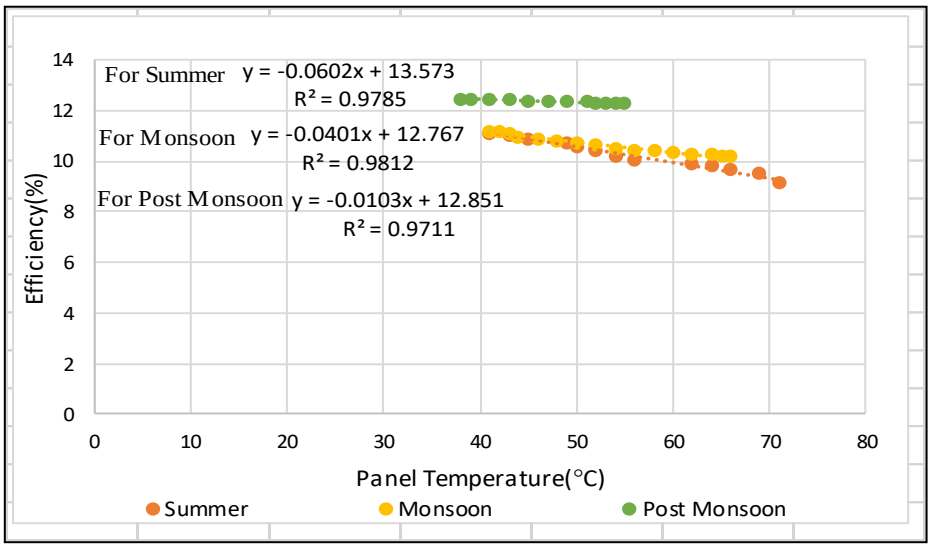

Fig.4.9 Correlation between PV panel temperature and efficiency in summer, monsoon, & post monsoon seasons

The PV panels' maximum efficiency is reached at T_P of 41°C in the summer and 48°C in the winter. In the summer, when the temperature rises above 41°C, panel efficiency drops by 0.06% for every degree. When T_P > 42°C, panel efficiency drops by 0.04% for every degree the temperature rises during the monsoon. For T_P > 39°C, panel efficiency decreases by 0.01% for every degree the temperature rises in the post-

monsoon period, as shown in Fig.4.9. In the winter, however, the modules achieve maximum efficiency with no loss of efficiency at a T_P of 48°C. The main reason for this is the regular natural cooling.

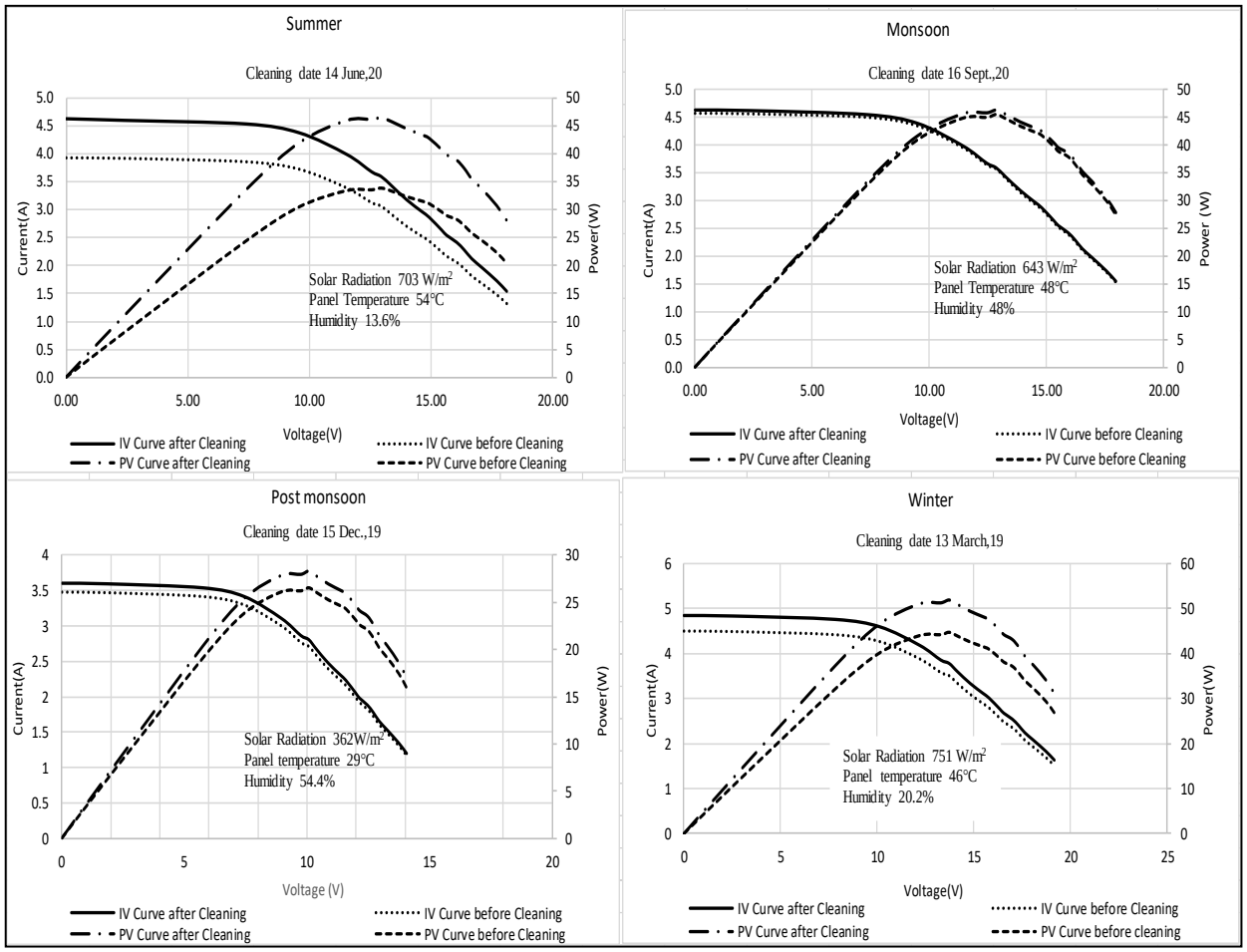

Fig.4.10 V-I & P-V curves for clean & dusty panels at the end of four seasons

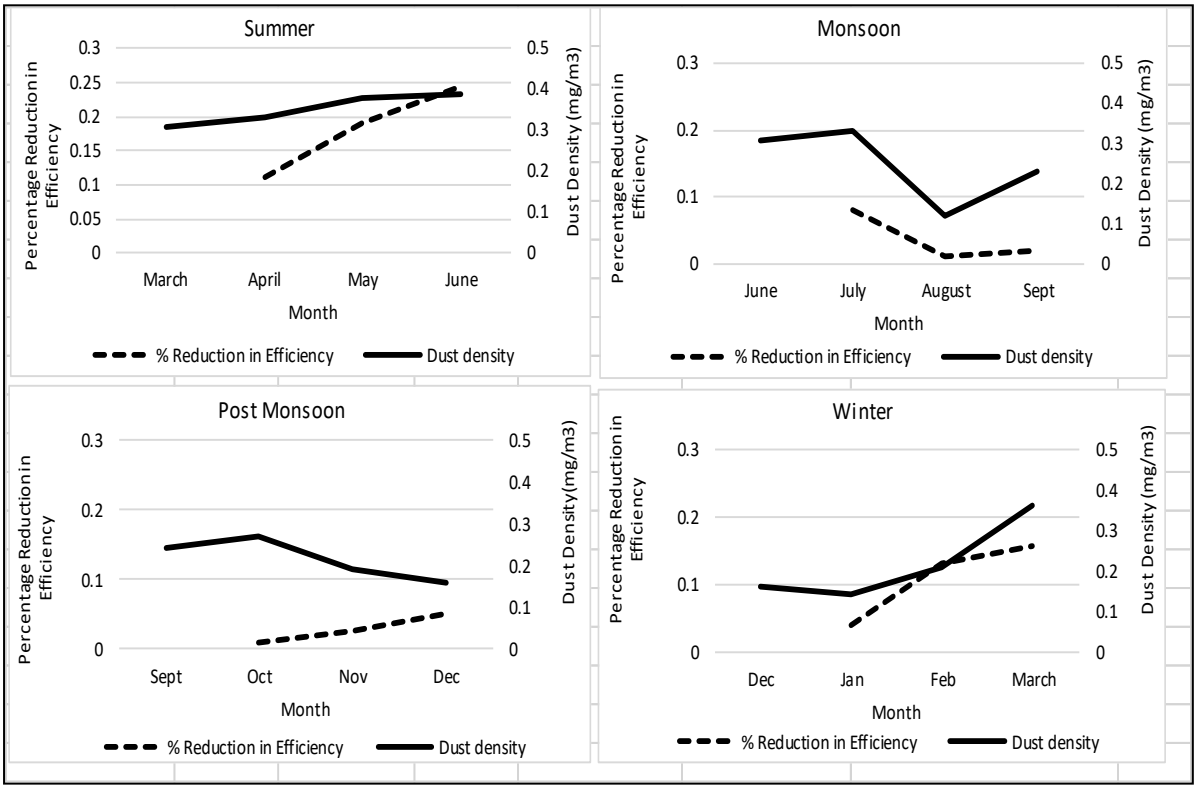

Fig.4.11 % Reduction in efficiency and air dust density month wise of all four seasons

In the summer, the average power was 33.5W in March, but after about four months, the average power was reduced to around 22W. The effect of the dirt on the panel reduces the amount of solar radiation on the surface of the panel and can be attributed to this. There were four dust storms that were observed in the months of May and June. The PV Panel's maximum power output increased rapidly, after cleaning the surface on 14th June, from 33.86W to 46.65W, due to the slight increase in sunlight and similar weather conditions. Then power begins to decrease with the soiling of panels. Fig. 4.10 shows the experimental V-I and P-V curves for dirty and washed PV panels at the end of four seasons. It should be noted that similar data was acquired for dusty and clean panels under the same sun irradiation, ambient temperature, and relative humidity conditions. It demonstrates that the power gain after cleaning is primarily due to a rapid

increase in short-current current, as shown in Fig. 4.10. We can conclude from the preceding discussion that an exposure of 12 months of the PV panels under different seasons in Jaipur reduces the efficiency of the PV system by 24.5% in summer, by 15.6% in winter, by 5.14% in post-monsoon and by 1.95% in monsoon as shown in Fig.4.11.

As usual, Jaipur has undergone climate change, namely rain and wind, during the investigation period. The month with the highest number of rainy days was August. Fig. 4.11 shows that panel efficiency increased in August by 7.5% as compared to July because of the rain, which provided natural cleaning and cooling. In the monsoon season, precipitation increases as the thundering activity begins. Clouds are common these days and humidity is also high, whereas in the post-monsoon, the hot and humid weather starts disappearing and the quality of the air becomes drastically better. The sky is clean, and the quality of solar radiation is improved because of fewer airborne particles. Rain reduces the amount of pollutant particles in the air. In post-monsoon season, the average output power, average solar radiation, and average panel temperature were 25.23 W, 359.15 W/m^2, and 33.4°C, respectively. The reduction in efficiency is only 5.14 %, which is very less as compared to others as shown in Fig.4.11. We received the highest average maximum efficiency, i.e., 11.29%, in this season, as shown in Fig.4.7.

The research, which has been done in Bangalore, revealed that the maximum efficiency of the SPV modules is at 45°C in the summer and 55°C in the winter. For T_p > 45°C in the summer, module efficiency decreases by 0.08% per degree increase in temperature. Maximum efficiency decreases by 0.04% per degree increase in temperature during the monsoon for T_p>35°C. Maximum efficiency is reduced by 0.06% per degree increase in temperature for module temperatures T_p > 38°C during the post-monsoon period [236]. Whereas in Jaipur, the PV panels' maximum efficiency is reached at T_p of 41°C in the summer and 48°C in the winter. In the summer, temperatures above 41°C reduce panel

efficiency by 0.6%. When T_p exceeds 42°C, panel efficiency decreases by 0.04% for every degree of temperature rise during the monsoon.

CHAPTER 5

DESIGN AND PERFORMANCE ANALYSIS OF THE SELF-CLEANING PV SLIDING SYSTEM

In this chapter, a self-cleaning and hail-storm protection mechanism for PV systems is proposed, and the effectiveness of the proposed self-cleaning PV siding system for solar power plant cleaning operations in a semi-desert environment is experimentally investigated. The goal of this research is to increase the efficiency of solar photovoltaic systems while minimising costs, ensuring effectiveness and adaptability. In this study, the cleaning performance of the proposed PV cleaning technique has been evaluated by considering a variety of factors, such as cleaning performance, cost, energy consumption, and land use.

In this developed technique, a self-cleaning PV sliding system covers the PV panels during the night and cleans them twice daily. The proposed self-cleaning PV sliding system also offers hailstorm protection.

5.1 Requirement of the novel Self-cleaning PV system

The decreasing PV panel energy generation efficiencies due to dirt deposition have prompted several researchers to develop practical and economical PV cleaning solutions. The literature mentions a variety of cleaning options, such as manual cleaning, mechanical cleaning, autonomous types & self-cleaning. Manual cleaning is one of the simplest ways to clean PV panels, depending on the water to unsoiled the PV panel’s surface. This traditional method, in addition to being expensive, necessitates the use of labor. Because water is a rare resource in hot desert conditions and desalination of water produces fresh water, which necessitates a large amount of thermal or electrical energy, this is not a good idea.

Studies show that a heavy hailstorm can affect the surface of the front glass and break the solar cell. A hailstorm reduces not just the total electricity generation but also the PV module life. In the last few years, it has been seen that the frequency and size of hailstorms have increased, which is not suitable for PV panels. The protection from hailstorm of the PV system is required.

In hot and dry climates like Rajasthan, water is scarce. The use of precious water resources for the purposes of PV cleaning is therefore contrary to the ultimate aims of economic and environmental sustainability. A cost-effective, efficient, and automated technique for cleaning dirt from PV systems and protecting them against hailstorms is required.

5.2 Essential parts of proposed Self-cleaning PV sliding system

The proposed self-cleaning PV sliding system comprises rails with three trackers, three 20W solar PV panels, rollers, an aluminum protective plate, Stud, a 12V DC motor, bearings, cleaning brushes, mechanical supporter, light-activated LDR, dark-activated LDR sensor, rain sensor, 5V magnetic reed switch sensor, and Arduino UNO. The rollers are attached to both sides of the solar panel to allow the solar PV panels to move easily on the tracker. To prevent rust, we have used plastic rollers here so that they can be moved freely for a long time. A 12-volt DC motor is connected to one end of the stud via a mechanical coupler, and the other end of the stud rests on a ball-bearing. The third solar panel is connected to the stud so that it can move linearly on the track with the motor. The strong threads are used to attach the PV solar panels together so that they can move forward throughout the uncovering process.

The second solar panel is linked to the third panel by a strong thread, and the first panel is linked to the second panel by a strong thread, so that when the motor rotates, the third panel, along with the first and second panels, is covered and uncovered according to command signals which are sent by LDRs and rain sensors. On the protecting plate, we fixed a brush in such a way that it cleans the first panel during covering and uncovering. We mounted the other brushes to clean the downward panels on the edges of the first and second panels. The front and rear views of the proposed self-cleaning PV sliding system are shown in Fig. 5.1 & 5.2. The block diagram of the motor controller of the proposed self-cleaning system is shown in Fig. 5.3.

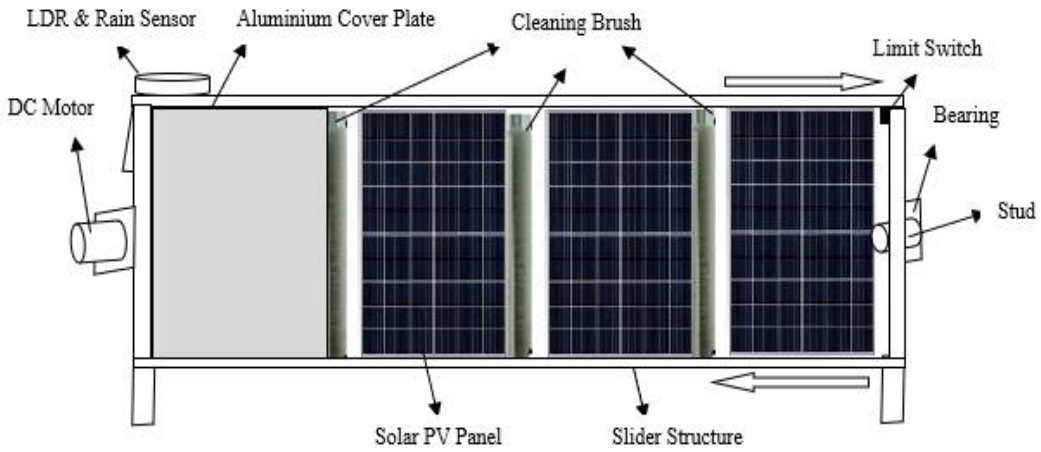

Fig. 5.1 Front view of Self- Cleaning PV sliding System

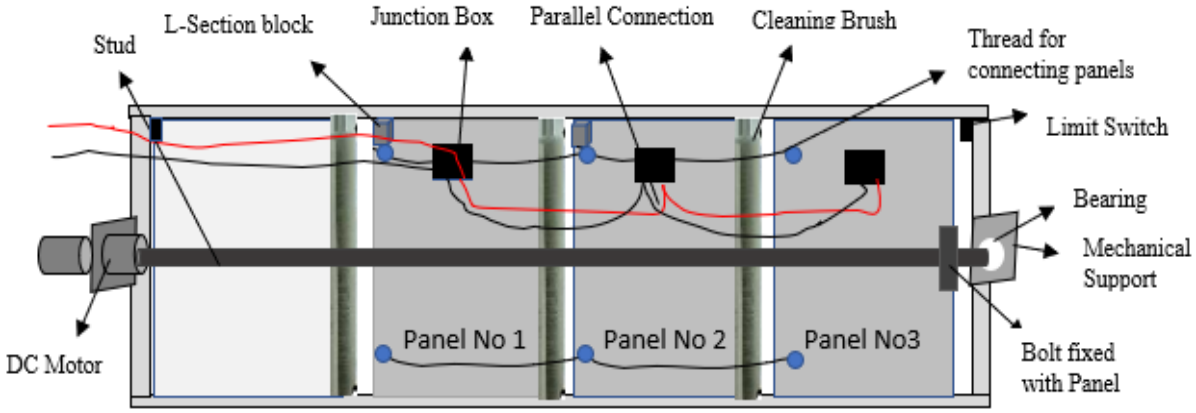

Fig. 5.2 Rear view of Self- Cleaning PV Sliding system

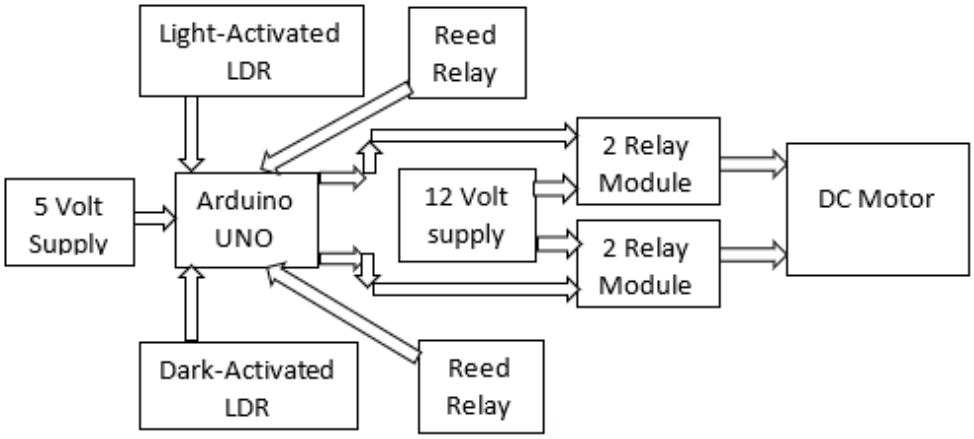

Fig. 5.3 Block Diagram of Motor Controller of Self- Cleaning PV Sliding system

Table 5.1 Mechanical Components for Proposed PV Sliding System

Name of Major Components	**Material**	**Function**
Track Rail System	Aluminium	To provide the sliding track for PV panels
Roller	Plastic	To provide the smoothness during sliding of PV panel
Bearing	Iron	To provide the frictionless support for stud
Stud	Iron	To move the PV Panel
Nut	Iron	To connect the PV panel to stud
Mechanical Coupler	Iron	To connect the motor shaft to stud
Cleaning Brush	Nylon	To clean the PV panels
Mechanical supports	Iron	For Bearing
L section	Aluminium	To provide the contact for another panel during covering
Thread	Nylon	To connect the PV panels
Protective Sheet	Aluminium	To cover the PV panels

Table 5.2 Electrical & Electronics Components for the Proposed PV Sliding System

Name of Major Components	**Quantity**	**Function**
DC Motor	1	To move forward and backward the PV panels
2 Relay Module	2	To control the direction of the motor
Light activated LDR	1	To send single to Arduino UNO for moving forward (to uncover) PV Panel
Dark activated LDR	1	To send single to Arduino UNO for moving backward (to cover) PV Panel
Rain Sensor	1	To send single to Arduino UNO for moving backward (to cover) PV Panel
Arduino UNO	1	Control the whole system
Magnetic reed switch sensor	2	To stop the motor when PV panels fully covered or uncover.
12 volts Supply	1	Input supply for motor
Magnet	2	For Reed switch sensor
PV panels	3	To generate electric energy

Table 5.3 Specifications of DC Motor used in the experiment

Specification	**Value**
Type	Gear
Input Voltage	12V
No-load Current	100mA
Maximum Load Current	3A
Rated Speed	300RPM
Stall Torque	8Kg-cm

Table 5.4 Specifications of solar panels at standard testing conditions

Specification	Value
Model	ELDORA 20P
Type	Polycrystalline
Maximum Power	20W
Open Circuit Voltage	21.44V
Short Circuit Current	1.27A
Maximum Voltage	17.15V
Maximum Current	1.18A

Table 5.1 & 5.2 shows the mechanical & electronics components of proposed self-cleaning PV sliding system and Table 5.3 shows the specifications of DC Motor used in the experiment. Table 5.4 shows the specifications of solar panels used in the experiment at standard testing conditions

5.3 Working of proposed Self-cleaning PV sliding system

Three sets of polycrystalline PV modules with the proposed self-cleaning system remain exposed in the natural environment. The rain sensor and LDRs are used for the detection of rain and sun light. When there is sunshine in the morning, the light activated LDR activates the relay module set, which rotates the DC motor to uncover and bring the solar panels into the sun's light. A flow chart of the proposed self-cleaning PV sliding mechanism is shown in Fig. 5.4. The brush on the top cover plate cleans the first panel, the brush on the first panel cleans the next panel, and the brush on the second panel cleans the third panel. All PV panels are cleaned in this manner during the uncovering process. When the sun sets in the evening, the dark-activated LDR triggers the second relay set, which rotates the DC motor in the opposite direction, allowing the panels to be placed beneath the protective plate. During this activity, the cleaning procedure takes place again. As a result, the suggested self-cleaning PV

sliding system performs the cleaning procedure twice daily and prevents dust particles from adhering to the PV panels. During hailstorms, rain drops on the rain sensor raise the rain sensor's output, which activates the relay, which starts the motor in such a way that all three panels come beneath the protective plate, shielding the solar panel from the hail. The reed relay switches, which are located on both ends of the track-rail system, disconnect the relay modules, stopping the motor, as soon as all the panels are completely uncovered and covered. L-section blocks are used to lock the third panel to the second and first panels during covering. Most of the dust deposition occurs at night-time or before the sun rises, as there is less traffic and less wind blowing. These conditions are very suitable for the stagnation of the small and large dust particles suspended in the air. The PV cell cools before sunrise and dew is formed when water mist in the air condenses, which interacts with the dust particles, increasing the cell surface adhesion forces and making the layers of dust deposition difficult to clean in a fair manner, resulting in significant losses in the generation of output power [8]. In this proposed technique, a self-cleaning PV sliding system covers the PV panels during the night and performs the cleaning procedure twice daily. As a result, the volume of dust deposited, and dew developed on the PV surface is greatly reduced. This technology is primarily designed to achieve maximum energy from the PV module and ensure protection against pollution and hailstorms for the PV module. Fig. 5.5 shows the developed self-cleaning PV sliding system.

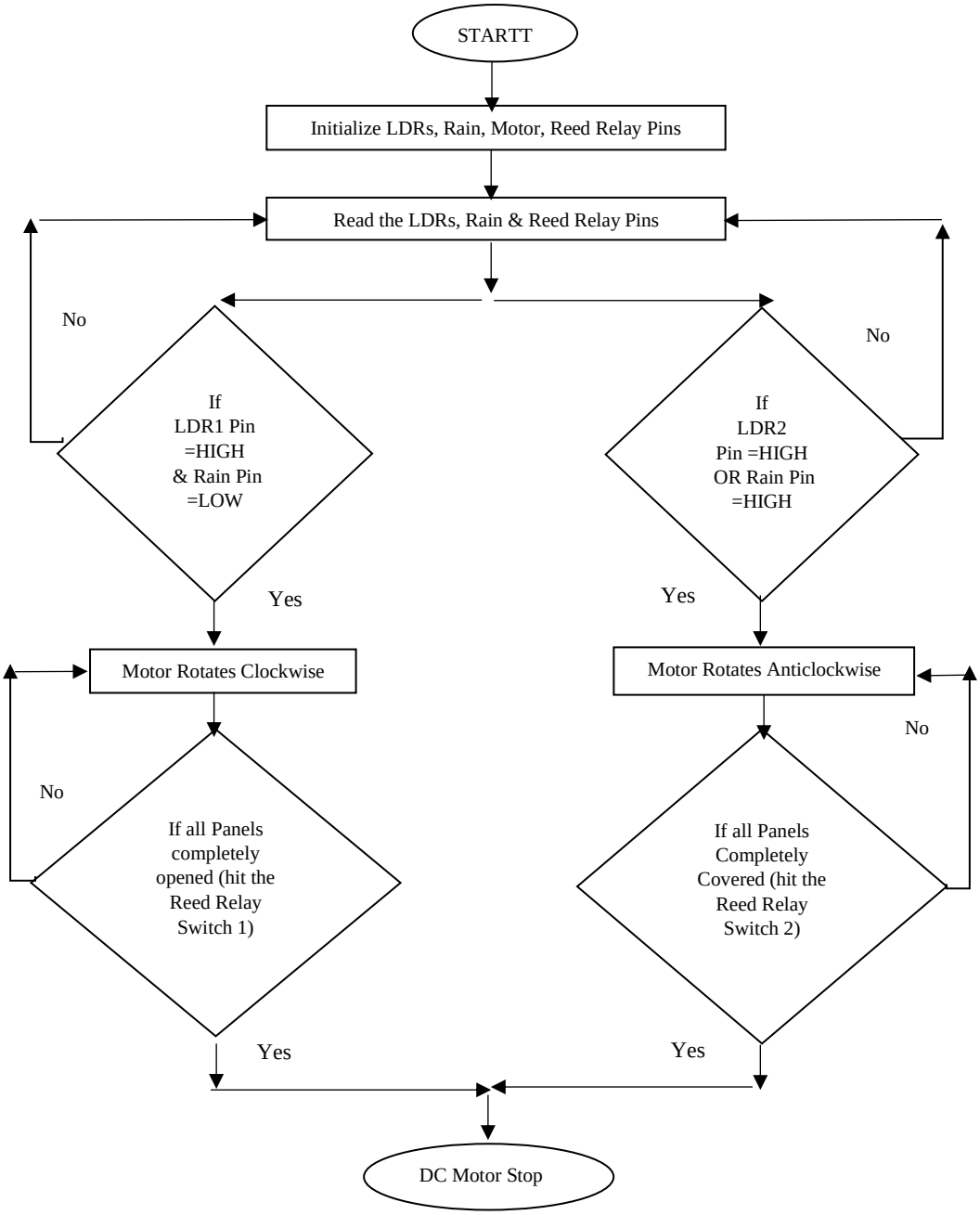

Fig. 5.4 Flow chart of proposed self-cleaning PV Sliding Mechanism

Fig. 5.5 Developed Self-cleaning PV sliding system

5.4 Experimental setup

To investigate the performance of the proposed self-cleaning PV sliding system, we incorporated three PV panels of 20W with a sliding structure and installed them on the rooftop of Manipal University Jaipur. The solar panels were connected in parallel, and the output terminals of the PV system were connected to the resistive load. Another set of 3 PV panels

of 20W was installed with a conventional method, i.e., fixed. The effectiveness of the proposed cleaning system was tested on photovoltaic panels in Jaipur, India, for all seasons. Both sets of three polycrystalline PV panels are mounted on a platform that is inclined 27° to the south. Fig. 5.6 shows the prototype of the self-cleaning PV system and the experiment setup.

We installed one set of three PV panels without any cleaning method, and on the second set of three PV panels, we implemented the proposed cleaning technique and measured the output power of both sets for one year. The proposed cleaning method uses no water. The performance of the proposed self-cleaning PV sliding system is determined based on cleaning efficiency and energy usage. A data logger is used to record the performance parameters. Table 5.5 shows the specifications of the test location.

(a) Proposed Self-cleaning PV system

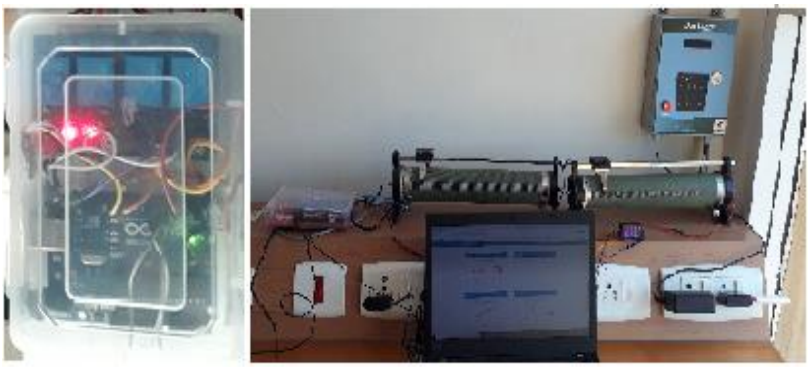

(b) Motor Controller (c) Load & Data logger

Fig. 5.6 Experimental setup of self-cleaning sliding system

Table 5.5 Specifics about the test location

Description	Value
Place	Academic Block 1, Manipal University Jaipur
Latitude	26.84
Longitude	75.56
Tilt angle	27°
Facing	South

5.5 Data Collection

An IOT-based monitoring system has been used, which collects real-time information and sends it to the ThinkSpeak cloud server. The system consists of an ESP8266 Wi-Fi module, INA 260 sensors, and the cloud platform ThingSpeak. ThingSpeak displays PV system variables such as generated voltage, current, and power. The sensors were verified and calibrated precisely. The readings of current and voltage measured by the INA260 and INA219 sensors are compared with the readings of a standard multimeter (Aplab VC97) at the same time. The entire calibration results were repeatable. For solar radiation, an EKO MS40M pyranometer is used. The Arduino-based data logger records the power consumed by the DC motor and stores the information on a micro-SD card. For this purpose, the INA219 sensor is used. Before each season, the calibration process was repeated

The experiment was divided into two sections. In the first section, we installed one set of three PV panels without any cleaning method, and on the second set of three PV panels, we implemented the proposed cleaning technique and measured the output power at an interval of 5 minutes from 7.00 am to 6.00 pm for the period of Dec. 2019 to Apr. 2021. For the summer, monsoon, post-monsoon, and winter seasons, data is collected for 58 days, 54 days, 68 days, and 64 days, respectively. The collected data has a P-value of less than 0.05, indicating that it is statistically significant.

The uncertainties of the measuring sensors INA260 (U_1), INA219 (U_2), pyranometer (U_3), and multimeter (U_4) used in this experiment are shown in Table 5.6. The verification reports for the sensors and measuring devices were used to determine the standard uncertainties for the components.

Table 5.6 Standard uncertainties for the components

U_1(%)	U_2(%)	U_3(W/m^2)	U_4(%)
0.5	0.5	1.5	0.5 for voltage 1.0 for current

5.6 Results and Discussion

To investigate the performance of the proposed self-cleaning PV sliding system, we incorporated three PV panels of 20W with a sliding structure, and another set of three PV panels of 20W was installed with a conventional method, i.e., fixed. Both sets of three polycrystalline PV panels are mounted on a platform that is inclined 27° to the south. There were two parts to the experiment. In the first part, we installed one set of three PV panels without any cleaning procedure, then applied the proposed cleaning methodology to the second PV set and measured the output power for all seasons. In the second part, we manually cleaned the first set of PV panels on a weekly and daily basis, while applying the proposed self-cleaning technique to the second set, and then measured the output power of both sets for four weeks and one month, respectively. The performance of the proposed self-cleaning PV slider system is determined based on the following points.

(i) Efficient Cleaning
(ii) Energy Consumption & Cleaning time
(iii) Cost considerations
(iv) Utilization of Land
(v) Effectiveness during hailstorm

(i) Efficient Cleaning

Fig. 5.7 (a), (b), (c) and (d) shows the variation in normalized efficiency of the PV system with and without the proposed self-cleaning mechanism. The ratio of the measured power to the power rating at STC compared to the irradiance divided by the STC irradiance gives the normalized efficiency as shown in equation 5.1.

$$\eta_N = \frac{P/P_{STC}}{I_m/I_{STC}} \quad \text{---------- (5.1)}$$

where P is the measured power, P_{STC} is the STC rated power, I_m is the measured irradiance, and I_{STC} is the reference irradiance (1,000W/m^2) [236,237].

Most of the dust deposition occurs at night-time or before the sun rises, as there is less traffic and less wind blowing. These conditions are very suitable for the stagnation of the small and large dust particles suspended in the air. The PV cell cools before sunrise and dew is formed when water mist in the air condenses, which interacts with the dust particles, increasing the cell surface adhesion forces and making the layers of dust deposition difficult to clean in a fair manner, resulting in significant losses in the generation of output power. In this proposed technique, a self-cleaning PV sliding system covers the PV panel during the night and performs the cleaning procedure twice daily. As a result, the possibility of dust deposited and dew development on the PV surface is reduced. As described above the proposed self-cleaning PV sliding system provides the cleaning process twice a day. It does not allow dust to be deposited on the PV panels and become adhesive dust. The results show that the cleaning system works significantly. It completely cleans large particles of dust, and it removes a substantial amount of small dust particles also. It has been observed that the cleaning system is unable to remove the bird droppings completely in one day cleaning. The result shows that the proposed solar cleaning system works well in winter, post monsoon and summer. Cleaning is not required in the monsoon season because of the

rain. It provides natural cleaning. During the monsoon season, the cleaning system performs the covering and uncovering process repeatedly due to the frequently appearing and disappearing of dark clouds, resulting in higher energy consumption. But the proposed system not only provides cleaning but also protection from hailstorms. So, it is very useful in the monsoon season also.

In post monsoon season, the hot and humid weather begins to fade, and the air quality improves noticeably. Because there are fewer airborne particles, the sky is clean, and the quality of solar radiation is improved. Rain reduces the amount of pollutant particles in the air. The efficiency drop in a PV system without a self-cleaning mechanism is 7.1%. This drop in efficiency is due to dust deposition. While the efficiency drop in a self-cleaning PV system is 0.85%, the overall efficiency gain is 6.40%. Results show that this mechanism is effective for the post-monsoon season.

In the winter season, the efficiency drop in PV systems without a self-cleaning mechanism is 14%. This drop in efficiency is not only due to dust accumulation; there are more factors involved, such as bird-dropping, insects, and leaves of trees because the autumn season starts, while the efficiency drop in a PV system with a self-cleaning mechanism is 2.2%. The overall gain in efficiency is 13.33%. Results show that this mechanism is effective for the winter season.

In the summer season, the reduction in efficiency in PV systems without a self-cleaning mechanism is 18.43%. During this season, the ambient temperature is very high and the humidity in the air is low, so the air easily lifts the dust particles and have accumulated on the PV panel, while the efficiency drop in a PV system with a self-cleaning mechanism is 3.3%. The overall gain in efficiency is 18.37%. Results show that this mechanism is effective for the summer season.

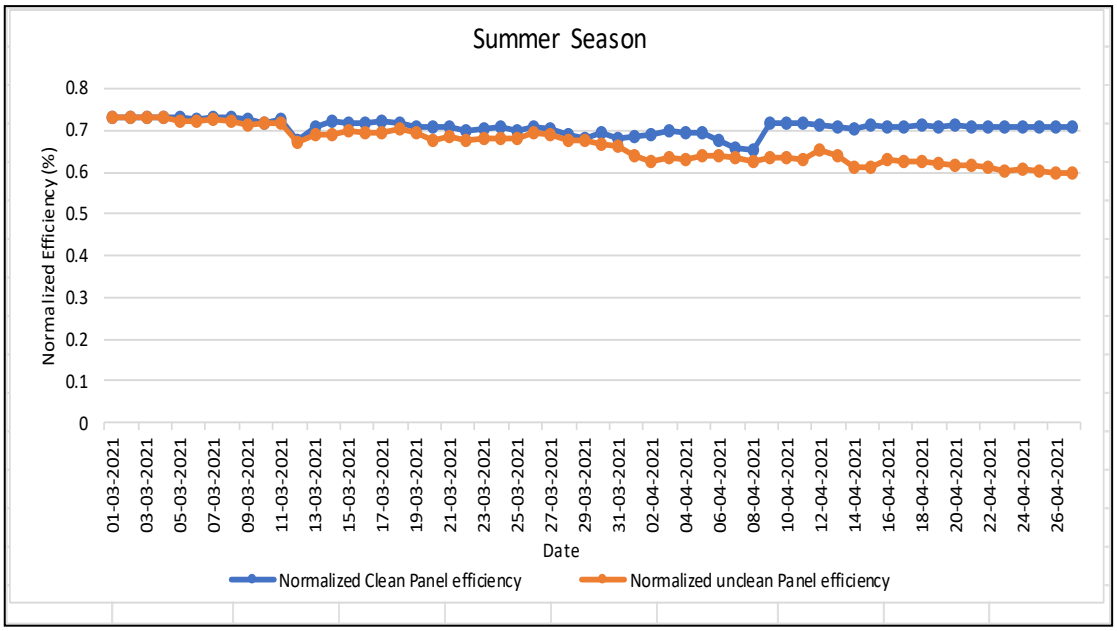
Summer Season
Normalized Efficiency (%)
0.8
0.7
0.6
0.5
0.4
0.3
0.2
0.1
0
01-03-2021
03-03-2021
05-03-2021
07-03-2021
09-03-2021
11-03-2021
13-03-2021
15-03-2021
17-03-2021
19-03-2021
21-03-2021
23-03-2021
25-03-2021
27-03-2021
29-03-2021
31-03-2021
02-04-2021
04-04-2021
06-04-2021
08-04-2021
10-04-2021
12-04-2021
14-04-2021
16-04-2021
18-04-2021
20-04-2021
22-04-2021
24-04-2021
26-04-2021
Date
Normalized Clean Panel efficiency
Normalized unclean Panel efficiency

(a)

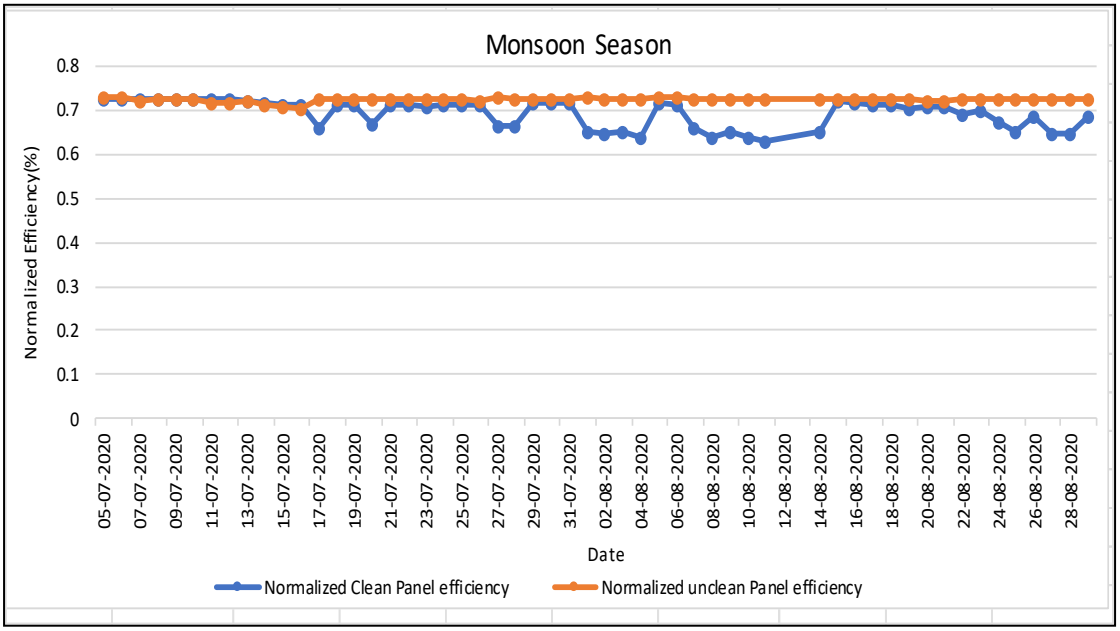
Monsoon Season
Normalized Efficiency(%)
0.8
0.7
0.6
0.5
0.4
0.3
0.2
0.1
0
05-07-2020
07-07-2020
09-07-2020
11-07-2020
13-07-2020
15-07-2020
17-07-2020
19-07-2020
21-07-2020
23-07-2020
25-07-2020
27-07-2020
29-07-2020
31-07-2020
02-08-2020
04-08-2020
06-08-2020
08-08-2020
10-08-2020
12-08-2020
14-08-2020
16-08-2020
18-08-2020
20-08-2020
22-08-2020
24-08-2020
26-08-2020
28-08-2020
Date
Normalized Clean Panel efficiency
Normalized unclean Panel efficiency

(b)

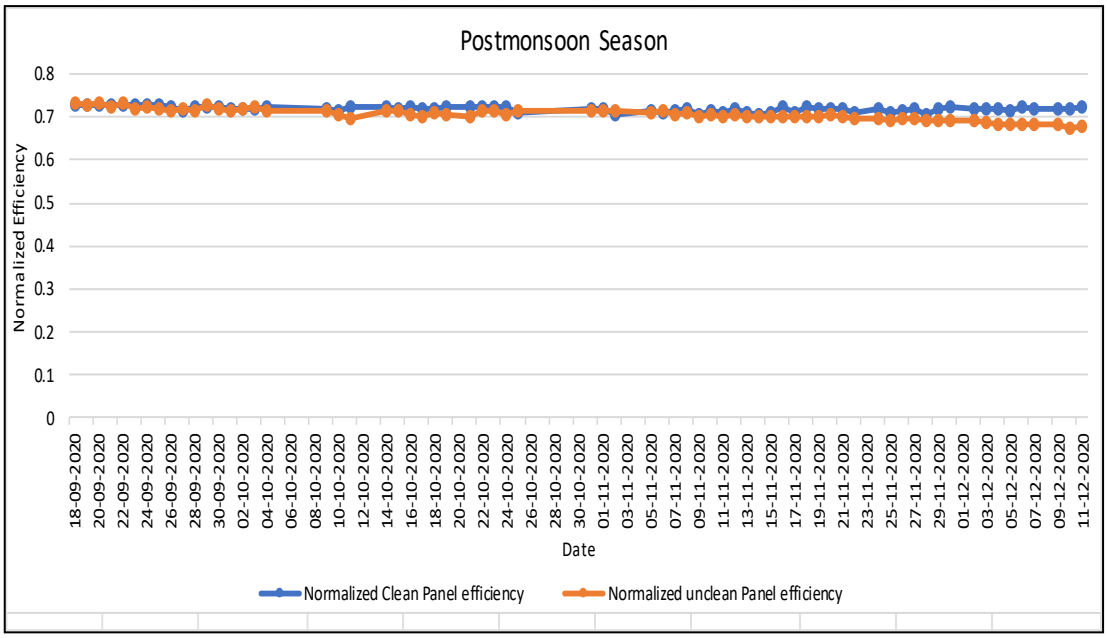

(c)

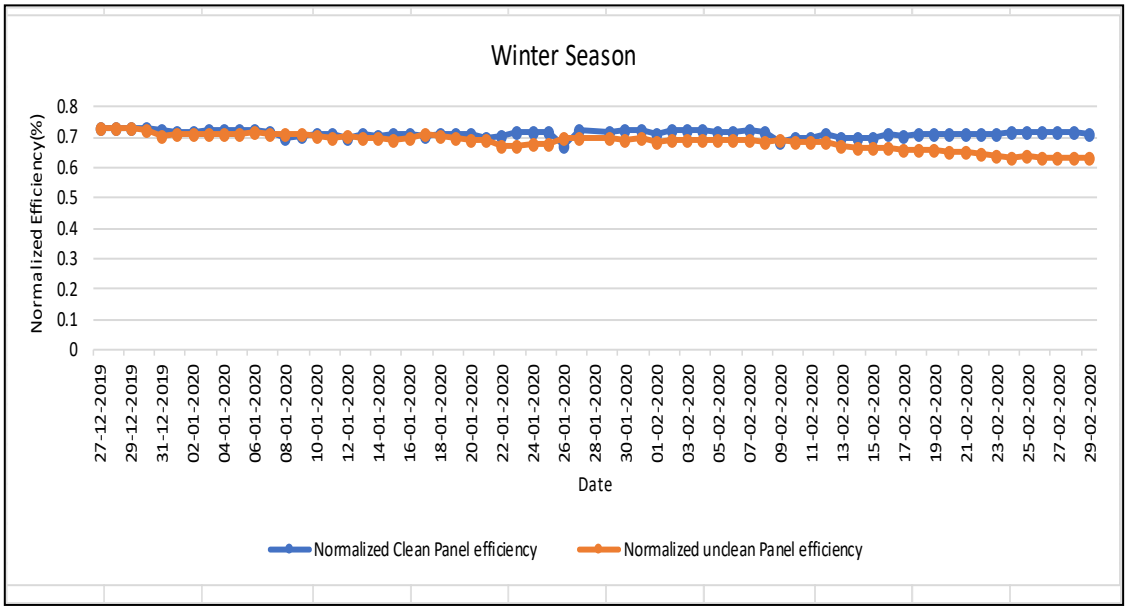

(d)

Fig.5.7 Variation in Efficiency of clean and unclean PV system in all seasons

During the monsoon season, PV systems without a self-cleaning mechanism lose 0.33% of their efficiency, while PV systems with a self-cleaning mechanism lose 5.5% of their efficiency. This drop in efficiency

is not due to dust accumulation; it is due to the repetition of the covering and uncovering process of panels when dark clouds appear and disappear. As a result, the PV system's exposure time was reduced. The overall drop in efficiency in the monsoon season is 5.4%. Result shows that cleaning is not required for the monsoon season. But the proposed system not only provides cleaning but also protection from hailstorms. So, it is very useful in the monsoon season also.

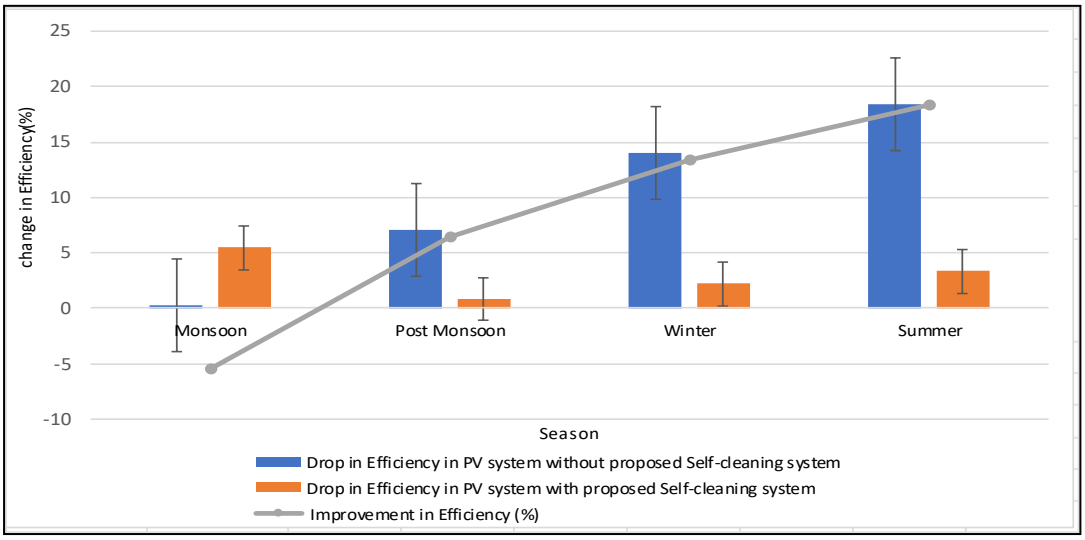

Fig. 5.8 Drop & improvement in efficiency of the PV system with & without the proposed cleaning mechanism for all seasons

Fig. 5.8 demonstrates that the proposed cleaning system's percent gain in efficiency is negative during the monsoon season, indicating that the cleaning mechanism of proposed system is not required in monsoon season. While the gain is positive in other seasons and the average energy consumption is very low, the proposed system is more effective and adaptable. The efficiency gains are 18.33%, 13.33%, and 6.4% in the summer, winter, and post-monsoon seasons, respectively.

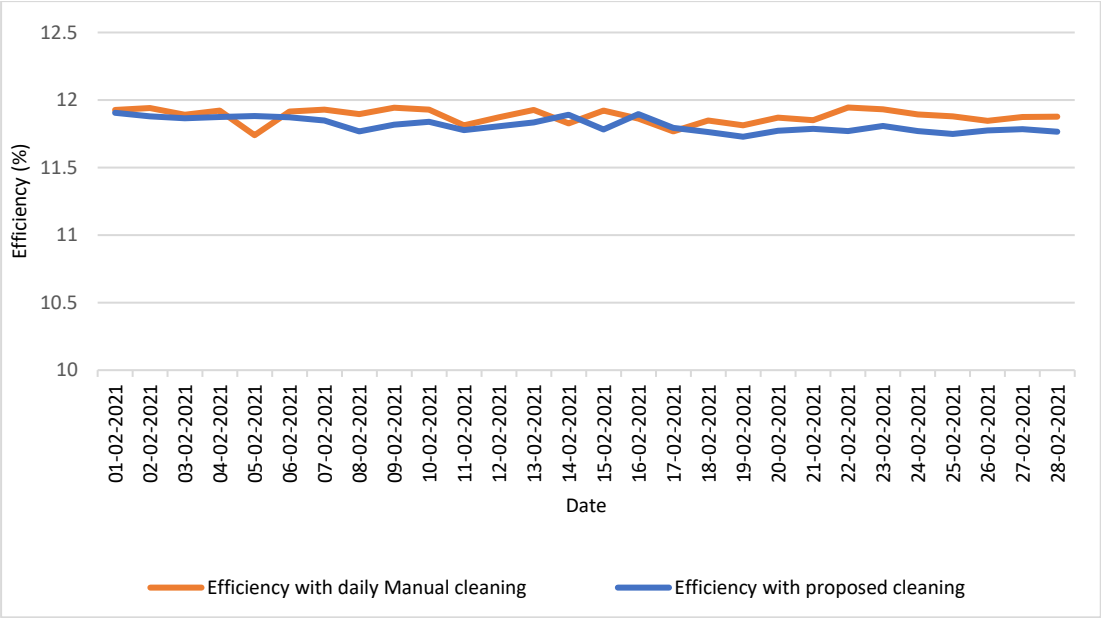

Fig. 5.9 Comparison of the performance of daily manual cleaning with the proposed cleaning method

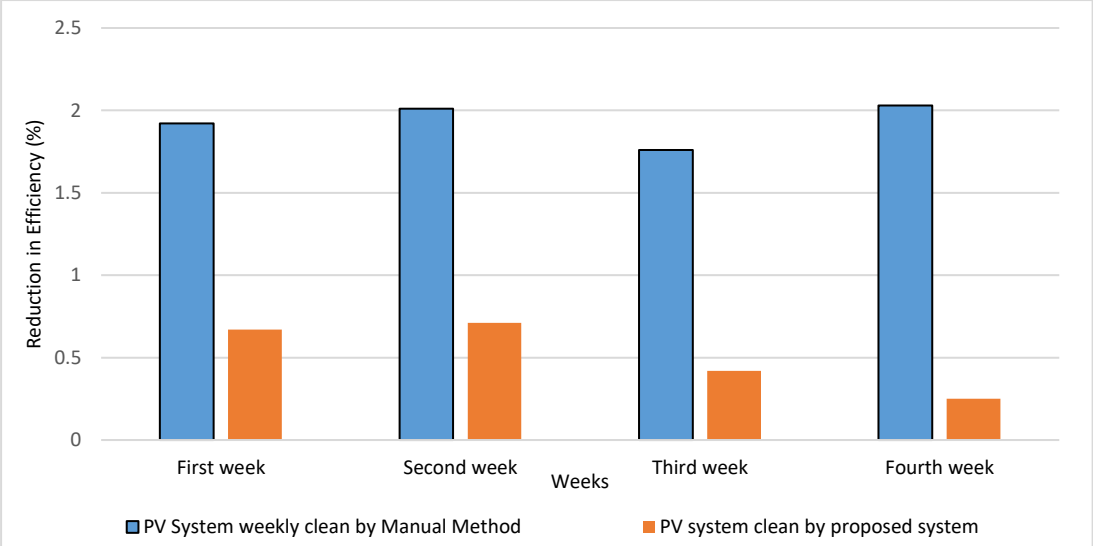

Fig. 5.10 Comparison of the performance of weekly manual cleaning with the proposed cleaning method

In the second part of the experiments, the efficiency of a fixed PV system with daily manual cleaning was compared to that of a proposed cleaning PV system for a month and found that the proposed cleaning PV system's efficiency was reduced by 1.13%. Whereas in the case of weekly cleaning

applied to a fixed PV system, the efficiency of a fixed PV system was reduced by 1.92%, 2.01%, 1.62%, and 2% after the first, second, third, and fourth weeks, respectively, whereas the efficiency of a proposed cleaning method was reduced by 0.67%, 0.67%, 0.42%, and 0.25%, as shown in Fig. 5.9 & Fig. 5.10.

(ii) Energy Consumption & Cleaning time

The energy consumption of the motor is primarily determined by the size and weight of the PV system's characteristics, although they are not the only factors. The efficiency of motors, the battery, and a variety of other elements all influence their energy usage. The proposed cleaning technique consumes energy while in use. As a result, the cleaning process' energy consumption is another important factor to consider when evaluating the cleaning method's viability for PV applications.

The self-cleaning solar PV sliding system that has been proposed uses relatively small amounts of energy. The motor draws an average current of 0.33A during uncovering when only the third panel is moved forward. The motor's average current jumps to 0.42A as soon as the second panel is pulled by the third panel. The motor's average current increases to 0.82A when the first panel is pulled by the second panel. However, the motor only needs an average current of 0.45A to pull the third panel throughout the covering operation. The motor requires an average current of 0.67A to pull two panels, and of 0.97A to pull all three panels. Fig.5.11 shows the average motor’s current during covering and uncovering with cleaning time for each panel. Table 5.7 shows the average current and cleaning time of individual PV panels in a self-cleaning PV sliding system.

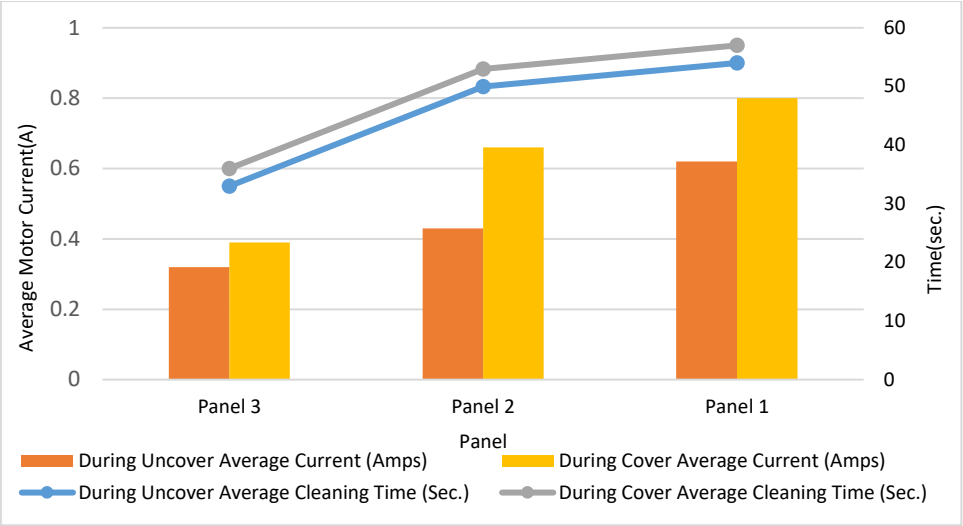

Fig. 5.11 Average motor's current during covering and uncovering with cleaning time for each panel

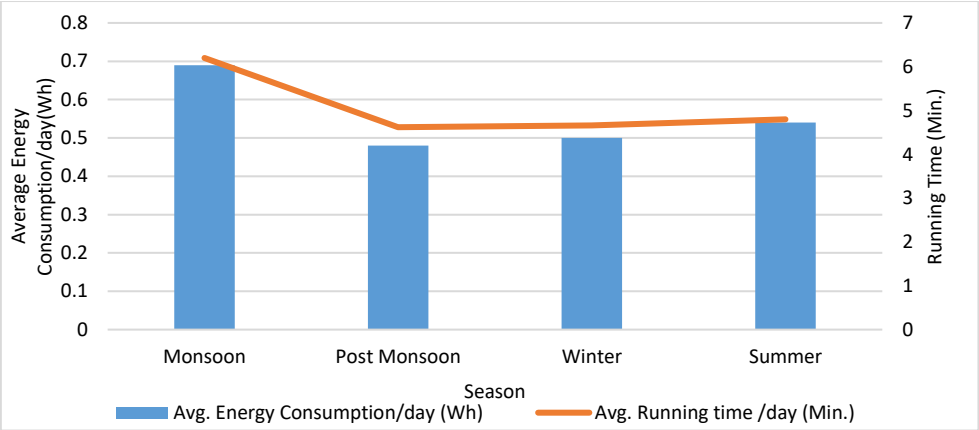

Fig. 5.12 Average energy consumption per day and cleaning timing for all seasons

Table 5.7 Average Energy Consumption of proposed self-cleaning solar PV sliding system*

	Average Running Time (Min.)	**Average Current (Amps)**	**Energy Consumption (Wh/day)**	**Monthly Energy Utilization (Wh)**
During Uncover	2.28	0.45	0.21	6.3
During Cover	2.42	0.62	0..3	9.0
		Total Energy Consumption		15..3 Wh

*Not include Monsoon season's energy consumption

Uncovering takes only 2 minutes and 28 seconds on average in the morning. During this time, a current of 0.4A was measured on average. In the evening, it takes an average of 2 minutes 42 seconds to cover and 0.58A of average current to do so. This method uses extremely little energy overall when it compares with power gain. In the summer season, it has been seen that the dust gets in between the track of the solar sliders, due to which the truck gets filled with friction and the load on the motor also increases, due to which the energy consumption slightly increases. In monsoon season, due to the frequent arrival and departure of dark clouds, the cleaning system has to be opened and closed frequently, resulting in increased energy consumption. The results show that the cleaning of solar PV panels is not required in the monsoon season because of the rain, which provides natural cleaning and cooling, and during this time, efficiency is not significantly reduced. Table 5.8 shows the performance of the proposed self-cleaning solar sliding system in all seasons. Fig. 5.12 shows the average energy consumption per day and cleaning timing for all seasons.

Table 5.8 Performance of Proposed self-cleaning solar PV sliding system in all seasons

Season	**Avg. Energy Consumption/day (Wh)**	**Avg. Running time /day (sec.)**	**Gain in Efficiency (%)**	**Suitability**
Monsoon	0.69	6.2	**-5.4**	**Effective**
Post Monsoon	0.48	4.62	**6.4**	**Effective**
Winter	0.50	4.66	**13.33**	**Effective**
Summer	0.54	4.8	**18.37**	**Effective**

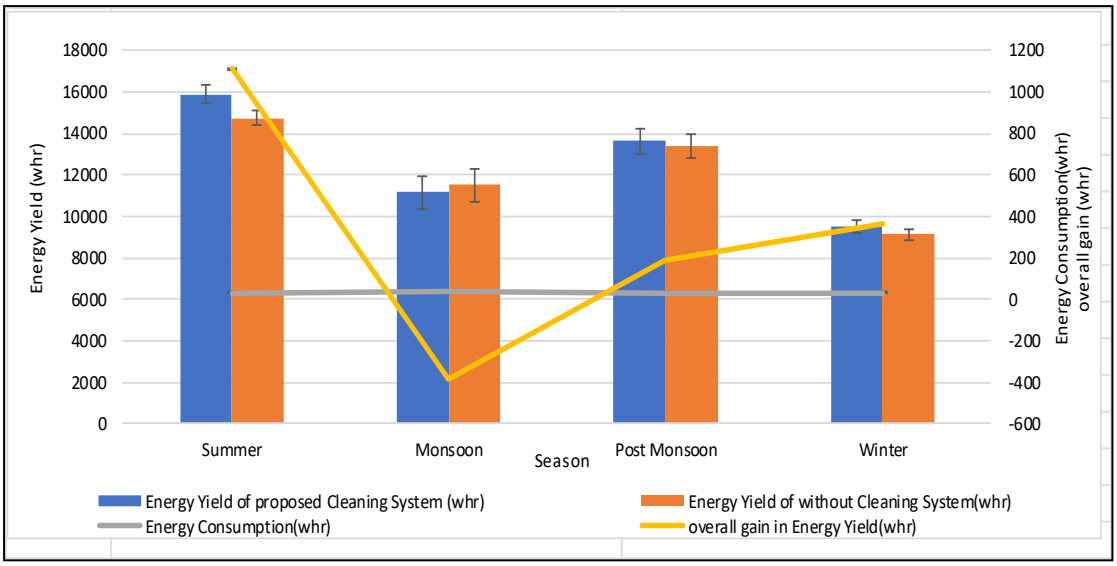

Fig.5.13 Energy yield of PV system with & without proposed cleaning mechanism, energy consumption and gain for all seasons

During the summer season, the suggested solar sliding PV system consumed 29.58Wh for 58 days, while the energy generation of the proposed system was 1145.6 Wh higher than the fixed PV panel. The total amount of energy gained was 1115.72 Wh. However, during the monsoon season, energy usage increases due to the repeated covering and uncovering of panels as dark clouds appear and disappear. As a result, the PV system's energy consumption was increased. For 54 days, a total energy loss of 345.4 Wh was measured. During the post-monsoon season, the energy generation of the proposed PV system was 221 Wh more than with a fixed PV system, while energy consumption was 32.64 Wh for 68 days. In the winter, the proposed system generated 396.8 Wh more energy than a fixed PV system, and the energy consumption was 31.36 Wh for 64 days. Fig.5.13 shows the energy yield of a PV system with and without the proposed cleaning mechanism, energy consumption, and gain for all seasons. Table 5.9 shows the comparison of the proposed self-cleaning PV sliding system with some literature studies for PV Cleaning.

Table 5.9 Comparison of Proposed Self-Cleaning PV sliding system with some literature studies for PV Cleaning

Reference	Cleaning Technique	Cleaning Frequency	Outcomes
Al-Shehri et al. [238]	Nylon brush, cloth, and silicon rubber foam		The maximum power output of solar panels cleaned with silicone rubber brush increased by about 1% on average when compared to the unbrushed initial power output.
Al-Shehri et al. [239]	Brush	1	The right brush must be chosen to achieve the required level of cleaning while avoiding damage to the solar panels' surface.
Arabatzis et al. [240]	Self-cleaning & Anti-reflective glass coating	16 days and 86 days	The coated PV panels showed an average gain of 5–6% for the tested period of time Under outdoor real conditions.
Urrejola et al. [241]	Brushing with water	Monthly cleaning (suggested optimum cleaning period: 45 days)	Lowest decay values in summer 2015: 0.14 percent, highest values in autumn 2015 seasonal average: 0.56%/day, the performance ratio has deteriorated by 17.36% monthly.
Al-Housani, et al. [242]	Drone incorporated with Brush, Microfiber cloth wiper, Vacuum cleaner	1 day 1 week 1 month	In the winter, the weekly power losses for microfiber based-cloth wiper + vacuum cleaner, mechanical brush + vacuum cleaner, microfiber based-cloth wiper, mechanical brush are 3.42 percent, 2.95 percent, 3.63 percent, and 2.28 percent, respectively.
Proposed Cleaning System	Sliding Structure with brush	2 time per day	The efficiency gains are 18.3%, 13.3%, and 6.4% in the summer, winter, and post-monsoon seasons, respectively. The proposed self-cleaning system protects the PV system from dust deposition and hailstorms.

(iii) Cost Considerations: -

The acceptability of PV cleaning techniques mainly depends on the cost of cleaning. Only three-track rail bars and rollers are required to construct the suggested system. For installation, rollers and the three-track bars are replaced by basic bars, which are required for sliding structure installation. Apart from that, a motor controller circuit and sensors are required, which are a low-cost, one-time investment in this system. This strategy can be implemented without incurring additional installation costs. Only a minor change has been made to the current installation process. Furthermore, there is no requirement for staff, specialised cleaning equipment, or water. It only uses a small amount of energy to run. However, it gains more energy than it consumes.

The costs of operation and maintenance, such as brush replacement and grease for mechanical parts, are also relatively low. The most of the existing solar cleaning techniques and equipment necessitate the use of separate mechanical structures, electricity, personnel, and water. There are various self-cleaning systems on the market that do not require water, but they are very expensive and require separate mechanical structure. Despite their high cost, they only provide cleaning services, not hailstorm protection. To determine the acceptability of the proposed self-cleaning solar slider technique, we compared the capital cost of solar cleaning devices available in the market. The capital cost of the proposed system is included in the installation cost and depends on the rating of the power plant's size. The proposed self-cleaning solar sliding system provides good cleaning and hailstorm protection at a marginally increased cost. Table 5.10 shows the comparison of the proposed self-cleaning system with drone-based PV Cleaning Technique and Table 5.11 shows the cost estimation of the proposed self-cleaning solar sliding PV system for a 60W PV system. Table 5.12 shows the cost comparison of the proposed self-cleaning PV sliding system with available cleaning devices.

Table 5.10 Comparison of the Proposed Self-Cleaning PV sliding system with drone-based PV Cleaning Technique [242-243]

Parameters	**Drone based Cleaning System**		**Developed Self-cleaning PV Sliding System**	
	Summer	**Winter**	**Summer**	**Winter**
Improvement in average power output (W/day)	0.4	0.5	1.98	0.77
Average Improvement (%)	7	4.8	18.33	13.3
Average Cleaning Cost (USD/ m^2)	0.0578	0.0578	0.0001	0.000097
Average Cleaning Time (min./panel)	0.75-2	0.75-2	0.33-0.57	0.33-0.57
Average Energy Consumption	Yes	yes	0.51Wh/day	0.49Wh/day
Capital Cost	High	High	Relatively low	Relatively low
Cleaning frequency per day	One Time	One Time	Two Time	Two Time
Manpower	Require	Required	No	No
Water	No	No	No	No

Table 5.11 Cost Estimation of proposed Self-cleaning solar slider PV system for 60W

S No.	**Name of Major Components**	**No./ Length/Area**	**Rate**	**Cost Rs.**	**Cost ($)**
1	Track Rail System	62-inch x 27-inch	150/- sq. feet	1500/-	20
2	Roller	12	30/- each	360/-	4.8
3	Bearing	1	25/- each	25/-	0.34
4	Stud	6 feet	20/- per feet	120/-	1.6
5	Mechanical Coupler	1	150/-	150/-	2
6	Cleaning Brush	6 feet	30/- per feet	180/-	2.4
7	Mechanical supports	1	60/- each	60/-	0.8
8	L section block	4	15/- each	60/-	0.8
9	Thread	2 meters	20/ per meter	40/-	0.6
10	Protective Sheet	16-inch x 27-inch	16/- sq. feet	50/-	0.7
11	DC Motor	1	380/- each	380/-	5
12	LDR	2	45/- each	90/-	1.2
13	Rain Sensor	1	120/- each	120/-	1.6
14	Arduino UNO	1	450/- each	450/-	6
15	Reed Relay Switch	2	215/- each	430/-	6
16	12 volts,3A Supply	1	275/- each	275/-	4
17	Two Relay Module	2	90/- each	180/-	2.4
Total Cost				**4600/-**	**61.5**

Table 5.12 Cost comparison of Proposed self-cleaning PV sliding system with available cleaning devices [244-247]

Type of Solar Cleaning Devices	Cost $	Requirements	Function
Pole with Cleaning Brush & wiper with or without water jet [244]	33-200	Manpower, Water	Only cleaning
Pole with rotating brush with water jet [245]	300-500	Manpower, Water, Electricity	Only cleaning
Double head automatic solar panel cleaning brush [246]	500$-800	Electricity, Water	Only cleaning
automatic intelligent solar panel cleaning robot [247]	1950-3800	Electricity, Separate mechanical structure	Only cleaning
Proposed novel PV cleaning system	Depend on PV system size (Installation structure)	Electricity	Two- Time/day Cleaning & Hailstorms Protection

(iv) Utilization of Land: -

Two major factors influence the amount of land required for a given total power capacity. The first is PV module efficiency, and the second is row-row spacing to avoid shading, which is determined by the slope of the PV module row, latitude, and seasons. PV module efficiency may have a significant impact on the area needed for a PV power plant; the higher the efficiency, the less land is required. PV panels containing tracking systems also generate roughly 20% more annual energy than fixed panels. A fixed PV panels takes up around half of the space required by a PV tracker system in terms of land use.

Total Power Output = Total Area x Solar Irradiance x Efficiency

Häberlin [248] proposed that the field (land) required for a ground-based or rooftop PV generator equals the total area of the PV modules multiplied by a factor known as a land factor (between 2 and 6 in Central Europe) for shading avoidance for a large solar PV plant where PV panels are arranged in behind each other.

When we consider the single row of PV panels for a 60W PV system, the area covered by the self-cleaning solar slider system installed at a 27° tilt angle is 10.35sq. feet. Whereas conventional fixed panels cover 7.5sq. feet of area as shown in Fig.5.14. There are several rows of PV panels in large PV plants. Apart from the row-row spacing to avoid shading, we have to leave more space for movement between rows by the installation and maintenance (cleaning) teams. The following assumptions have been included in the hypothetical PV power plants of rating 1200W using proposed and conventional fixed methods and Table 5.13 shows the details of test conditions:

- PV panels facing south and Installed with a yearly tilt angle corresponding to the local latitude with both methods.
- From 7:00 a.m. to 6:00 p.m., there is a sun window (sunny hours each day).
- Each row has a single line of PV modules. In both methods, PV plant has ten rows of 6 panels.
- In fixed method, space between rows keeps two time of D_r.

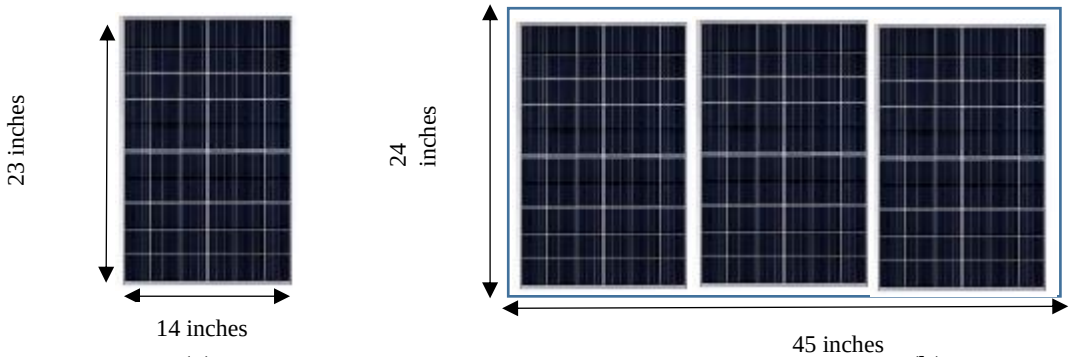

(a) (b)

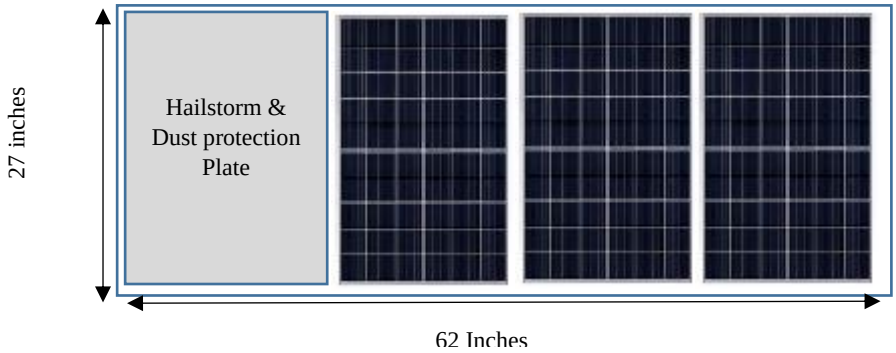

(c)

Fig.5.14 Layout of proposed self-cleaning PV Sliding Mechanism

The shadow length D_s is the distance between two rows in the direction of the sun, can be calculated using the Fig. 5.15,

$$D_s = Y/\tan\alpha$$

D_r is the distance between two rows in the south direction as shown in Fig. 5.15 is given by the following expression:

$$D_r = D_s \cos z$$

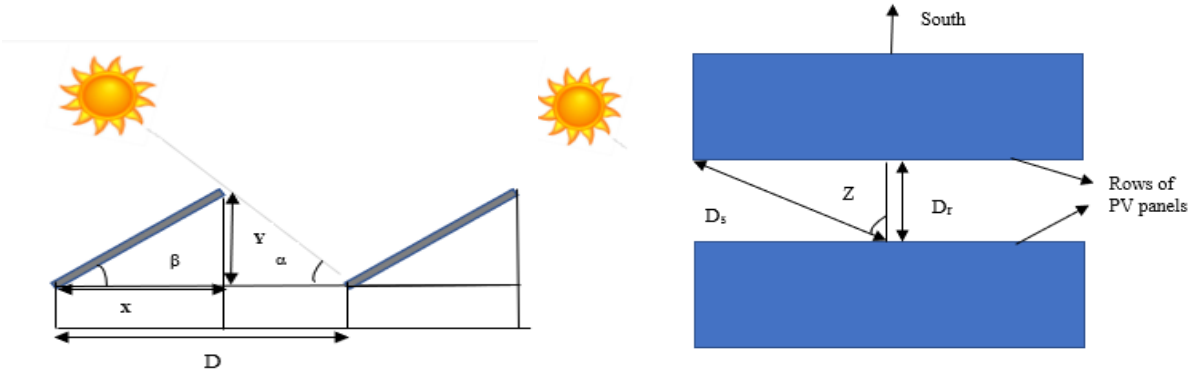

Fig.5.15 Layout of the PV system with spacing

Spacing between rows:

$$Y = 27 \sin(26.91°)$$

$$Y = 12.21 \text{ inches}$$

$$D_s = Y / \tan\alpha = 28.61 \text{ inches}$$

$$D_r = 28.61 * \cos(180°-131.5°) = 16.9 \text{ inches}$$

$$D_r = 17 \text{ inches}$$

The value of D_r spacing between rows is not practically true because for cleaning and maintenance we require 2 times more space [248].

Table 5.13 Specifics about the test location's parameters during land used analysis

Parameters	**Values**
Latitude	26.91
Longitude	75.78
Time Region	+5.5
Worst Solar Day	Dec. 21
Time	9.00 am
Solar Noon	12.24 pm
Solar Azimuth	131.5°
Solar Inclination	23.3°

Table 5.14 Utilizations of Land in proposed Self-cleaning PV sliding system and Fixed PV panels for 1200W PV system

Type of PV System	**Area covered by Panels without Self-cleaning Mechanism**	**Area covered by Panels with Self-cleaning Mechanism**	**Difference**
Without space for cleaning and maintenance	245 sq. feet	364 sq. feet	48.5%
With space for cleaning and maintenance	341 sq. feet	364 sq. feet	6.7%

The proposed self-cleaning solar PV sliding system takes 48.5% more space as compared to conventional fixed without cleaning space. Table 5.14 shows that for 1200W PV systems, the percentage difference in land use is 6.7% more in the case of the proposed self-cleaning solar sliding system. So, as far as utilisation of land is concerned, there is no big issue

because large PV plants are installed in semiarid or dessert areas on barren land where solar PV panel cleaning is more needed than land use.

(v) Effectiveness during hailstorm

Hailstorms are common in India. The frequency and intensity of hailstorms have increased in India in the last few years, which is a threat to PV panel life. There is no method to protect them from heavy hailstorms. The proposed solar sliding system also provides protection from hailstorms, along with the self-cleaning of PV panels. Two hailstorms were observed on March 5, 2020, and November 17, 2020, in Jaipur. The hailstorm that happened on March 5th was very deadly.

Fig. 5.16 shows the intensity and size of deadly hailstorms. There are a lot of PV panels installed on the top of Manipal University Jaipur without any protection. As shown in Fig. 5.17 (b), one of the 300W PV panels was completely damaged during the massive hailstorm, and some have cracks in the front glass. The proposed system kept the PV panels safe, but the corner of the protective plate was damaged, as shown in Fig. 5.17 (a). Tables 5.15 shows the Self-cleaning PV sliding system's potential benefits and drawbacks.

Fig. 5.16 Deadly hailstorm on 5 March 2020, Jaipur

(a) (b)

Fig. 5.17 (a). Proposed system after deadly hailstorm, (b) 300W PV panel damaged during deadly hailstorm on 5 March 2020

Table 5.15 Self-cleaning PV sliding system's potential benefits and drawbacks

Benefits	Drawbacks
• Cleaning procedures are automated. • Cleaning two time/day, which not allows to stick the dust. • Cleaning time very less. • Low power consumption. • Not only provides cleaning but also provides protection from hailstorms. • No costlier. • No Water required	• Maintenance required. • In monsoon, more power consumes because of dark cloud. • It is prone to corrosion because it is made of iron rod and iron mechanical support. • Required to change the brushes or clean the brushes in four to six months, depends on local climate

CHAPTER 6

CONCLUSION

An economical, reliable, and affordable data acquisition system for sensing and monitoring of the PV system is required for researchers and academia. Existing wired and wireless data collecting systems are expensive and difficult to use because they are based on licence software and cloud services. Wired DAQ systems have limitations in that they are only accessible close to the PV system and require humans to operate. Wired DAQ systems have restrictions in that they are only accessible near the PV system and are either continuously connected to supply or operated, which necessitates the use of labour to control the system near the remote PV plant. Some wireless data gathering systems make use of open-source software and cloud services, but they only monitor and record a few parameters of low value at a significant cost. These problems can be solved by implementing the proposed IoT enabled DAQ system. Open-access software and cloud services were used to construct the suggested IoT-enabled data acquisition system. The developed DAQ system can be remotely turned on and off using a Wi-Fi enabled switch, depending on the requirements. This work presents a design of a cost-effective data acquisition system for gathering operational data of the PV system for assessment purposes with omnipresent access. The developed IoT enabled data acquisition system can record nine parameters with a voltage range of 0-36V and a current range of 15A. This method can save 58% of energy (assuming a daily operation time of 10 hours). The results of the experiments reveal that the created DAQ system is more durable, economical, trustworthy, and reliable and that it can be operated in harsh environments to observe and collect operational data from the PV system in order to study its behavior. This proposed DAQ system provides a more

affordable method for sensing and monitoring systems in the field of domestic and industrial standards to actualize the IoT.

Most of the research on the impact of dust on PV cell performance has been done in either an indoor or non-desert environment in semi-arid regions, especially in India. The performance of PV systems installed in various places is influenced by climatic and local factors. It becomes critical to conduct field experiments and scientific data analysis at the location. In this article, the authors present details on the behaviour of PV panels in various seasons in the Jaipur (semi-arid) region. The average annual PV system's efficiency is around 10.8%. The monthly average maximum efficiency of 11.6% was recorded in the month of December (winter) and the seasonally average maximum efficiency of 11.3% was recorded in the post monsoon season. In the summer, the average air dust density was 0.35 mg/m^3, reducing efficiency by 24.5% over four months. Despite the decrease in air dust density in winter, especially in the month of January, the reduction in efficiency of the panel is high, because bird-droppings are more in this period. In the summer, when the panel temperature rises above 41°C, panel efficiency drops by 0.06% for every degree. When T_P > 42°C in the monsoon, panel efficiency drops by 0.04% for every degree the panel temperature rises. For T_P > 39°C, panel efficiency decreases by 0.01% for every degree of temperature rise in the post-monsoon period. In the winter, however, the modules achieve maximum efficiency with no loss of efficiency at a T_P of 48°C. This is primarily due to natural cooling that occurs on a regular basis. The post-monsoon season has a higher efficiency of 11.3% than the summer, winter, and monsoon seasons. It is critical to keep the PV panel surface clean and at a low temperature, especially during the summer, in order to get the maximum output power from a PV system. The key finding of this investigation is that dust deposition on the PV panels also depends on seasonal changes, and the post monsoon season is more suitable for PV systems.

Most existing solar cleaning technologies rely on water and separate cleaning systems, which can be prohibitively expensive and inefficient. In hot and dry climates like Rajasthan, water is scarce. The use of precious water resources for the purposes of PV cleaning is contrary to the ultimate aims of economic and environmental sustainability. Hailstorms reduce not only total electricity generation but also the life of PV modules. There is no method for protecting the PV system from hailstorms. The proposed self-cleaning system protects the PV system from dust deposition and hailstorms. In this proposed technique, a self-cleaning PV sliding system covers the PV panels during the night and performs the cleaning procedure twice daily. As a result, the volume of dust deposited and dew developed on the PV surface is greatly reduced. This technology is primarily designed to achieve maximum energy in the PV module and ensure protection against pollution and hailstorms for the PV module. Results show that the proposed self-cleaning PV sliding system improves efficiency by 18.37%, 13.33%, and 6.4% when compared to fixed systems in the summer, winter, and post-monsoon seasons, respectively. The efficiency of a fixed PV system using weekly cleaning drops by 1.92%, 2.01%, 1.6%, and 2% after the first, second, third, and fourth weeks, respectively, whereas the efficiency of a proposed cleaning method drops by 0.67%, 0.67%, 0.422%, and 0.25%. For one month, the efficiency of a fixed PV system with daily manual cleaning was compared to that of a proposed cleaning system, and the proposed system's efficiency was reduced by 1.13%. The results of this study show that there is a significant improvement in PV efficiency, and hence an increase in the production of electricity in semi-desert climate conditions. This proposed cleaning mechanism provides a more affordable, efficient, and energy-efficient technique for cleaning and protecting the PV systems throughout the year. The following conclusions have been drawn.

- The developed data acquisition system is appropriate and effective for monitoring and gathering operational information of the PV

system to assess its performance under outdoor conditions for a long time.

- Water and separate cleaning systems are used in most existing solar cleaning technologies, which can be prohibitively expensive and inefficient.
- Hailstorms reduce electricity generation as well as the lifespan of PV modules. There is no way to keep the PV system safe from hailstorms.
- The suggested self-cleaning technique cleans the PV system without using water.
- The proposed self-cleaning system protects the PV system from dust and hailstorms.
- In this proposed technique, a self-cleaning PV sliding system covers the PV panels during the night and cleans them twice daily. As a result, the amount of dust deposited on the PV surface and the formation of dew are greatly reduced.

FUTURE WORK

There is a substantial amount of significant research work that can be done in the future to solidify and improve the proposed IoT based data acquisition system and self-cleaning solar PV sliding system. Firstly, the energy consumption of the proposed self-cleaning system is higher in the monsoon season. Therefore, it is necessary to make further improvements to the proposed self-cleaning PV sliding system. Some useful insights towards future work are highlighted as

- In practical application, there are several types of cleaning brushes. Therefore, it is necessary to investigate the performance of the self-cleaning solar PV sliding system with different types of cleaning brushes.
- Learn about the challenges of putting this technology into practice on a commercially large scale.
- For the proposed IoT based data acquisition system, we required a Wi-Fi connection at the point of PV installation. For remote and dessert PV systems, it may not be available. Therefore, it is necessary to make it work on a self-created Wi-Fi module.

REFERENCES

[1] Country Analysis Executive Summary: India. https://www.eia.gov/international/analysis/country/IND-2020.

[2] Jaszczur, M., Teneta, J., Styszko, K., Hassan, Q., Burzyńska, P., Marcinek, E., Łopian, N. (20180), The field experiments and model of the natural dust deposition effects on photovoltaic module efficiency. Environ. Sci. Pollut. Res., 1–16. https://doi.org/10. 1007/s11356-018-1970-x.

[3] Annual Report https://mnre.gov.in/annual report2019-20.

[4] Indian power Industry reports https://www.ibef.org/industry/power-sector-india.aspx2020.

[5] Javed, W., Wubulikasimu, Y., Figgis, B., Guo, B. (2017), Characterization of dust accumulated on photovoltaic panels in Doha. Qatar. *Sol. Energy*, 142: 123–135.

[6] Tanesab J, Parlevliet D, Whale J, et al. T. (2019), The effect of dust with different morphologies on the performance degradation of photovoltaic modules. *Sustainable Energy Technologies and Assessments*, 31:347-354.

[7] Salimi H, Lavasani A M, Danesh-Ashtiani H A. (2019), Effect of dust concentration, wind speed, and relative humidity on the performance of photovoltaic panels in Tehran. *Energy Sources, Part A: Recovery, Utilization, Environmental Effects*, 1-11.

[8] Razykov, T.M., Ferekides, C.S., Morel, D., Stefanakos, E., Ullal, H.S., Upadhyaya, H.M. (2011), Solar photovoltaic electricity: current status and future prospects. *Sol Energy*, 85 (8), 1580–1608.

[9] Said, S.A.M., Walwil, H.M. (2014), Fundamental studies on dust fouling effects on PV module performance. *Sol. Energy*, 107, 328–337

[10] Saidan, M., Albaali, A.G., Alasis, E., Kaldellis, J.K. (2016) Experimental study on the effect of dust deposition on solar photovoltaic panels in desert environment. *Renew. Energy*, 92:499–505.

[11] Mani, M., Pillai, R. (2010), Impact of dust on solar photovoltaic (PV) performance: Research status, challenges and recommendations. *Renew. Sustain. Energy Rev.*, 14(9), 3124–3131.

[12] Haeberlin, H., Graf, J.D. (1998), Gradual reduction of PV generator yield due to pollution. In: Proceedings of the 2nd *World Conference on Photovoltaic Solar Energy Conversion*, Vienna, Australia.

[13] Bombach, E. (2006), Technical experience during thermal and chemical recycling of a 23-year-old PV generator formerly installed on Pell worm island. 21st European Photovoltaic Solar Energy Conference.

[14] Kazem H A, Chaichan M T, Al-Waeli A H. (2020), A review of dust accumulation and cleaning methods for solar photovoltaic systems, *Journal of Cleaner Production*, 276:123187.

[15] Dhimish M, Holmes V, Mehrdadi B. (2017), The impact of cracks on photovoltaic power performance. *Journal of Science: Advanced Materials and Devices*,2(2):199-209. https://. doi: 10.1016/j.jsamd.2017.05.005.

[16] Siddiqui, R., Bajpai, U. (2012), Correlation between thicknesses of dust collected on photovoltaic module and difference inefficiencies in composite climate. *Int. J. Energy Environ. Eng.*, 3 (1), 1–7.

[17] Kaldellis, J.K., Kokala, A. (2012), Quantifying the decrease of the photovoltaic panels' energy yield due to phenomena of natural air pollution disposal. *Energy*, 35, 4862–4869.

[18] Zhang, P. (2013), Reliability assessment of photovoltaic power systems: Review of current status and future perspectives. *Appl. Energy*, 104, 822–833.

[19] Gooré Bi, E., Monette, F., Gasperi, J. (2015), Analysis of the influence of rainfall variables on urban effluents concentrations and fluxes in wet weather. *J. Hydrol*, 523,320–332.

[20] Mazumder, M.K., Sharma, R., Biris, A.S., Zhang, J., Calle, C., Zahn, M. (2007), Self-cleaning transparent dust shields for protecting solar panels and other devices. *PartSci. Technol*., 25 (1), 5–20.

[21] Pachauri R K, Mahela O P, Khan B, Kumar A, Agarwal S, Alhelou H H, Bai J. (2021), Development of arduino assisted data acquisition system for solar photovoltaic array characterization under partial shading conditions. *Computers & Electrical Engineering*, 92:107175. https://doi.org/10.1016/j.compeleceng.2021.107175.

[22] Touati F, Al-Hitmi M A, Chowdhury N A, Hamad J A, Antonio J.R. Gonzales S P. (2016), Investigation of solar PV performance under Doha weather using a customized measurement and monitoring system, *Renewable Energy,* 89:564-577.

[23] Herteleer B, Huyck B, Catthoor F. (2017), Normalised efficiency of photovoltaic systems: Going beyond the performance ratio, *Solar Energy*,157:408-418. https://doi.org/10.1016/j.solener.2017.08.037.

[24] Adouane M, Al-Qattan A, Alabdulrazzaq B. (2020), Comparative performance evaluation of different photovoltaic modules technologies under Kuwait harsh climatic conditions, *Energy Reports*, 6: 2689-2696. https://doi.org/10.1016/j.egyr.2020.09.034.

[25] Oh S. (2019), Analytic and Monte-Carlo studies of the effect of dust accumulation on photovoltaics. *Solar Energy*, 188:1243–1247.

[26] Zaihidee, F.M., Mekhilef, S., Mahmoudian, Seyed, Horan, H. (2016), Dust as an unalterable deteriorative factor affecting PV Panel's efficiency: Why and How. *Renew. Sustain.Energy Rev*., 65, 1267–1278.

[27] Zhe Song and Jia Liu and Hongxing Yang. (2021), Air pollution and soiling implications for solar photovoltaic power generation: A comprehensive review, *Applied Energy*, 298: 117-247

[28] El-Shobokshy, M.S., Hussein, F.M. (1993), Degradation of photovoltaic cell performance due to dust deposition on to its surface. *Renew. Energy*; 3 (6), 585–590.

[29] Hassan AH, Rohoma UA, Elminir HK, Fathy AM. (2005). Effect of Airborne dust concentration on the performance of PV modules. *Journal of Astronomical Society Egypt*;13(1):24–38.

[30] Asl-Soleimani E, Farhangi S, Zabihi MS. (2001). Effect of tilt angle, air pollution on performance of photovoltaic systems in Tehran. *Renewable Energy*; 24:459–68.

[31] Molki A. (2010), Dust affects solar-cell efficiency. *Physics Education*;45:456–8.

[32] Sulaiman SA, Hussain HH, Nik Leh NSH, Razali MSI. (2011), Effects of dust on the performance of PV panels. *World Academy of Science, Engineering and Technology*;58:588–93.

[33] Kaldellis JK, Fragos P, Kapsali M. (2011), Systematic experimental study of the pollution deposition impact on the energy yield of photovoltaic installa- tions. *Renewable Energy*;36(10):2717–24.

[34] Jiang H, Lu L, Sun K. (2011), Experimental investigation of the impact of airbourne dust deposition on the performance of solar photovoltaic (PV) modules. *Atmospheric Environment*;45(25):4299–304.

[35] Zorrilla-Casanova, J., Piliougine, M., Carretero, J., Bernaola, P., Carpena, P., Mora-López, L., Sidrach-de-Cardona, M., (2011), Analysis of dust losses in photovoltaic modules. In:Proceedings of the *World Renewable Energy Congress*, Link¨oping, Sweden, pp.2985–2992.

[36] Adinoyi, M.J., Said, S.A. 2013. Effect of dust accumulation on the power outputs of solar photovoltaic modules. *Renew. Energy*;60, 633–636.

[37] Kazem H A,Khatib T,Sopian K, (2013), Effect of dust deposition on the performance of multi-crystalline photovoltaic modules based on experimental measurements, *Renew. Energy*;3, 850–853.

[38] Rajput DS, Sudhakar K. (2013), Effect of dust on the performance of solar PV panel. *Int J ChemTech Res*.;5(2):1083–6.

[39] Weber, B., Quinones, A., Almanza, R., Duran, M.D. (2014), Performance reduction of PV systems by dust deposition. *Energy Procedia*.,57, 99–108.

[40] Rao A., Pillai R, Mani M., Ramamurthy P. (2014), Influence of dust deposition on photovoltaic panel performance, Energy Procedia; 54, 690-700.

[41] Mejia, F.; Kleissl, J.; Bosch, J.L. (2014), The Effect of Dust on Solar Photovoltaic Systems. *Energy Procedia*, 49, 2370–2376.

[42] Ketjoy N, M Konyu, (2014), Study of dust effect on photovoltaic module for photovoltaic power plant, *Energy Procedia*, 52:431-437.

[43] Klugmann-Radziemska, E. (2015), Degradation of electrical performance of a crystalline photovoltaic module due to dust deposition in northern Poland. *Renew. Energy*,78, 418–426.

[44] Chaichan, M.T., Mohammed, B.A., Kazem, H.A. (2015), Effect of pollution and cleaning on photovoltaic performance based on experimental study. *Int. J. Sci. Eng. Res*.,6 (4), 594–601.

[45] Kumar, B. S., & Sudhakar, K. (2015), Performance evaluation of 10 MW grid connected solar photovoltaic power plant in India. *Energy Reports*, 1, 184–192.

[46] Dastoori K, Al-Shabaan G, Kolhe M, Thompson D, Makin B. (2016), Impact of accumulated dust particles' charge on the photovoltaic module performance. *J Electrostatic*,79:20–4.

[47] Stamber A., Ramírez R., Juan J., Milón G., Karim N. C., Sergio L. B., (2022), Influence of dust deposition, wind and rain on photovoltaic panels efficiency in Arequipa Peru, *International Journal of Sustainable Energy*,1-14. https://doi.org/10.1080/14786451.2022.2052290

[48] Abderrezek, M., Fathi, M.(2017), Experimental study of the dust effect on photovoltaic panels' energy yield. *Sol. Energy*, 142: 308–320.

[49] Gholami, A., Khazaee, I., Eslami, S., Zandi, M., Akrami, E. (2018), Experimental investigation of dust deposition effects on photovoltaic output performance. *Sol. Energy,* 159:346–352.

https://doi.org/10.1016/j.solener.2017.11.010.

[50] Darwish Z A, Sopian K, Fudholi A. (2021), Reduced output of photovoltaic modules due to different types of dust particles. *Journal of Cleaner Production,* 280:124317. https://doi.org/10.1016/j.jclepro.2020.124317.

[51] Enaganti P K, Bhattacharjee A, Ghosh A. (2022), Experimental investigations for dust build-up on low-iron glass exterior and its effects on the performance of solar PV systems, *Energy,* 239:122213. https://doi.org/10.1016/j.energy.2021.122213.

[52] Chanchangi Y N, Ghosh A, Baig H. (2021), Soiling on PV performance influenced by weather parameters in Northern Nigeria, *Renewable Energy,* 180: 874-892. https://doi.org/10.1016/j.renene.2021.08.090.

[53] Maag, C.R. (1977), Outdoor weathering performance of solar electric generators. *J. Energy*,1 (6), 376–381.

[54] Sayigh, A.A.M., Charchafchi, S., Al-Habali, A. (1979), Experimental evaluation of solar cells in arid zones. In: Izmir *International Symposium on Solar Energy Fundamentals and Applications*. Izmir, Turkey, pp. 909–932.

[55] Nimmo, B., Said, S.A.M. (1979), Effects of dust on the performance of thermal and photovoltaic flat plate collectors in Saudi Arabia preliminary results. In: *2nd International Conference on Alternative Energy Sources*. Miami Beach, FL, pp. 145–152.

[56] Hoffman, A.R., Maag, C.R. (1980), Photovoltaic Module Soiling Studies May 1978 October 1980. Tech. Rep.,1012-49, Department of Energy/ Jet Propulsion Laboratory.

[57] Khoshaim, B., Huraib, F., Al-Sani, A., Salim, A.A., Imamura, M. (1984), Performance of 350 kW photovoltaic power system for Saudi Arabian villages after 30 months. In: 17th *IEEE Photovoltaic Specialists Conference* (PVSC), 1–4 May. Orlando, FL, pp. 1426–1432.

[58] El-Shobokshy, M.S., Mujahid, A., Zakzouk, A.K.M. (1985), Effects of dust on the performance of concentrator photovoltaic cells. *IEE Proc. I (Solid-State Electron Dev.*),132 (1), 5–8.

[59] Al-Busairi, H., Al-Kandari, A. (1987), Performance evaluation of photovoltaic modules in Kuwait. In: 3rd *International Photovoltaic Science and Engineering Conference.* Tokyo, Japan, pp. 323–326.

[60] Salim, A.A., Huraib, F.S., Eugenio, N.N., V. (1988), Power-study of system options and optimization. In: 8th *International Photovoltaic Solar Energy Conference*. Florence, Italy,pp. 688–692.

[61] Bajpai, S.C., Gupta, R.C. (1988). Performance of silicon solar cells under hot & dusty environmental conditions. *Ind. J. Pure Appl. Phys*., 26, 364–369.

[62] Ryan, C.P., Vignola, F., McDaniels, D.K. (1989), Solar cell arrays: degradation due to dirt. In: *American Section of the International Solar Energy Society.* Denver, CO, pp. 234–237.

[63] Said, S.A.M. (1990), Effects of dust accumulation on performances of thermal and photovoltaic flat-plate collectors. *Appl. Energy*, 37 (1), 73–84.

[64] Yahya, H.N., Sambo, A.S. (1991), The effect of dust on the performance of photovoltaic modules in Sokoto. Niger. *J. Renew. Energy*, 2 (1), 36–42.

[65] Pande, P.C. (1992), Effect of dust on the performance of PV panels. In: 6th *International Photovoltaic Science and Engineering Conference*. New Delhi, India, pp. 539–542.

[66] Becker, H., Vaassen, W., Hermann, W. (1997), Reduced output of solar generators due to pollution. In: 14th *European Photovoltaic Solar Energy Conference*, 30 June–4 July. Barcelona, Spain, pp. 251–255.

[67] Townsend, T.U., Hutchinson, P.A. (2000), Soiling analysis at PVUSA. In: *Solar 2000 Conference*, 16–21 June. Madison, WI, pp. 417–420.

[68] Asl-Soleimani, E., Farhangi, S., Zabihi, M.S. (2001), The effect of tilt angle, air pollution on performance of photovoltaic systems in Tehran. *Renew. Energy*;24 (3-4), 459–468.

[69] Pang, H., Close, J., Lam, K. (2006), Study on effect of urban pollution to performance of commercial copper indium diselenide modules. In: 4th *IEEE World Conference on Photovoltaic Energy Conversion*, 7–12 May. Waikoloa, HI, pp. 2195–2198.

[70] Boykiw, E.. (2011), The Effect of Settling Dust in the Arava Valley on the Performance of Solar Photovoltaic Panels. *Senior thesis*, Allegheny College, Meadville, PA.

[71] Cano, J. (2011), Photovoltaic Modules: Effect of Tilt Angle on Soiling. *Master's thesis*, Arizona State University, Tempe, AZ.

[72] Ibrahim, A. (2011), Effect of shadow and dust on the performance of silicon solar cell. *J. Basic Appl. Scient. Res.m*,1 (3), 222–230.

[73] Pavan, A.M., Mellit, A., Pieri, D.D.(2011), The effect of soiling on energy production for large-scale photovoltaic plants. *Solar Energy*, 85 (5), 1128–1136.

[74] Rahman, M.M., Islam, M.A., Karim, A.H.M.Z., Ronee, A.H. (2012), Effects of natural dust on the performance of PV panels in Bangladesh. *Int. J. Mod. Edu. Comp. Sci.*, 4 (10), 26–32.

[75] Liqun, L., Zhiqi, L., Chunxia, S.Z.L. (2012), Degraded output characteristic at atmospheric air pollution and economy analysis of PV power system: a case study. *Przegl. Elektrotech*. (Electr. Rev.), 88 (9A), 281– 284.

[76] Kalogirou, S.A., Agathokleous, R., Panayiotou, G. (2013), On-site PV characterization and the effect of soiling on their performance. *Energy*, 51, 439–446.

[77] Piliougine, M., Can˜ ete, C., Moreno, R., Carretero, J., Hirose, J., Ogawa, S., Sidrach-de-Cardona, M.. (2013), Comparative analysis of energy produced by photovoltaic modules with anti-soiling coated surface in arid climates. *Appl. Energy*,112, 626–634.

[78] Mejia, F.; Kleissl, J.; Bosch, J.L. (2014), The Effect of Dust on Solar Photovoltaic Systems. *Energy Procedia*, 49, 2370–2376.

[79] Ketjoy N, M Konyu, (2014), Study of dust effect on photovoltaic module for photovoltaic power plant, *Energy Procedia*, 52:431-437.

[80] Sulaiman S A, Guangul F M, Mat M N H, Mohammed A B. (2015), Real-time study on the effect of dust accumulation on the performance of solar PV panels in Malaysia. In: 1st *IEEE conference on Electrical and Information technologies,*;pp. 269-274.

[81] Kazem, H.A., Chaichan, M.T. (2016), Experimental analysis of the effect of dust's physical properties on photovoltaic modules in Northern Oman. *Sol. Energy*, 139, 68–80.

[82] Guan Y, Zhang H, Xiao B, Zhou Z, Yan X. (2017), In-situ investigation of the effect of dust deposition on the performance of polycrystalline silicon photovoltaic modules. *Renew Energy*,101:1273–84.

[83] Garg, H. (1974), Effect of dirt on transparent covers in flat-plate solar energy collectors. *Sol. Energy*,15 (4), 299–302.

[84] Nahar, N., Gupta, J.P. (1990), Effect of dust on transmittance of glazing materials for solar collectors under arid zone conditions of India. *Sol. Wind Technol.*,7 (2), 237–243.

[85] Hasan A, Sayigh AA. (1992), Effect of sand and dust accumulation on the light transmittance, reflectance, and absorbance of the PV glazing. In: *Renewable energy: technology and the environment: Proceedings of the 2nd world renewable energy congress*, pp. 461–6.

[86] Al-Hasan AY. (1998), A new correlation for direct beam solar radiation received by photovoltaic panel with sand dust accumulated on its surface. *Solar Energy*, 63(5);323-33.

[87] Qasem H, Betts TR, Müllejans H, AlBusairi H, Gottschalg R. (2014), Dust-induced shading on photovoltaic modules. *Prog Photovolt Res Appl*., 22(2):218–26.

[88] Monto, M., Rohit, P. (2010), Impact of dust on solar photovoltaic performance: Research status, challenges and recommendations. *Renew. Sustain. Energy Rev.*, 14: 3124–3131.

[89] Gholami, A., Saboonchi, A., Alemrajabi, A.A. (2017), Experimental study of factors affecting dust accumulation and their effects on the transmission coefficient of glass for solar applications. *Renew. Energy*, 112, 466–473.

[90] Hoffman, A.R., Maag, C.R. (1980), Airborne particulate soiling of terrestrial photovoltaic modules and cover materials. In: 26th *Annual Technical Meeting of Institute of Environmental Sciences*, 12–14 May. Philadelphia, PA, pp. 229–236.

[91] Sayigh, A.A.M., Al-Jandal, S., Ahmed, H. (1985), Dust effect on solar flat surfaces devices in Kuwait. In: *Workshop on Physics of Non-Conventional Energy Sources and Material Science for Energy*. Trieste, Italy, pp. 353–367.

[92] Mastekbayeva, G.A., Kumar, S. (2000), Effect of dust on the transmittance of low density polyethylene glazing in a tropical climate. *Solar Energy*, 68 (2), 135–141.

[93] Hegazy, A.A. (2001), Effect of dust accumulation on solar transmittance through glass covers of plate-type collectors. *Renew. Energy*,22 (4), 525–540.

[94] El-Nashar, A.M. (2003), Effect of dust deposition on the performance of a solar desalination plant operating in an arid desert area. *Solar Energy*, 75 (5), 421–431.

[95] El-Nashar, A.M. (2009), Seasonal effect of dust deposition on a field of evacuated tube collectors on the performance of a solar desalination plant. *Desalination*, 239 (1–3), 66–81.

[96] Appels, R., Muthirayan, B., Beerten, A., Paesen, R., Driesen, Poortmans, J. (2012), The effect of dust deposition on photovoltaic modules. In: 38th *IEEE Photovoltaic Specialists Conference (PVSC)*, 3–8 June. Austin, TX, pp. 001886–001889.

[97] Hee, J.Y., Kumar, L.V., Danner, A.J., Yang, H., Bhatia, C.S. (2012), The effect of dust on transmission and self-cleaning property of solar panels. *Energy Proc*.,15, 421–427.

[98] Ghazi S, Ip K, Sayigh A. (2013), Preliminary study of environment solid particles on solar flat surfaces in the UK. *Energy Proc*., 42, 765-774.

[99] Qasem H, Betts TR, Müllejans H, AlBusairi H, Gottschalg R. (2014), Dust-induced shading on photovoltaic modules. *Prog Photovolt Res Appl* , 22(2):218–26.

[100] Semaoui S, Arab A H, Boudjeithia E K, Bacha S, Zerabla H. (2015), Dust effect on optical transmittance of photovoltaic module glazing in desert region. *Energy Proc*.,74, 1347-1357.

[101] Helene P., Johann S., Josefine S. (2016), Effect of soiling on photovoltaic modules in Norway. *Energy Procedia, (*92); 585-589.

[102] Dorobantu L, Popescu M O, Popescu C, Craciunesc A. (2011), The effect of surface impurities on photovoltaic panels. In: *Proceedings of the international conference on renewable energies and power quality* (icrepq'11). Spain: LasPal- mas dEGranCanaria..

[103] Goossens, D., Van Kerschaever, E., (1999), Aeolian dust deposition on photovoltaic solar cells: the effects of wind velocity and airborne dust concentration on cell performance. *Sol. Energy*, 66:277–289.

[104] Weber P, Sastry OS, Tiwari GN. (2017), Effect of irradiance, temperature exposure and an Arrhenius approach to estimating weathering acceleration factor of Glass, EVA and Tedlar in a composite climate of India. *Sol Energy*, ,144:267–77.

[105] Goossens, D., Offer, Z.Y., Zangvil, A., (1993), Wind tunnel experiments and field investigations of aeolian dust deposition on photovoltaic solar collectors. *Sol. Energy*, 50:75–84.

[106] Jaszczur, M., Teneta, J., Styszko, K., Hassan, Q., Burzyńska, P., Marcinek, E., Łopian, N. (2018), The field experiments and model of the natural dust deposition effects on photovoltaic module efficiency.

Environ. Sci. Pollut. Res., 1–16. https://doi.org/10. 1007/s11356-018-1970-x.

[107] Jiang, Y., Lu, L., Ferro, A.R., Ahmadi, G. (2018), Analyzing wind cleaning process on the accumulated dust on solar photovoltaic (PV) modules on flat surfaces. *Sol. Energy*, 159, 1031e1036. https://doi.org/10.1016/j.solener.2017.08.083.

[108] Goossens, D., Offer, Z.Y. (1995), Comparisons of day-time and night-time dust accumulation in a desert region. *J. Arid Environ*.1995; 31 (3), 253–281.

[109] Clarke L, Elatrash M S, L.Ã S. (2006), Field measurements of desert dust deposition in Libya. vol. 40, pp. 3881–3897.

[110] Elminir, H.K., Ghitas, A.E. (2006), Effect of dust on the transparent cover of solar collectors. *Energy Convers. Manage*., 47 (18), 3192–3203.

[111] Kohli R, Mittal KL.(2011), Developments in surface contamination and cleaning. Volume three, methods for removal of particle contaminants. *Amsterdam; Boston: Elsevier*.

[112] Schneider H, Subtask I of Spacecraft Cleaning and Decontamination Techniques, Ch. 6 of Planetary Quarantine, *Ann. Rev. Space echnology and Research*, Jet Propulsion Laboratory TR-900-597. (February 1973).

[113] Mekhilef S, Rahman S, Kamalisarvestani M. (2012), Effect of dust, humidity and air velocity on efficiency of photovoltaic modules. *Renewable and Sustainable Energy Reviews*, 16:2920–5.

[114] Gostein, M., J.R. Caron, and B. (2014), Littmann Measuring soiling losses at utility- scale PV power plants. in *Photovoltaic Specialist Conference (PVSC)*, IEEE 40th, 2014 IEEE.

[115] Figgis, B., D. Martinez Plaza, and Mirza T. (2014), PV Soiling Rate Variation over Long Periods.

[116] Kim, Y., Wellum, G., Mello, K., Strawhecker, K.E., Thoms, R., Giaya, A., Wyslouzil, B.E. (2016), Effects of relative humidity and

particle and surface properties on particle resuspension rates. *Aerosol. Sci. Technol*., 50 (4), 339–352.

[117] Isaifan R J, Johson D, Ackermann L,,Figgis B, Ayoub M. (2019), Evaluation of the adhesion forces between dust particles and photovoltaic module surfaces. *Solar Energy Materials & solar Cells*,191;413-421.

[118] Kimber A, Mitchell L, Nogradi S, Wenger H. (2006), Effect of soiling on large grid- connected photovoltaic systems in California and the Southwest region of the United States. In: *Proceedings of the photovoltaic energy conversion: record of the 2006 IEEE 4th world conference*. pp. 2391–5.

[119] Bethea, R.M., Barriger, M.T., Williams, P.F., Chin, S. (1981), Environmental effects on solar concentrator mirrors. *Solar Energy*; 27 (6), 497– 511.

[120] Cuddihy, E., Coulbart, C., Gupta, A., Liang, R.. (1981), Electricity from Photovoltaic Solar Cells: Flat-Plate Solar Array Project Final Report. Volume VII: Module encapsulation. Tech. Rep., DOE/JPL-1012-125, Jet Propulsion Laboratory (October).

[121] Caron J R , Littmann B. (2013), Direct monitoring of energy lost due to soiling on first solar modulesin California. *Photovolt IEEEJ*, 3(1):336–40.

[122] Hassan G, Yilbas BS, Said SAM, Matin A. (2016), Chemo-Mechanical Characteristics of Mud Formed from Environmental Dust Particles in Humid Ambient Air. *Nat. Publ. Gr*., pp. 1–14.

[123] Brown K, Narum T, Jing N. (2012), Soiling test methods and their use in predicting performance of photovoltaic modules in soiling environments. In: *Proceedings of the 38th IEEE Photovoltaic Specialists Conference (PVSC)*, pp. 1881–1885.

[124] Corn M. (1961), The adhesion of solid particles to solid surfaces, I. A review. *J Air Pollute Control Assoc*., 11(11):523–8.

[125] Penney EW. (1962), Contact Potentials and the Adhesion of Dust, pp. 200–204.

[126] Kazmerski LL, Diniz ASAC, Maia CB, Viana MM, Costa SC, Brito PP, Campos CD, Neto LVM, Hanriot S De Morais, Oliveira LR De. (2016), Fundamental studies of adhesion of dust to PV module surfaces: chemical and physical relationships at the microscale. *IEEE J Photovolt* ,6(3):719–29.

[127] Kazmerski LL, Sonia A, Diniz AC, Brasil C, Machado M, Costa SC, Brito PP, Dias C, De Morais S, Oliveira LR De. (2016), Soiling particle interactions on PV modules: surface and inter - particle adhesion and chemistry effects. Pvsc:2–4.

[128] Hammond, R., Srinivasan, D., Harris, A., Whitfield, K., Wohlgemuth, J. (1997), Effects of soiling on PV module and radiometer performance. In: 26th *IEEE Photovoltaic Specialists Conference (PVSC*), 29 September– 3 October. Anaheim, CA. pp. 1121–1124.

[129] Al-Ammri . (2013), Dust effects on the performance of PV Street light in Baghdada city, *IEEE conference*.

[130] Cano, J., (2014), Effect of tilt angle on soiling of photovoltaic modules.in *Photovoltaic Specialist Conference(PVSC)*,14IEEE40th, IEEE

[131] Xu R, Ni K, Hu Y, Si J, Wen H, Yu D. (2017), Analysis of the optimum tilt angle for a soiled PV panel. *Energy Convers Manag*, 148:100–9.

[132] Haghdadi N, Copper J, Bruce A, Macgill I. (2017), A method to estimate the location and orientation of distributed photovoltaic systems from their generation output data. *Renew Energy*,108:390–400.

[133] Kaddoura TO, Ramli MAM, Al-turki YA. (2016), On the estimation of the optimum tilt angle of PV panel in Saudi Arabia. *Renew Sustain Energy Rev*., 65:626–34.

[134] Singh R, Banerjee R. (2016), Impact of solar panel orientation on large scale rooftop solar photovoltaic scenario for Mumbai [no. December 2015]. *Energy Procedia*, 90:401–11.

[135] Goossens D, Offer Z. (1990), A wind tunnel simulation and field verification of desert dust deposition (Avdat Experimental Station, Negev Desert). *Sedimentology*,37(1):7–22.

[136] ParkY-B, (2011), Self-cleaning effect of highly water-repellent micro shell structures for solar cell applications. *JMaterChem*,21(3):633–6.

[137 Barbón A., Bayón-Cueli C, Bayón L, Rodríguez-Suanzes C. (2022), Analysis of the tilt and azimuth angles of photovoltaic systems in non-ideal positions for urban applications. *Applied Energy*, 305,117802.

[138] Neil S. Beattie, Robert S. Moir, Charlslee Chacko, Giorgio Buffoni, Simon H. Roberts, Nicola M. Pearsall, (2012), Understanding the effects of sand and dust accumulation on photovoltaic modules, *Renew. Energy* 48, pp 448-452.

[139] Bhushan, B., Jung Y. C., and Nosonovsky M. (2012), Hierarchical structures for super hydrophobic surfaces and methods of making, *Google Patents.*

[140] Torma M, Loget G, Corn R M. (2014). Flexible teflon nanocone array surfaces with tunable super hydrophobicity for self-cleaning and aqueous droplet patterning. *ACS Appl Mater Interfaces*.

[141] Tian W, Wang Y, Ren J, Zhu L. (2007), Effect of urban climate on building integrated photovoltaics performance. *Energy Convers Manag*.,48(1):1–8.

[142] Berthet, C., Dessens, J. and Sanchez, J., (2011), Regional and yearly variations of hail frequency and intensity in France. *Atmospheric Research* 100, pp. 391–400.

[143] Hughes, P., and R. Wood, (1993).. Hail: The white plague, *Weatherwise*, pp.16-21.

[144] Browning, K.A. (1977), The structure and mechanisms of hailstorms. Monograph 38, *American Meteorological Society*, Review of Hail Science and Hail Suppression, pp. 1-48.

[145] Brandes, E., Vivekanadan, J., Tuttle, J. and Kessinger, G., (1997), Hail production in Northeast Colorado hailstorms, *Proceedings 27th Conference on Radar Meteorology, American Meteorological Society*, Boston, MA, pp. 527-530.

[146] Dessens, J., (1986). Hail in Southwestern France: Hailfall characteristics and hailstorm environment. *Journal of Applied Meteorology* 25, pp. 35-47.

[147] Edwards, R., and Thompson, R.L., (1998), Nationwide comparisons of hail size with WSR-88D vertically integrated liquid water and derived thermodynamic sounding data. Weather and Forecasting 13, pp.277-285.

[148] Gokhale, N.R. (1975), Hailstorms and hailstone growth. State University of New York Albany Press, pp.465.

[149] Changnon S. A. (2012), Hailstorms Across the Nation: An Atlas about Hail and Its Damages.

[150] www.noaa.gov and www.torro.org.

[151] Morrison, S. (1997), Causes and extent of damage related to structure, material, and architectural failure. Hail, Hail The Disaster's Here, Employers Reinsurance Corp. Overland Park, KS,pp. 12.

[152] K€ontges M., Siebert M, Hinken D, Eitner U., Bothe K., Potthof T. (2009), Quantitative analysis of PV-modules by electroluminescence images for quality control, in: 24th *European Photovoltaic Solar Energy Conference*, Hamburg, Germany, pp. 21-24.

[153] Berardone I, Corrado M, Paggi M. (2014), A generalized electric model for mono and polycrystalline silicon in the presence of cracks and random defects. *Energy Procedia*, 55:22-9.

[154] Moore D, Wilson A, (1978), Photovoltaic Solar Panel Resistance to Simulated Hail. Jet Propulsion Laboratory, Pasadena, California.

[155] Koentges M, Kunze I, Kajari-Schroeder S, Breitenmoser X, Bjørneklett B. (2011), The risk of power loss in crystalline silicon based photovoltaic modules due to micro-cracks. *Sol Energ Mat Sol Cells*, 95:1131-37.

[156] Kajari-Schroeder S, Kunze I, Eitner U, Koentges M. (2011), Spatial and orientational distribution of cracks in crystalline photovoltaic modules generated by mechanical load tests. *Sol Energ Mat Sol Cells*, 95:3054-59.

[157] Kajari-Schroeder S, Kunze I, Koentges. (2012), Criticality of cracks in PV modules. *Energy Procedia*, 27:658-63.

[158] Morlier A., Haase F, K€ontges M. (2015), Impact of cracks in multicrystalline silicon solar cells on PV module powerda simulation study based on field data, *IEEE J. Photovolt*., 5 (6); pp1735-1741.

[159] Paggi M., Corrado M., Rodriguez M A, (2013), A multi-physics and multi-scale numerical approach to microcracking and power-loss in photovoltaic modules, *Compos. Struct*. 95; pp 630-638.

[160] K€ontges M, Kajari-Schr€oder S, Kunze I, Jahn U., (2011), Crack statistic of crystalline silicon photovoltaic modules, in: 26th *European Photovoltaic Solar Energy Conference and Exhibition*, pp.5-6.

[161] M€olken V. J. I., Yusufo U.A, Safiei A., Windgassen H., Khandelwal R., Pletzer T.M., Kurz H., (2012), Impact of micro-cracks on the degradation of solar cell performance based on two-diode model parameters, *Energy Procedia* 27; pp167-172.

[162] Kaplani E., (2016), Degradation in field-aged crystalline silicon photovoltaic modules and diagnosis using electroluminescence imaging, in: Presented at *8th International Workshop on Teaching in Photovoltaics* (IWTPV'16),7.

[163] Dallas W., Polupan O., Ostapenko S. (2007), Resonance ultrasonic vibrations for crack detection in photovoltaic silicon wafers, *Meas. Sci. Technol.* 18 (3) , 852.

[164] Muehleisen W, Eder G C, Voronko Y, Spielberger M, Sonnleitner H, Knoebl K, Ebner R, Ujvari G, Hirschl C. (2018),. Outdoor detection and visualization of hailstorm damages of photovoltaic plants, *Renewable Energy*, 118: p. 138-145.

[165] http://www.indexmundi.com

[166] Qasem H, Betts TR, Müllejans H, AlBusairi H, Gottschalg R. (2014), Dust-induced shading on photovoltaic modules. *Prog Photovolt Res Appl*., 22(2):218–26.

[167] Smith M K, (2013), Effects of natural and manual cleaning on photovoltaic output. *J Sol Energy Engg* ,135(3):034505.

[168] Cuddihy EF. (1980), Theoretical considerations of soil retention. *Solar Energy Materials,*3:21–33.

[169] Mohamed AO, Hasan A. (2012), Effect of dust accumulation on performance of photovoltaic solar modules in Sahara environment. *J Basic Appl Sci Res.* 2(11):11030–6.

[170] El-Nashar AM. (1994), Effect of dust accumulation on the performance of evacuated tube collectors. *Solar Energy,* 53:105–15.

[171] Kimber A. (2007), The effect of soiling on photovoltaic systems located in arid climates. In: *Proceedings of the 22nd European PV solar energy conference*. Milan, Italy, WIP, Germany

[172] Moharram K. (2013), Influence of cleaning using water and surfactants on the performance of photovoltaic panels. *Energy Convers Manag,*, 68:266–72.

[173] Freese JM. (1979), Effects of outdoor exposure on the solar reflectance properties of silvered glass mirrors. Sandia laboratory report SAND 78-1649; November 1978. In: *Proceedings of the international solar energy meeting;* 1979. p.1340–4.

[174] Tejwani, R. and C. Solanki. (2010), 360° sun tracking with automated cleaning system for solar PV modules .in *Photovoltaic Specialists Conference* (PVSC),2010 35th IEEE; 2010.IEEE.

[175] Lamont LA, Chaar L. (2011). Enhancement of a stand-alone photovoltaic system's performance: reduction of soft and hard shading. *Renew Energy,* 36 (4):1306–10.

[176] Williams RB, Tanimoto R, Simonyan A. (2007), Vibration characterization of self-cleaning solar panels with piezoceramic actuation. Collection of technical papers. In: *Proceedings of the 48th*

AIAA/ASME/ASCE/AHS/ASC structures, structural dynamics, and materials conference, p. 512–20.

[177] Masuda, S., Fujibayashi, K., Ishida, K., Inaba, H. (1972), Confinement and transportation of charged aerosol clouds via electric curtain. *Electr. Eng. Japan*, 92 (1), 43–52.

[178] Masuda, S., Matsumoto, Y. (1973), Contact-type electric curtain for electro dynamical control of charged dust particles. In: *2nd International Conference on Static Electricity*. No. 72, March. Frankfurt, Germany, 1973; pp. 1370–1409.

[179] Mazumder MK, Sharma R, Biris AS, Zhang J, Calle C, Zahn M. (2007), Self-cleaning transparent dust shields for protecting solar panels and other devices. *Part Sci Technol*,25(1):5–20.

[180] Guo B, Figgis B, Javed W.(2019), Measurement of electrodynamic dust shield efficiency in field conditions; *Journal of Electrostatics*, 9726-30.

[181] Mazumder, M.K., Horenstein, M.N., Stark, J.W., Girouard, P., Sumner, R., Henderson, B., Sadder, O., Hidetaka, I., Biris, A.S., Sharma, R. (2013), Characterization of electrodynamic screen performance for dust removal from solar panels and solar hydrogen generators. *IEEE Trans. Indust. Appl*., 49 (4), 1793–1800.

[182] Derakhshandeh J. F.,AlLuqman R, Mohammad S, AlHussain H, AlHendi G, AlEid D, Ahmad Z. (2021), A comprehensive review of automatic cleaning systems of solar panels. *Sustainable Energy Technologies and Assessments*,47,101518. https://doi.org/10.1016/j.seta.2021.101518.

[183] Ju, F., Fu, X. (2011), Research on impact of dust on solar photovoltaic (PV) performance. In: *International Conference on Electrical and Control Engineering (ICECE)*, 16–18 September. Yichang, China, pp. 3601–3606.

[184] Cuddihy, E.F. (1983), Surface soiling: theoretical mechanisms and evaluation of low- soiling coatings. in *Proceedings of the Flat-Plate Solar Array* Project Research Forum..

[185] Brophy, B., Abrams, Z.R., Gonsalves, P., and Christy, K. (2015), Field performance and persistence of anti-soiling coatings on photovoltaic glass. In 31st *European Photovoltaic Solar Energy Conference and Exhibition*, Hamburg (Germany), pp 2598-2602.

[186] Abrams, Z.R., Gonsalves, P., Brophy, B., and Posbic, J. (2014), Field and Lab Verification of Hydrophobic Anti-Reflective and Anti-Soiling Coatings on Photovoltaic Glass. *In 29thEuropean Photovoltaic Solar Energy Conference and Exhibition*, pp. 2759–2764.

[187] He G, Zhou C, LiZ. (2011), Review of self-cleaning method for solar cell array. *Procedia Eng.*,16:640–5.

[188] Dahlioui D, Laarabi B, Barhdadi A. (2022), Review on dew water effect on soiling of solar panels: Towards its enhancement or mitigation, *Sustainable Energy Technologies and Assessments*,49,101774. https://doi.org/10.1016/j.seta.2021.101774.

[189] Checco A, Rahman A,Black CT. (2014), Robust super hydrophobicity in large-area nanostructured surfaces defined by block-copolymer self-assembly. *Adv Mater,* 26(6):886–91.

[190] Verma L K. (2011), Self-cleaning and antireflective packaging glass for solar modules. *RenewEnergy*,36(9):2489–93.

[191] Midtdal K, Jelle B P. (2013), Self-cleaning glazing products: a state-of-the-art review and future research pathways. *Sol Energy Mater Sol Cells*, 109:126–41.

[192] Yong Sheng K. (2014), Optimal orientation and tilt angle for maximizing in- plane solar irradiation for PV applications in Singapore. *IEEEJ*;4(2):647–53.

[193] Hong L, Pan T. (2011), Surface microfluidics fabricated by photo pattern able super- hydrophobic nano composite. *Microfluid Nanofluidics*, 10(5):991–7.

[194] Nair, V., Dave B. C. (2014), Tuning the anti-reflective, abrasion resistance, anti-soiling and self-cleaning properties of transparent coatings for different glass substrates and solar cells, Google Patents.

[195] Smitha V S. (2013), U V curable hydrophobic inorganic–organic hybrid coating on solar cell covers for photo catalytic self-cleaning application. *J Mater Chem A*,1(40):12641–9.

[196] Polizos, G. (2014), Enhanced durability transparent super hydrophobic anti- soiling coatings for CSP applications .in *ASME 20148th International Conference on Energy Sustainability* collocated with the ASME 2014 12th Inter- national Conference on Fuel Cell Science, Engineering and Technology. American Society of Mechanical Engineers.

[197] Chanchangi Y N, Ghosh A, Sundaram S, Mallick T K. (2021). Angular dependencies of soiling loss on photovoltaic performance in Nigeria, *Solar Energy*,225, pp108-121. https://doi.org/10.1016/j.solener.2021.07.001.

[198] Drelich J, Chibowski E. (2010), Super hydrophilic and super wetting surfaces: definition and mechanisms of control. *Langmuir*, 26(24):18621–3.

[199] Son J. (2012), A practical super hydrophilic self-cleaning and antireflective surface for outdoor photovoltaic applications. *Sol Energy Mater Sol Cells*, 98:46–51.

[200] http://www.theultimatefinish.co.uk/ .

[201] Solar facts and advice. ⟨http://www.solar-facts-and-advice.com/solar-panel- cleaning.html07/01/2014⟩.

[202] SERBOTLG Solar Panel. ⟨http://www.serbot.ch/index.php/en/⟩.

[203] Self-cleaning solar panels maximize energy efficiency. ⟨https://www.asme.org/engineering-topics/articles/energy/self-cleaning-solar-panels-maximize- efficiency⟩.

[204] Nayshevsky, I.; Xu, Q.; Lyons, 2018. Hydrophobic-Hydrophilic Surfaces Exhibiting Dropwise Condensation for Anti-Soiling Applications." 2018 *IEEE 45th Photovoltaic Specialists Conference* (PVSC).

[205] Nayshevsky, I.; Xu, Q.; Barahman, G.; Lyons, A., 2017. Self-Cleaning Effects of the Anti-Soiling and Anti-Reflective Textured Fluoropolymer Nano coatings. *IEEE 44rd Photovoltaic Specialists Conference* (PVSC).

[206] Mondal, B.; Eain, M.M.G.; Xu, Q.; Egan, V.M.; Punch, J.; Lyons, A.M., 2015. Design and Fabrication of a Hybrid Super hydrophobic–Hydrophilic Surface That Exhibits Stable Dropwise Condensation. *ACS Applied Materials & Interfaces*, vol. 7, no. 42, pp. 23575–23588.

[207] Fraunhofer ISC. (2017), The need for modified surfaces on solar Application in the MENA region, In *intersolar middle east conference*.

[208] (https://www.duramat.org/hybrid-coating.html)

[209] Mondal S.; Mondal A. K.; Sharma A.; Devalla V.; Rana S.; Kumar S.; Pandey J. K. (2018). An overview of cleaning and prevention processes for enhancing efficiency of solar photovoltaic panels, *Current Science*,115 (6), 25.

[210] Mukaro R., Carelse X.F. (1999), A microcontroller-based data acquisition system for solar radiation and environmental monitoring, *IEEE Trans. Instrum. Measur.* 48 ,1232–1238.

[211] Koutroulis E., Kalaitzakis K.(2003), Development of an integrated data-acquisition system for renewable energy sources systems monitoring, *Renew. Energy,* 28, 139–152.

[212] Anwari M., Hidayat A., Hamid M.I., Taufik I., (2009), Wireless data acquisition for photovoltaic power system, in: *International*

Congress: Telecommunications Energy Conference, Incheon, Korea, pp. 1–4, Oct 2009.

[213] Forero N., Hernandez J., Gordillo G. (2006), Development of a monitoring system for a PV solar plant, *Energy Convers. Manage.* 47; 2329–2336.

[214] Zou X., Bian L., Yonghui Z., Haitao L. (2012), Performance monitoring and test system for grid-connected photovoltaic systems, in: *IEEE Power and Energy Engineering Conference (APPEEC),* Asia-Pacific, pp. 1–4.

[215] Balan M., Damian M., Jäntschi L. (2008), Preliminary results on design and implementation of a solar radiation monitoring system, *Sensors* 8;963–978.

[216] Thomas A., Ganesan A., Mujeeb S.A. (1993), Solar irradiance monitor, *Renew. Energy*,3; 599–606.

[217] Aristizabal A.J., Arredondo, C.A Hernandez J, Gordillo G. (2006), Development of equipment for monitoring PV power plants, using virtual instrumentation, *IEEE 4th World Conference on Photovoltaic Energy Conversion*, vol. 2, pp. 2367–2370.

[218] Alex S. Kok Bin, S. Weixiang, O. Kok Seng, S. Ramanathan, L. I-Wern, (2006), Development of a LabVIEW-based test facility for standalone PV systems. In: *Proceedings of the Third IEEE International Workshop on Electronic Design, Test and Applications*.

[219] Belmili H., Cheikh S., Haddadi M., Larbes C. (2010), Design and development of a data acquisition system for photovoltaic modules, *Renewable Energy* 35(7):1484-1492.

[220] Benghanem M. (2009), Measurement of meteorological data based on wireless data acquisition system monitoring, *Appl. Energy*,86(12), pp. 2651–2660.

[221] Gagliarducci M., Lampasi D. A., and Podestà L. (2007), GSM-based monitoring and control of photovoltaic power generation, *Measurement*,40(3), pp. 314–321.

[222] Van Dyk E. E, Gxasheka A. R., and Meyer E. L. (2005), Monitoring current-voltage characteristics and energy output of silicon photovoltaic modules, *Renew. Energy*,30(3), pp. 399–411.

[223] Belmili H., Ait Cheikh S. M, Haddadi M., and Larbes C. (2010), Design and development of a data acquisition system for photovoltaic modules characterization, *Renew. Energy*,35(7), pp. 1484–1492.

[224] Mlakić, D., Baghaee, H. R., Nikolovski, S., Vukobratović, M., & Balkić, Z. (2019), Conceptual Design of IoT-Based AMR Systems Based on IEC 61850 Microgrid Communication Configuration Using Open-Source Hardware/Software IED. *Energies*, 12(22), 4281.

[225] Ulieru V.D., Cepisca C., Ivanovici T. D, Pohoata A., Husu A., Pascale L. (2010). Measurement and analysis in PV systems, in: *Proceedings of the International Conference on Circuits, WSEAS*, pp37-142.

[226] Torres M., Mu~noz F.J., Mu~noz J.V., Rus C. (2012). Online monitoring system for standalone photovoltaic applications-analysis of system performance from monitored data, *J. Sol. Energy Eng*.,3;134.

[227] Chouder A., Silvestre S., Taghezouit C., Karatepe E. (2013), Monitoring, modelling and simulation of PV systems using LabVIEW, *Sol. Energy*, 91; pp337-349.

[228] Congedo P.M., Malvoni M., Mele M., Giorgi M.G.D (2013), Performance measurements of monocrystalline silicon PV modules in South- eastern Italy, *Energy Convers. Manag*,68; pp1-10.

[229] Fuentes M., Vivar M., Burgos J. M., Aguilera J. Vacas J. A. (2014), Design of an accurate, low-cost autonomous data logger for PV system monitoring using Arduino™ that complies with IEC standards, *Sol. Energy Mater. Sol. Cells*; 130, pp529-543.

[230] Ferdoush S., Li X., (2014), Wireless sensor network system design using raspberry Pi and Arduino for environmental monitoring applications, Proc. *Comput. Sci.*,34; pp. 103-110.

[231] Hegazy Rezk, Igor Tyukhov, Mujahed Al-Dhaifallah, Anton Tikhonov, (2017), Performance of data acquisition system for monitoring PV system parameters. *Measurement*,104, pp.204-211.

[232] Parra JMP, Aroca AM, Ninirola GS, Bueso MC, García AM. (2018), PV module monitoring system based on low-cost solutions: wireless raspberry application and assessment. *Energies,* 11: pp. 1–20.

[233] Jiang B, Iqbal MT. (2019), Open-source data logging and data visualization for an isolated PV system. *Electronics* (Basel), 8:1–16.

[234] Motahhir S, Hammoumi AE, Ghzizal AE, Derouich A. (2019), Open hardware/software test bench for solar tracker with virtual instrumentation. *Sustain Energy Technol Assess,* 31:9–16.

[235] Shravanth M.V., Srinivasan J., Sheela K. (2016), Performance of solar photovoltaic installations: Effect of seasonal variations, *Solar Energy*, 131: 39-46. https://doi.org/10.1016/j.solener.2016.02.013.

[236] Herteleer B, Huyck B, Catthoor F. (2017), Normalised efficiency of photovoltaic systems: Going beyond the performance ratio, *Solar Energy*,157:408-418. https://doi.org/10.1016/j.solener.2017.08.037.

[237] Adouane M, Al-Qattan A, Alabdulrazzaq B (2020), Comparative performance evaluation of different photovoltaic modules technologies under Kuwait harsh climatic conditions, *Energy Reports*,6, pp.2689-2696. https://doi.org/10.1016/j.egyr.2020.09.034.

[238] Shehri A A, Parrott B, Carrasco P. (2017), Accelerated testbed for studying the wear, optical and electrical characteristics of dry-cleaned PV solar panels. *Solar Energy*, 146:8–19.

[239] Shehri A A, Parrott B, Carrasco P. (2016), Impact of dust deposition and brush-based dry cleaning on glass transmittance for PV modules applications. *Solar Energy*, 135:317–24 https://doi.org/10.1016/J.SOLENER.2016.06.005.

[240] Arabatzis I, Todorova N, Fasaki I. (2018), Photocatalytic, self-cleaning, antireflective coating for photovoltaic panels: characterization

and monitoring in real conditions. *Solar Energy*,159:251–9. https://doi.org/10. 1016/J.SOLENER.2017.10.088.

[241] Urrejola E, Antonanzas J, Ayala P. (2016), Effect of soiling and sunlight exposure on the performance ratio of photovoltaic technologies in Santiago, Chile. *Energy Convers Manage*, 114:338–47.

[242] Al-Housani M, Bicer Y, Koç M. (2019), Experimental investigations on PV cleaning of large-scale solar power plants in desert climates: Comparison of cleaning techniques for drone retrofitting, *Energy Conversion and Management*,185:800-815. https://doi.org/10.1016/j.enconman.2019.01.058.

[243] Al-Housani M, Bicer Y, Koç M. (2019), Assessment of Various Dry Photovoltaic Cleaning Techniques and Frequencies on the Power Output of CdTe-Type Modules in Dusty Environments. *Sustainability*,11(10):2850. https://doi.org/10.3390/su11102850.

[244]https://www.amazon.in/Water-Fed-Pole-Kit-Lightweight/dp/B07YLLRT S7

[245]https://www.amazon.in/Zoom-Renewables-Cleaning-Water-fed-Telescopic/dp/B07VPP6TDF

[246]https://www.sweeping-brush.com/sale-13782344-double-head-automatic-solar-panel-cleaning-brush-and-pole-kit-solar-panel-cleaning-rotating-brush-cl.html

[247]https://www.alibaba.com/product-detail/Extenclean-electric-rotating-double-head-window_1600320267634.html?spm=a2700.galleryofferlist.normal_offer.d_title.1014225eUxnnA0&s=p

[248] Häberlin, H. (2012), Photovoltaics system design and practice: John Wiley & Sons.

List of Publications

1. Gupta, V., Sharma, M., Pachauri, R.K., Babu K. N. D., (2019). Comprehensive review on effect of dust on solar photovoltaic system and mitigation techniques. *Solar Energy* 191, 596–622. https://doi.org/10.1016/j.solener.2019.08.079. **(I.F.4.67) (Q1).**

2. Gupta, V., Sharma, M., Pachauri, R.K., Babu K. N. D., (2022). Impact of hailstorm on the performance of PV module: a review, *Energy Sources, Part A: Recovery, Utilization, and Environmental Effects,* 44(1),1923-1944. https://doi.org/10.1080/15567036.2019.1648597. **(I.F.3.44) (Q1).**

3. Gupta V, Sharma M, Pachauri R.K., Babu K. N. D., (2021). A low-cost real-time IOT enabled data acquisition system for monitoring of PV system, *Energy Sources, Part A: Recovery, Utilization Environ Effects,* 43(20), 2529-2543. https://doi.org/10.1080/15567036.2020.1844351. **(I.F.2.66) (Q2).**

4. Gupta, V., Sharma, M., Pachauri, R.K., Babu K. N. D., (2022). Performance Analysis of Solar PV system using customized wireless data acquisition system and novel cleaning technique, *Energy Sources, Part A: Recovery, Utilization, and Environmental Effects*, 44(2), 2748-2769. https://doi.org/10.1080/15567036.2022.2061091. **(I.F.3.44) (Q1).**

5. Gupta, V., Sharma, M., Pachauri, R.K., Babu, K.D., Design and development of self-cleaning PV sliding system, Clean Energy, 6(3), 392–403, https://doi.org/10.1093/ce/zkac015. **(I.F.2.98) (Q2).**

6. Gupta, V., Sharma, M., Pachauri, R.K., Babu K. N. D., Performance enhancement of solar photovoltaic system using waterless PV cleaning system, *Energy Sources, Part A: Recovery, Utilization, and Environmental Effects***.** (Under Review).

PHD THESIS@Vinay Gupta

ORIGINALITY REPORT

9%	7%	4%	2%
SIMILARITY INDEX	INTERNET SOURCES	PUBLICATIONS	STUDENT PAPERS

PRIMARY SOURCES

1	P Pandiyan, S Saravanan, T Chinnadurai, Tiwari Ramji, N Prabaharan, S Umashankar. "Mitigation Techniques for Removal of Dust on Solar Photovoltaic System", Wiley, 2021 Publication	1%
2	www.ijert.org Internet Source	<1%
3	academicworks.cuny.edu Internet Source	<1%
4	Touati, Farid, M.A. Al-Hitmi, Noor Alam Chowdhury, Jehan Abu Hamad, and Antonio J.R. San Pedro Gonzales. "Investigation of solar PV performance under Doha weather using a customized measurement and monitoring system", Renewable Energy, 2016. Publication	<1%
5	ore.exeter.ac.uk Internet Source	<1%
6	"The Effects of Dust and Heat on Photovoltaic Modules: Impacts and Solutions", Springer	<1%